

NASA Contractor Report 4399

IN-35
40360
P. 131

Advanced Optical Sensing
and Processing Technologies
for the Distributed Control
of Large Flexible Spacecraft

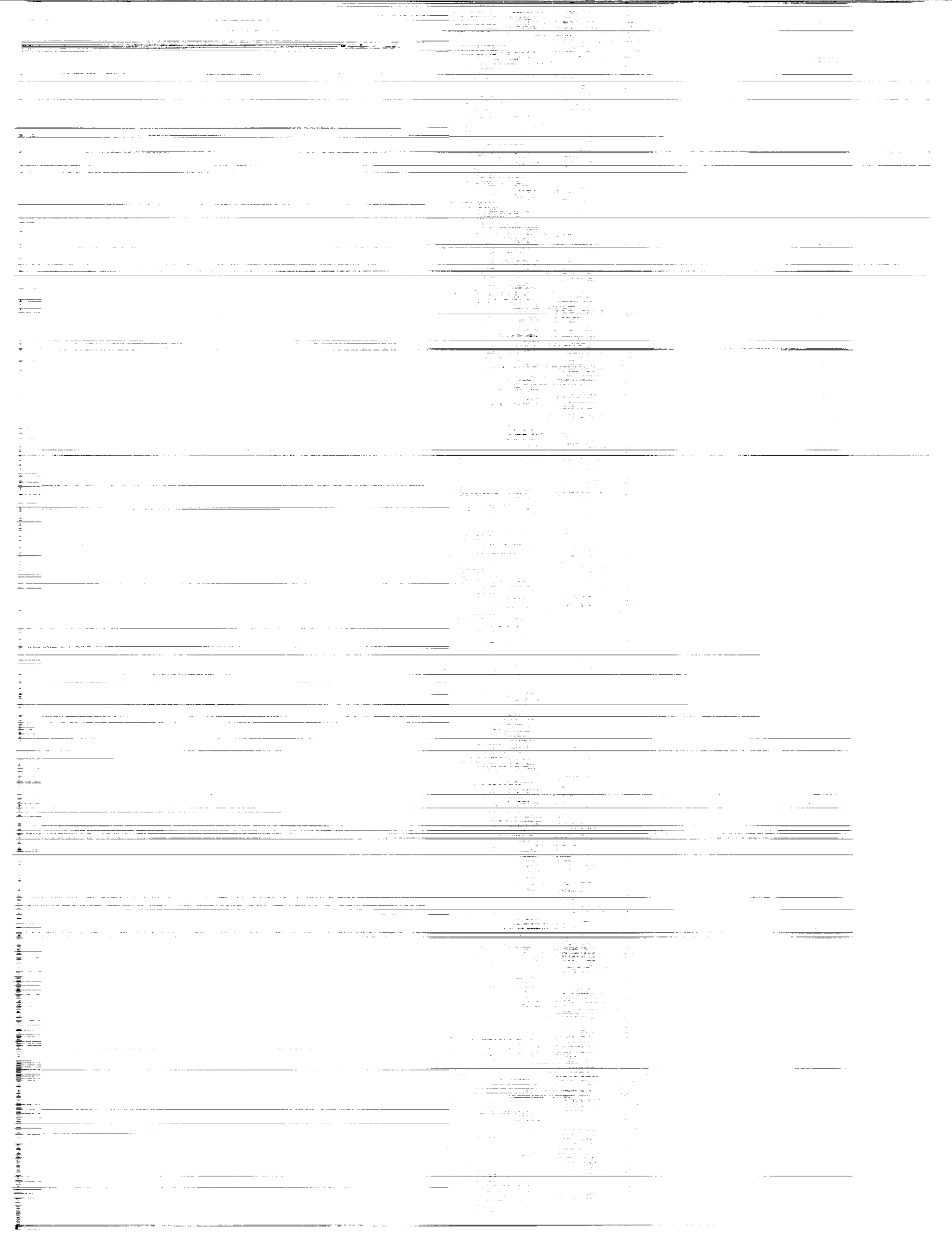
G. M. Williams and J. C. Fraser

CONTRACT NAS1-18763
OCTOBER 1991

(NASA-CR-4399) ADVANCED OPTICAL SENSING AND PROCESSING TECHNOLOGIES FOR THE DISTRIBUTED CONTROL OF LARGE FLEXIBLE SPACECRAFT Final Report (Photon Research Associates) 131 p
CSCL 20F H1/35 0040360

Unclas
0040360





NASA Contractor Report 4399

Advanced Optical Sensing and Processing Technologies for the Distributed Control of Large Flexible Spacecraft

G. M. Williams and J. C. Fraser
Photon Research Associates
Cambridge Research Division
Cambridge, Massachusetts

Prepared for
Langley Research Center
by Photon Research Associates
for McDonnell Douglas Space Systems Company
under Contract NAS1-18763



National Aeronautics and
Space Administration

Office of Management

Scientific and Technical
Information Program

1991

PREFACE

This is the final report for McDonnell Douglas Corporation subcontract number 89521150H, NASA contract number NAS1-18763, entitled "Optical Sensing and Processing for Distributed Control of Flexible Spacecraft". This report covers work performed during the period from June 1989 to February 1990.

Contributions to the program were made by the entire staff of Photon Research Associates, Cambridge Division. Program Management was conducted by Dr. Keto Soosaar and Dr. James C. Fraser. The engineering staff included Laura Larkin (Project Engineer), George M. Williams, Karen Swiech, and Dr. Leslie Matson.

TABLE OF CONTENTS

1.0 INTRODUCTION 1

2.0 REVIEW AND ASSESSMENT OF PROPOSED NASA MISSION 3

 2.1 CANDIDATE "OPTICAL TECHNOLOGIES" MISSIONS DESCRIPTION 3

 2.1.1 PRECISION OPTICAL SYSTEMS 3

 2.1.2 CANDIDATE LARGE ANTENNA SYSTEMS 6

 2.1.3 SELECTION OF A BASELINE MISSION 8

3.0 LDR SYSTEM REQUIREMENTS 15

4.0 STRAWMAN LDR CONTROL SYSTEM 20

 4.1 INTRODUCTION 20

 4.2 OVERALL CONTROL SYSTEM APPROACHES 20

 4.3 KEY DEVICES AND FUNCTIONS 23

 4.3.1 SENSORS 23

 4.3.2 ACTUATORS (SLOW-ACTING EXCEPT WHERE NOTED) 24

 4.4 MAJOR CONTROL SYSTEMS 24

 4.4.1 PRECISION OVERALL OPTICS ALIGNMENT 25

 4.4.2 OPTICAL FORM MAINTENANCE 25

 4.4.3 STRUCTURE MODE CONTROL 25

 4.4.4 VIBRATION DAMPING 26

 4.5 SUMMARY 26

5.0 ASSESSMENT OF TRADITIONAL TECHNOLOGY 27

 5.1 SOA ELECTRONIC PROCESSING TECHNOLOGY 27

 5.2 SOA CONVENTIONAL SENSOR TECHNOLOGY 32

 5.3 SOA CONVENTIONAL ACTUATOR TECHNOLOGY 38

6.0 ASSESSMENT OF ADVANCED OPTICAL PROCESSING MATERIALS, DEVICES, AND APPLICATIONS 43

 6.1 MATERIALS 43

 6.1.1 PHOTOREFRACTIVE CRYSTALS 44

 6.1.2 NLO POLYMERS 52

 6.1.3 SEMICONDUCTORS 53

 6.1.4 SUMMARY OF MATERIALS 56

 6.2 SPATIAL LIGHT MODULATORS 56

 6.3 OPTICAL COMPUTERS 65

 6.3.1 OPTICOMP COMBINATORIAL PROCESSOR 68

 6.3.2 BIMODAL OPTICAL COMPUTER 69

 6.3.3 OPTICAL LINEAR ALGEBRAIC PROCESSOR 75

6.3.4	RESIDUE MATHEMATICS	75
6.4	OPTICAL NEURAL NETWORKS	79
6.5	REAL-TIME CORRELATION	85
6.6	DETECTOR ARRAYS	87
7.0	DEVELOPMENT PLAN FOR THE IMPLEMENTATION OF ADVANCED OPTICAL PROCESSING TECHNOLOGIES FOR THE CONTROL OF LARGE FLEXIBLE SPACECRAFT	88
7.1	INTRODUCTION	90
7.2	CURRENT RESEARCH INTEREST	91
7.3	DEVELOPMENT OF MATERIALS	92
7.3.1	PHOTOREFRACTIVE CRYSTALS	96
7.3.2	NLO POLYMERS	98
7.3.3	III-V MATERIALS	99
7.4	DEVELOPMENT OF EO DEVICES AND APPLICATIONS	101
7.4.1	NEURAL NETWORKS	102
7.4.2	OPTICAL COMPUTING	104
7.4.3	PATTERN RECOGNITION	106
7.4.4	WAVEFRONT SENSING AND WAVEFRONT CORRECTION DEVICES	108
8.0	A PROPOSED DEMONSTRATION PLAN	110
8.1	INTRODUCTION	110
8.2	POTENTIAL APPLICATIONS	111
8.3	ELECTRO-OPTICAL STRUCTURAL CONTROLS EXPERIMENT	111
8.3.1	EXPERIMENT OVERVIEW AND CONFIGURATION	111
8.3.2	OBJECTIVE	113
8.3.3	APPROACH	113
8.3.4	MILESTONE PLAN	116
9.0	REFERENCES	121

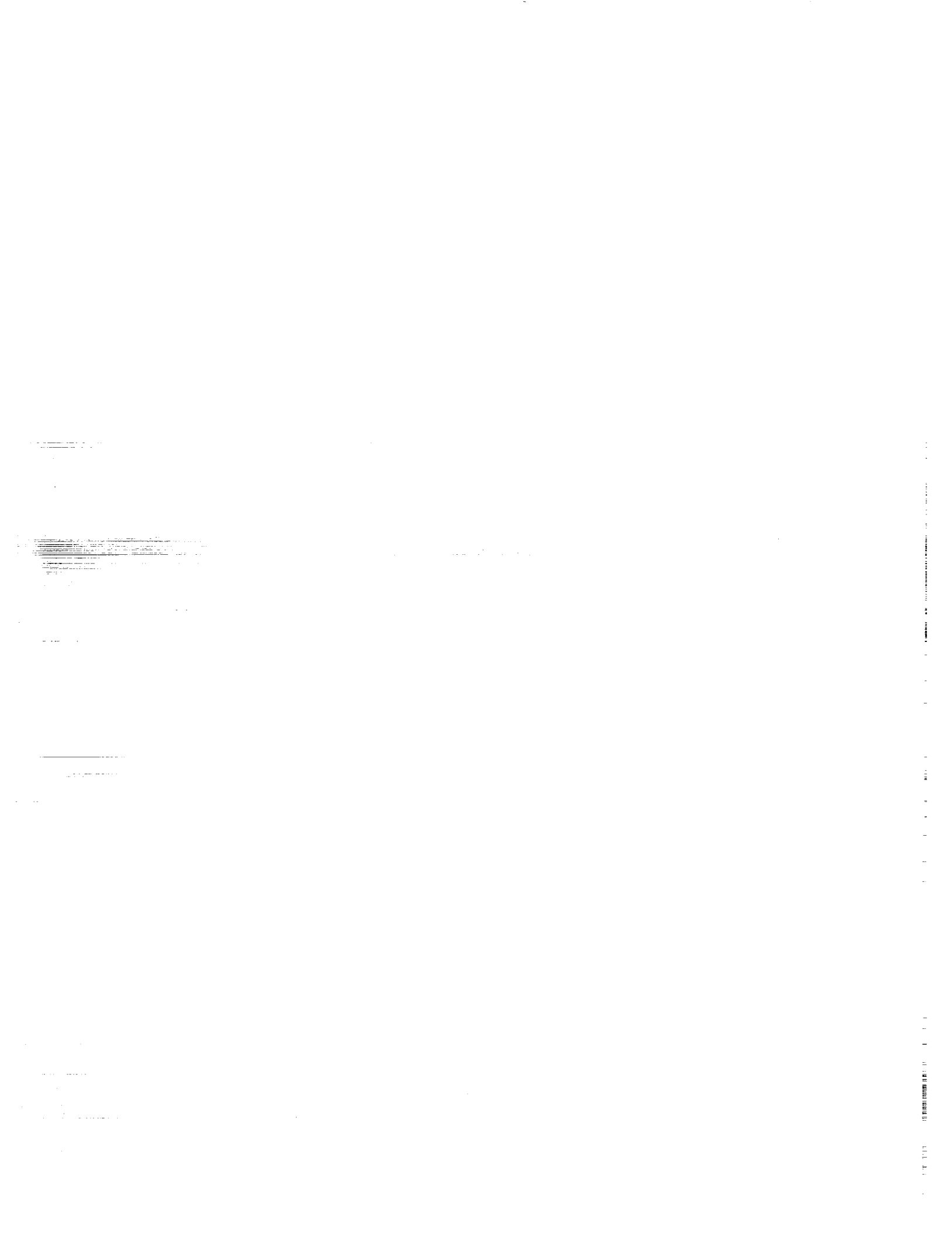
LIST OF FIGURES

1.	CANDIDATE PRECISION OPTICAL MISSIONS	4
2.	CANDIDATE LARGE ANTENNA MISSIONS	7
3.	JPL LDR SYSTEM CONCEPT	17
4.	IN-LINE 2 STAGE LDR OPTICS	18
5a.	STEADY STATE INDEX CHANGE IN BaTiO ₃ AS A FUNCTION OF GRATING PERIOD FOR APPLIED FIELDS, E _o = 0, 10 kV/cm	49
5b.	STEADY-STATE INDEX CHANGE IN BSO AS A FUNCTION OF GRATING PERIOD FOR APPLIED FIELDS, E _o = 0, 10 kV/cm	49
6a.	RESPONSE TIME OF BaTiO ₃ AS A FUNCTION OF GRATING PERIOD FOR APPLIED FIELDS, E _o = 0, 10 kV/cm, AND MEAN IRRADIANCE I _o = 1w/cm ²	50
6b.	RESPONSE TIME OF BSO AS A FUNCTION OF GRATING PERIOD FOR APPLIED FIELDS, E _o = 0, 10 kV/cm, AND MEAN IRRADIANCE I _o = 1 w/cm ²	50
7.	ENERGY PER UNIT AREA TO WRITE A 1% DIFFRACTION EFFICIENCY GRATING IN BSO AND BaTiO ₃ AS A FUNCTION OF GRATING PERIOD FOR APPLIED FIELDS, E _o = 0, 10 kV/CM. NO CURVE IS GIVEN FOR BSO WITH E _o = 0 BECAUSE A 1% DIFFRACTION EFFICIENCY CANNOT BE REACHED IN A 1 mm PATH LENGTH	51
8.	SLM CLASSIFICATION	57
9.	SLM PARAMETERS	58
10.	PRINCIPLE OF OPERATION OF SEMETEX "SIGHT-MOD"	61
11.	REFLECTIVE-READOUT PHOTOADDRESSED SPATIAL LIGHT MODULATOR	63
12.	DEFORMABLE MIRROR DEVICE	64
13.	PRINCIPLE OF SEED DEVICES	65
14a.	INPUT INTENSITY vs. OUTPUT INTENSITY FOR OPTICAL BISTABLE DEVICE	66
14b.	BISTABLE OPTICAL DEVICE	66
15.	OPTICOMP OPTICAL COMPUTER HARDWARE FOR GENERAL PURPOSE PROGRAMMABLE COMBINATORIAL LOGIC PLA COMPUTATION ELEMENTS	70
16.	THE BIMODAL OPTICAL PROCESSOR	71
17a.	THE LOG(ERROR) AS A FUNCTION OF THE NUMBER OF ITERATIONS. THE BOC STARTED WITH 30% ERROR [17]	72
17b.	THE LOG(ERROR) AS A FUNCTION OF THE NUMBER OF ITERATIONS. THE BOC STARTED WITH 100% ERROR [17]	72
18a.	PLOT OF LOG OF THE RATIO A _n IN TERMS OF THE SIZE OF THE MATRIX [19]	76
18b.	PLOT OF THE LOG OF THE RATIO B _n IN TERMS OF THE SIZE OF THE MATRIX [19]	76
19.	OPTICAL LINEAR ALGEBRAIC PROCESSOR	77
20.	DATA FLOW ARRANGEMENT FOR PARTITIONING MATRIX [20]	78
21.	ADDITION PERFORMED USING BASE 3,5 RESIDUE MATHEMATICS	79
22.	OPTO-ELECTRONIC ANALOG OF A NERVE CELL	80
23.	MODEL OF A NEURAL CELL	82

24.	OPTICAL PROCESSOR SHOWING COMPONENT OF HOPFIELD NEURAL MODEL	83
25.	VOLUME HOLOGRAM CONNECTING $N \times N$ INPUT AND OUTPUT FRAMES	84
26.	INPUT/OUTPUT CONSIDERATIONS FOR GRATING FORMATION IN VOLUME HOLOGRAMS	85
27.	VANDERLUGT OPTICAL CORRELATOR	86
28.	REAL-TIME OPTICAL CORRELATOR	87
29.	SEVERAL OF THE OPTICAL APPLICATIONS OF MATERIALS	94
30.	SUMMARY OF STATUS OF ADVANCED OPTICAL MATERIALS	95
31.	DEMONSTRATION PLAN FOR PHOTOREFRACTIVE CRYSTALS	97
32.	DEMONSTRATION PLAN FOR NLO POLYMERS	98
33.	DEMONSTRATION PLAN FOR III-V SEMICONDUCTOR MATERIALS	100
34.	DEMONSTRATION PLAN FOR OPTICAL NEURAL NETWORKS APPLIED TO NASA CONTROL SYSTEM DESIGNS.	103
35.	DEVELOPMENT PLAN FOR OPTICAL COMPUTING CONCEPT IMPLEMENTATION FOR THE CONTROL OF FLEXIBLE SPACECRAFT	105
36.	DEVELOPMENT PLAN FOR UTILIZING REAL-TIME PATTERN RECOGNITION AND CORRELATORS FOR SPACECRAFT CONTROL.	107
37.	DEVELOPMENT PLAN FOR THE DEVELOPMENT OF WAVEFRONT SENSING APPLICATIONS FOR NASA CONTROL SYSTEMS	108
38.	PANCAKE TRUSS ARRANGEMENT	112
39.	TRUSS ELEMENT CONFIGURATION EXAMPLES	114
40.	MODAL PATTERN RECOGNIZING SYSTEM	115
41.	DETAIL OF OPTICAL ASSOCIATIVE MEMORY	117
42.	CONTROLLERS FOR PANCAKE TRUSS	118
43.	MILESTONE PLAN	119

LIST OF TABLES

1.	PROPOSED CONTROLS HARDWARE - PRECISION OPTICAL SYSTEMS	9
2.	FUTURE MISSION REQUIREMENTS - PRECISION OPTICAL SYSTEMS	10
3.	FUTURE MISSION REQUIREMENTS - LARGE ANTENNAS	11
4.	MISSION SELECTION CRITERIA	13
5.	LDR PARAMETERS AND REQUIREMENTS	16
6.	AC-100	29
7.	MAST 1750A COMPUTER	31
8.	CONVENTIONAL SENSORS	33
9.	CONVENTIONAL SENSORS, OVERVIEW SUMMARY	37
10.	CONVENTIONAL ACTUATORS	39
11.	CONVENTIONAL ACTUATORS - OVERVIEW SUMMARY	41
12.	FERROELECTRIC NON-LINEAR MATERIALS	45
13a.	CUBIC NON-LINEAR MATERIALS	46
13b.	SEMICONDUCTOR - NON-LINEAR MATERIALS	46
14.	NLO POLYMER CLASSES	54
15.	SPATIAL LIGHT MODULATOR TECHNOLOGY	60
16.	FIGURE OF MERIT FOR HIGHLY CONNECTED PROCESSORS	81
17.	LARGE FORMAT CCD ARRAYS	88
18.	LDR CONTROL REQUIREMENTS COMPARED TO OPTICAL TECHNOLOGY PERFORMANCE CHARACTERISTICS	93



1.0 INTRODUCTION

This document is the final report for NASA contract NAS1-18763, McDonnell Douglas Contract No. 89521160H. The report represents work performed on the contract during the period from June 1989 through February 1990. The objective of this study effort was to examine state-of-the-art optical sensing and processing technology and determine the viability and effectiveness of applying this technology to control the motion of flexible spacecraft.

Proposed large flexible space systems, such as optical telescopes and antennas, will require control over vast surfaces. Most likely distributed control will be necessary involving many sensors to accurately measure the surface. Some proposed control schemes use many conventional electrical or electro-mechanical sensors placed at strategic locations (e.g. structural nodes) to determine the system response. Information from these myriad sensors must be processed rapidly. After an appropriate complex control algorithm determines actuator commands, a similarly large number of conventional actuators must act upon the system. Potential bottlenecks to this type of control system includes too large of a processing time due to both the number of components and the transmission delay times, and excessive weight, cost, and complexity due to the large number of components. Recent advances in optical technologies may provide very lightweight and rapid sensors and processors. Also, optical technologies most likely would have reduced power requirements, increased reliability, lower cost, reduced complexity, and an improved ability to calibrate. In addition, a possibility exists to correct system errors due to structural flexibility solely in the optical domain. Therefore, the use of advanced optical components may be either enhancing or truly enabling for future NASA missions.

Advanced electro-optical techniques, for the purposes of this study, are defined as either utilizing a few complex sensors each of which handles a large amount of data or using optical processing and computing techniques, or possibly the ability to provide complete wavefront correction without mechanical components.

The technical approach used to meet this study goal included reviewing proposed NASA missions to assess system needs and requirements. From these space systems, a candidate mission was chosen as a baseline study spacecraft for comparison of conventional and optical control components. Control system requirements of the baseline system were used for designing both a "conventional" control system (containing current off-the-shelf components) and an "optical" system (utilizing electro-optical devices for sensing and/or processing). State-of-the-art surveys of conventional sensor, actuator, and processor technologies

and advanced optical technologies were performed to provide the background and database to develop candidate control systems. The potential benefits of electro-optical control system components warranted a technology development plan. This proposed plan presents a logical, effective way to develop and integrate this technology. The last portion of this study effort was the development of a demonstration plan. Potential laboratory experiments which would investigate and use electro-optical components were described in detail.

Section 2.0 reviews planned NASA missions including controls requirements to identify large flexible space systems where distributed controls approaches may benefit from advanced optical technologies. Optical and radar systems are examined in detail and these missions are narrowed down to one focus or baseline mission. The requirements and a detailed description of the baseline mission, the Large Deployable Reflector (LDR), is presented in Section 3.0. Section 4.0 describes a strawman control system using advanced optical components. Details of the sensors, actuators, and processors are provided. Section 5.0 contains a state-of-the-art survey of conventional control technologies. This study includes the traditional electrical, mechanical, and electro-mechanical sensors, actuators, and computing equipment used for spacecraft control. Section 6.0 contains a state-of-the-art assessment of the materials, devices, and applications of advanced optical processing technologies including materials, spatial light modulators, optical computers, optical neural networks, optical correlators and detector arrays. Section 7.0 presents a development plan, whose goal is to develop the optical technologies required for implementing distributed electro-optical control systems. The demonstration plan in Section 8.0 details an experiment to develop and demonstrate an optical processing concept for the optical control of flexible spacecraft.

2.0 REVIEW AND ASSESSMENT OF PROPOSED NASA MISSION

Several future NASA missions were considered while investigating the potential benefits of electro-optical sensors and processors. The candidate missions most likely to benefit from advanced optical sensors or processors are those large flexible space structures operating at short wavelengths which have very stringent pointing and stability requirements. Additionally, some improvements may accrue from performing control calculations in the optical domain for optically-performing systems rather than converting to electro-mechanical response. Space systems may be classified by three broad categories - precision optical systems (e.g. large telescopes), large multi-instrument platforms, and large antennas. The primary two space systems areas investigated for this study were precision optical systems and systems with large antennas, either radar or microwave.

2.1 CANDIDATE "OPTICAL TECHNOLOGIES" MISSIONS DESCRIPTION

2.1.1 PRECISION OPTICAL SYSTEMS

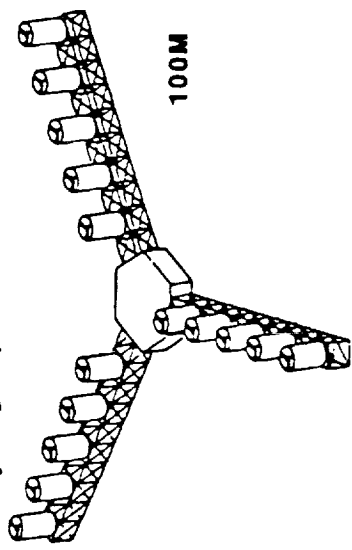
The seven precision large optical systems researched are described below. A brief description of the mission purpose, spacecraft size, and other parameters are provided. Conceptual illustrations of several of the large optical systems are shown in Figure 1.

Large Deployable Reflector (LDR) - The LDR is a dedicated astronomical space observatory operating in the spectral region between 30 micrometers and 1 millimeter. The baseline concept consists of a Cassegrain telescope with a segmented, actively controlled 20 meter primary reflector composed of 37 segments. Active control of the optics utilizing edge sensors, wavefront error measurements, or directed laser range finding will control the position and orientation of each optical segment. In addition, active pointing and structural (vibration) control will be required.

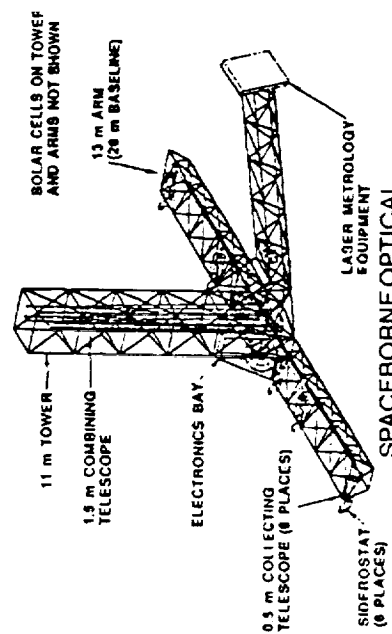
Advanced X-Ray Astrophysics Facility (AXAF) - The AXAF will be an advanced version of the HEAO-2 (Einstein) observatory with a capability 50 - 100 times that of HEAO-2. AXAF is a grazing incidence x-ray telescope with nested pairs of mirrors and a 9 - 12 meter focal length. The overall spacecraft length will be approximately 13 - 16 meters.

Infrared Interferometer (I2) - I2 will contain three SIRTf-class telescopes mounted on a 100 meter beam. The three telescopes allow observations with higher angular resolution than a single mirror telescope. The center telescope will be

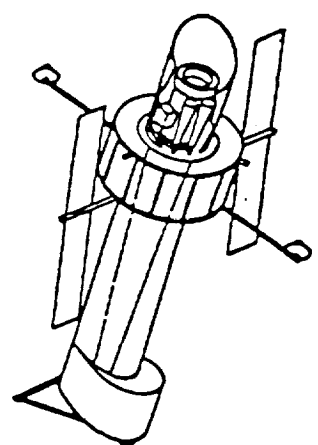
Very large optical interferometer



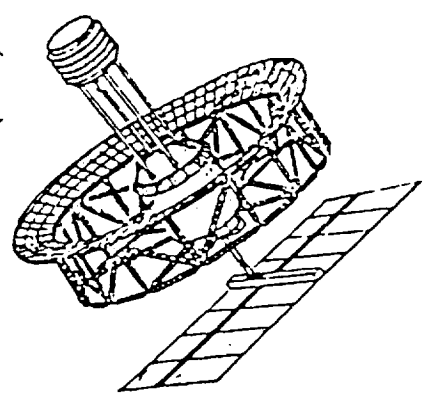
INFRARED INTERFEROMETER (I)



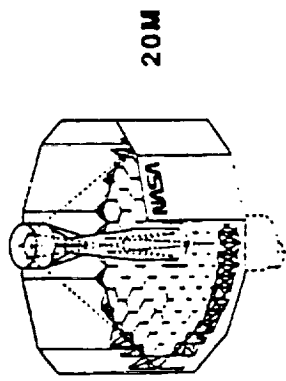
SPACEBORNE OPTICAL INTERFEROMETER (SOI)



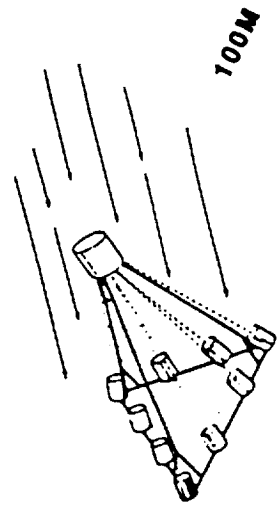
ADVANCED X-RAY ASTROPHYSICS FACILITY (AXAF)



THINNED APERTURE TELESCOPE (TAT)



LARGE DEPLOYABLE REFLECTOR (LDR)



COHERENT SYSTEM OF MODULAR IMAGING COLLECTORS (COSMIC)

Figure 1. CANDIDATE PRECISION OPTICAL MISSIONS

fixed and each one at the beam endpoint will be movable via remote control which permits baseline settings from the heterodyne interferometer. Telescope and beam attitude positioning will be accomplished by a star tracker with a focal plane array tracking system. The baseline length of 100 meters between the optical paths will allow spatial resolution nearly an order of magnitude better than that obtained from an individual SIRTf of the LDR. The long beam structure will most likely require active structural control.

Coherent Optical System of Modular Imaging Collectors (COSMIC) - The full-cross COSMIC facility is an optical interferometer consisting of modules of identical telescopes, a system of mirrors for beam combination and a set of focal plane detectors. This will allow images of astronomical sources at milli-arc-sec angular resolution down to very faint stellar magnitudes. Each of the four arms contains four Afocal Interferometer Telescopes (AIT) and one Beam Combining Telescope (BCT) all with 1.8 meter square primary mirrors. The optics, fine guidance system, and aspect system are mounted on a rectangular metering truss. This is then mounted on an aluminum shell which is designed to handle launch loads and provide a stable thermal environment. The full cross version would be 31 by 34 meters. Proposed actuators include magnetic torquers and double gimbals control moment gyros. Sensors might include sun sensors, magnetometers, fixed-head star trackers, rate gyros, and CCD fine guidance sensors.

Thinned Aperture Telescope (TAT) - The 100 meter TAT would provide a 30-fold increase in image resolution and a 1000-fold increase in astrometric precision over the Space Telescope. The large aperture telescope would be deployed in low earth orbit using advanced assembly techniques. The basic structure would be constructed and then instrumented with retro-reflectors to improve dimensional stability using laser gage interferometry. The individual elements are mounted to this structure and then controlled to form a coherently phased array. Interferometric sensors in the focal plane are used to detect wavefront errors for each element for image compensation and figure control. Total dimension will be 100 meters in diameter. The primary mirrors will be 4 by 4 meters. Secondary mirrors must be articulated for image motion compensation and background chopping.

Spaceborne Optical Interferometer (SOI) - The SOI is the JPL CSI focus mission which emphasizes microprecision controlled structures. This mission is seen as enabling for the class of large optical systems and enhancing for large precision antenna systems. The criteria for the selection of this as a focus mission were the importance of the mission to NASA, the mission's need for CSI technology, the ability to drive development of general purpose CSI technology, and the JPL emphasis on microprecision structures. The spacecraft is composed

of four arms. The 11 meter tower contains a 1.5 meter combining telescope. The two 13 meter arms (one 26 meter beam) contains siderostats in six locations and 0.5 meter collecting telescopes in six locations. The fourth arm contains laser metrology equipment. Disturbance sources have been identified and include reaction wheels/control moment gyros, siderostat motor cogging, ripple, and imbalance, bearing noise, slew reaction torques, trombone nonlinearities, slew reaction forces, and motor and bearing noise, and tape recorders start/stop transients and noise. A fairly detailed list of potential structural control options have been proposed. Passive damping could include viscous and viscoelastic means. Vibration isolation options include magnetic, piezoelectric, electrodynamic, viscous, and elastomeric. Control actuator options include piezo/inch worm actuators, voice coil/screw jack actuators, torque wheel actuators, and proof-mass actuators. Feedback sensor options are microgravity accelerometers, load cell force sensors, strain gage capacitive displacement sensors, laser metrology displacement sensors, eddy current rate sensors, and angular rate/acceleration sensors. Structural control requirements have also been identified and are as follows: 300 micrometers at DC, 30 micrometers at 1 Hz, 30 nanometers at 10 Hz, 0.3 nanometers at 100 Hz and above.

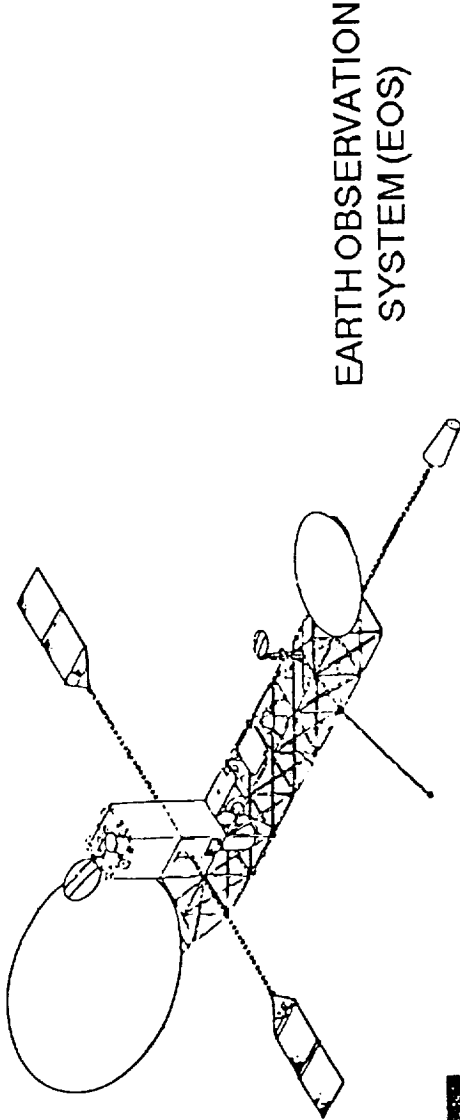
Advanced Space Telescope (AST) - The AST would be a large, 8 meter aplanatic Cassegrain telescope. Critical technology needs include positioning to 1/65 of a wavelength of a 3 meter pie-shaped segment with an off-axis figure, techniques for control of structure alignment, precision positioning of components, optical diagnostic sensors and controls for figure control to wavefront error of $\lambda/40$. Piezoelectric methods are thought to be promising at this point.

2.1.2 CANDIDATE LARGE ANTENNA SYSTEMS

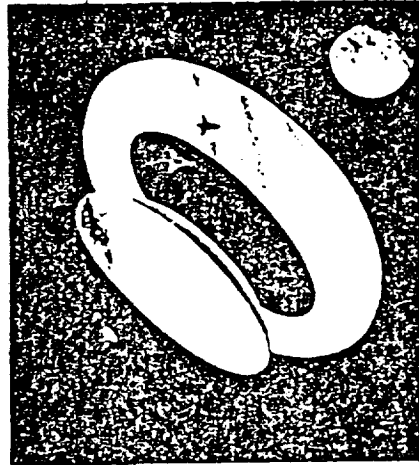
The large antenna systems included in the study are described in the following text. Conceptual illustrations of the large antenna systems are shown in Figure 2.

Very Long Baseline Interferometer (VLBI) - The VLBI Observatory system requires a 15 - 20 meter deployable parabolic mesh antenna with receivers to augment the ground-based VLBI array. Pointing of the antenna probably will require two stages with a 3-axis or spin stabilized attitude control system and a movable Cassegrain subreflector for pointing refinement.

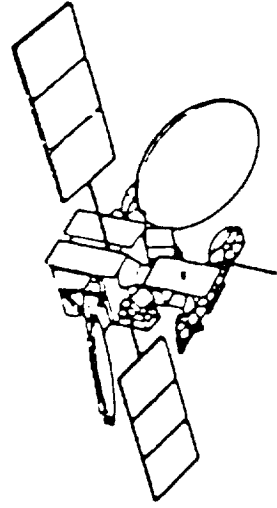
Earth Observation System (EOS) - EOS would establish a global observation system in space which would include experiments and free-flying platforms, in polar, low-inclination and geostationary orbits to perform integrated long-term



EARTH OBSERVATION SYSTEM (EOS)



SEARCH FOR EXTRATERRESTRIAL INTELLIGENCE (SETI)



ADVANCED COMMUNICATIONS TECHNOLOGY SATELLITE (ACTS)

Figure 2. CANDIDATE LARGE ANTENNA MISSIONS

measurements. One portion of the EOS would be the Geostationary Platform. This platform satellite would contain several instruments (perhaps more than 20) and contain both a fine and coarse passive microwave radiometer. The size of these antennas is not yet firmly fixed. Estimates range from 15 to 100 meters.

Search for Extra-Terrestrial Intelligence (SETI) - The SETI satellite would be designed to detect transmitted radio signals and also provide general investigations of radio sources. One concept for a system consists of a spherical primary reflector made of lightweight mesh, with three Gregorian subreflectors and feed assemblies that permit three different stars to be searched simultaneously. A disk-shaped shield placed between the antenna and the Earth protects against radio frequency interference (RFI). One concept envisions a 300 meter diameter lightweight spherical reflecting antenna and a 600 meter diameter RFI shield.

Advanced Communication Technology Satellite (ACTS) - The ACTS project would develop multibeam communications technology to permit a more efficient use of orbit and spectrum resources and allow for new forms of communication and data transfer. The ACTS satellite would provide three fixed beams or two scanning beams and a single fixed beam. Isolation between beams will be provided through the combined use of orthogonal polarization and spatial separation.

2.1.3 SELECTION OF A BASELINE MISSION

With potential systems identified, some criteria were needed to narrow this list down to a few focus missions. Since the final goal is to identify and define an equivalent or improved optically-based system, current thoughts on appropriate conventional sensors, actuators, and controls strategies were investigated. These findings for many of the precision optical systems are listed in Table 1. Several systems are quite immature at this time. With the configuration indeterminate for a few of these missions, control strategies are difficult to propose. Both LDR and JPL focus mission, SOI, have been planned in relatively great detail. This allows some estimates on the number and types of sensors and actuators required to achieve pointing goals.

Requirements for these future missions were investigated and the results for the proposed optical systems are shown in Table 2. Table 3 shows the requirements for the proposed large antenna missions.

Several issues can be raised from these numbers: Can conventional sensors and actuators meet range and resolution requirements? What types and combinations of control systems will be needed to meet control attenuation needs?

Table 1. PROPOSED CONTROLS HARDWARE - PRECISION OPTICAL SYSTEMS

<u>MISSION</u>	<u>SENSORS</u>	<u>ACTUATORS</u>	<u>STRATEGY/COMMENTS</u>
LDR	Shack interferometer, weak diffraction gratings, figure sensor - optical lever, multiple wf interferometer, electronic capacitive.	adaptive structures, proof-mass, reaction wheels, cmg's	Reference concept employs 2-stage optical design in which primary figure errors are compensated for by means of a closed-loop servo system that measures the wf error and quasi-statically controls individual segments in a quaternary mirror which is conjugate to the primary. Critical technology areas are dynamic figure control, modeling and performance prediction, wf and figure control, los guidance.
COSMIC	Sun, magnetometer, fixed-head star tracker, rate gyro, CCD fine guidance sensor	NOT DEFINED	NOT DEFINED
TAT	Retroreflectors for laser gauge interferometry, interferometric sensors	NOT DEFINED	Individual elements mounted to base structure & then controlled to form a coherently phased array. Interferometric sensors in the focal plane used to detect wf errors for each element for image compensation and figure control. Articulated secondary mirrors for image motion compensation and background chopping.
SOI	micro-g accelerometers, load cell force sensors, strain gauge force displacement, linear displacement voltage transducers, capacitive displacement, laser metrology displacement, eddy current rate, angular rate/acceleration sensors.	viscous, visco-elastic dampers, Isolation - magnetic, piezoelectric, electrodynamic, viscous, elastomeric, Piezo/inch-worm, voice coil/screw jack, torque wheel, proof-mass	Identified disturbance sources include reaction wheels/cmg's; siderostat motor cogging, ripple, and imbalance; bearing noise; slew reaction torques, trombone nonlinearities; slew reaction forces; motor & brg. noise; tape recorder transients. Structural control requirements have been identified and are 300 micrometers at DC, 30 micrometers at 1 Hz, 30 nm at 10 Hz, 0.3 nm at 100 Hz.

MISSION	OPERATIONAL POINTING REQIMNTS.		RANGE FIG/ALIGN	RESOLUTION FIG/ALIGN	CONTROL ATTENUATN REQUIRED
	WAVELENGTH (μm)	ACC. STAB. (μrad)			
LDR	30	.3-.5	300/3000 m	.3/3 m	200
AXAF	3×10^{-5} - 1×10^{-2} (x-rays)	150	150	?	10
I2	300	.8	3/30 mm	3/30 m	200
COSMIC	.4-.7 (vis)	1	5/50 mm	.005/.05 m	2×10^6
TAT	.4-.7 (vis)	.0005	?	.005/.05 m	$>10^6$
SOI/JPL	.1-1.5 (uv-ir)	.005	5 m	.001/.01 m	10^6
AST	.4-.7	.01	1/10 mm	.005/.05 m	5×10^4

continue

Table 2. FUTURE MISSION REQUIREMENTS - PRECISION OPTICAL SYSTEMS

<u>MISSION</u>	<u>OPERATIONAL WAVELENGTH</u>	<u>POINTING REQUIREMENTS ACCURACY</u>	<u>STABILITY</u>	<u>RESOLUTION FIG/ALIGN</u>	<u>CONTROL ATTENUATION REQUIRED</u>
VLBI	8.3 - 200 mm	145 rad	50 rad		10
EOS	8 - 16 mm	1.5 rad	1.5 rad	.8 - 1.6 mm	20
SETI	radio	.2 - 5 mrad			
ACTS	100 - 500 mm	2 mrad	2 mrad		<10

ent16666

Table 3. FUTURE MISSION REQUIREMENTS - LARGE ANTENNAS

Are pointing requirements (accuracy and stability) beyond the current state-of-the-art?

Additional criteria were also utilized to determine an optical focus mission. Of primary importance was the relative urgency of the mission. A relatively near-term mission would be of more interest for evaluating the benefits of utilizing optical components wherever practical. Since many of the large, flexible space systems with stringent pointing requirements are not envisioned for the near future (less than 10 yrs. to launch), this reduced the candidates substantially. Also, since the focus of this effort is to examine the alternatives or promising optical methods to perform sensing and control tasks, a system which is already relatively well-defined with conventional technologies is preferred to a system which is ill-defined at this point. This criterion is satisfied by the same four missions as the previous one with the addition of the interesting JPL/SOI mission.

A third criterion used was the perceived influence of control/structure interaction (CSI). NASA is very interested in this area and has put significant energy into CSI phenomena. Therefore, it would be beneficial to tie this study of optical methods into the larger picture of CSI-impacted missions. NASA, JPL, MIT, Cambridge Division of PRA, and others have identified missions which will be critically impacted by controls/structure interaction. With these three factors, the initial set of eleven candidate missions was narrowed to three. Although only LDR and EOS satisfy all three criteria, SOI was retained for further investigation because of the large available data base. The selection criterion for the missions is shown in Table 4.

Pertinent attributes of the three missions retained for further investigation are listed in the following text in order of study preference. LDR will be utilized as a baseline for the EO study. The text reflects that other very favorable missions for an analysis and comparison of optical sensing and processing technologies would include EOS and JPL's SOI.

Large Deployable Reflector (LDR) - moderately large optical system with near-term interest. May require control of many structural modes (potentially more than one thousand). Conventional control sensors and actuators will require a large amount of power and have a complex computational burden. Advanced electro-optic techniques appear promising for surface and segment alignment control.

Earth Observation System, Geostationary Platform (EOS/GP) - large to very large microwave antenna, depending on concept, between 15 and 200 meters.

<u>MISSION</u>	<u>NASA-DEFINED CSI DRIVER?</u>	<u>NEAR TERM?</u>	<u>SYSTEM RELATIVELY WELL-DEFINED?</u>
LDR*	Y	Y	Y
AXAF	N	Y	Y
I2	Y	N	N
COSMIC	Y	N	N
TAT	N	N	N
SOI/JPL	Y~JPL	N	Y
AST	N	N	N
VLBI	N	N	N
EOS*	Y	Y	Y
SETI	N	N	N
ACTS	N	Y	Y

0815448

Table 4. MISSION SELECTION CRITERIA

Extreme interest in mission. The proposed ultra-lightweight and flexible antennas require surface control or electronic compensation.

Spaceborne Optical Interferometer (SOI) - Although this mission does not have as much near-term interest as the other two, it provides some interesting characteristics including micro-precision control over a very large distance (100 meters). Conventional device concerns relate to the number of sensors and actuators required along with processing requirements.

3.0 LDR SYSTEM REQUIREMENTS

This section lists system requirements dictated by the scientific objectives selected for this system, and introduces the overall configuration of the system. The next section discusses the rationales for the major control system functions and then defines a strawman implementation of the control functions using "conventional" approaches, as a point of departure for the advanced electro-optic approaches which are the subjects of this study.

LDR, a joint effort between the Jet Propulsion Laboratory and the Ames Research Center, had its beginnings in 1977. Since that time, continuing studies by the two centers, industry, and universities resulted in a recommendation by the National Academy of Sciences that LDR be one of the two major space efforts in astronomy for the 1980's.

A workshop was held at Asilomar, California, in June 1982 at which approximately 100 scientists and engineers defined the scientific objectives of LDR and discussed its technical feasibility. The present conceptual design represents a consensus of ASILOMAR III and is a balance between technical feasibility in the 1980's and scientific capability.

The Large Deployable Reflector (LDR) is to be a dedicated astronomical observatory in space. It will operate in the $30\mu\text{m}$ to 1 mm wavelength region where the Earth's atmospheric opacity makes ground-based observations nearly impossible. The primary mirror will be 20 m in diameter, made up of 37 individual segments. The reflector will be actively controlled to provide an overall surface accuracy of $<2\mu\text{m}$. The LDR will be placed in orbit by the Space Shuttle and revisited at approximately two-year intervals during its ten-year lifetime.

Table 5 lists the major system parameters and requirements and Figure 3 illustrates a configuration of the main telescope elements. The balance of the spacecraft is not detailed, but contains the science packages to which the telescope image is delivered and other systems such as solar arrays, steerable communication antennas, attitude control system components, etc. Figure 4 shows an exploded view of the main optics train being considered for LDR, the quaternary mirror being a flat at the image of the primary mirror. The quaternary mirror is therefore convenient to use for the "chopping" function (a nodding motion of the look direction to permit background cancellation by data processing). It also has been suggested that correction of wavefront errors due to the primary mirror be done here.

Table 5. LDR PARAMETERS AND REQUIREMENTS

Primary mirror diameter	20 m
84 hexagonal segments	(91 less 7 central)
f/number	0.5-0.7
Optical form	Two stage
Field of view	3 arc min
Chopping frequency	2 Hz
Amplitude	1 arc min
System f/number	~ 10
Wavelength band	30-1000 μm
Diffraction limit	30-50 μm
Pointing accuracy	0.1 arc sec
Pointing stability (jitter)	.02 arc sec
Slew rate	20 deg/min
Scan rate	1 deg/min
Tracking rate	0.2 deg/hr
System natural frequency	3 Hz
Number of significant vibration modes	~ 1000
Primary structure surface	100 μm rms
Primary mirror tolerances	
Assembly manufactured WFE	1.5 μm rms
Mirror WFE unassembled	1.0 μm rms
Radius mismatch error	0.5 μm rms
Misalignment error	1.0 μm rms
Tilt error (each component)	0.6 μrad
Piston error	1.3 μm

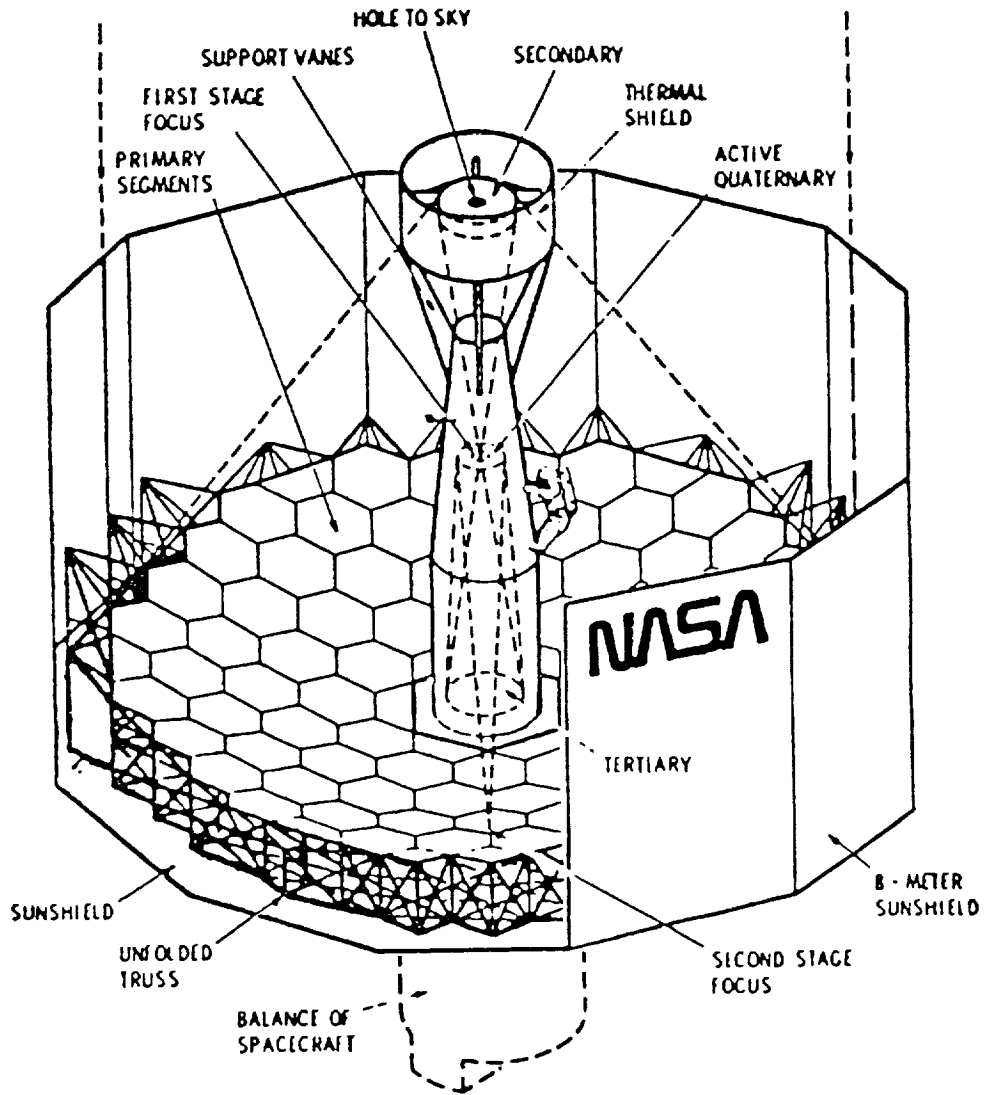


Figure 3. JPL LDR SYSTEM CONCEPT

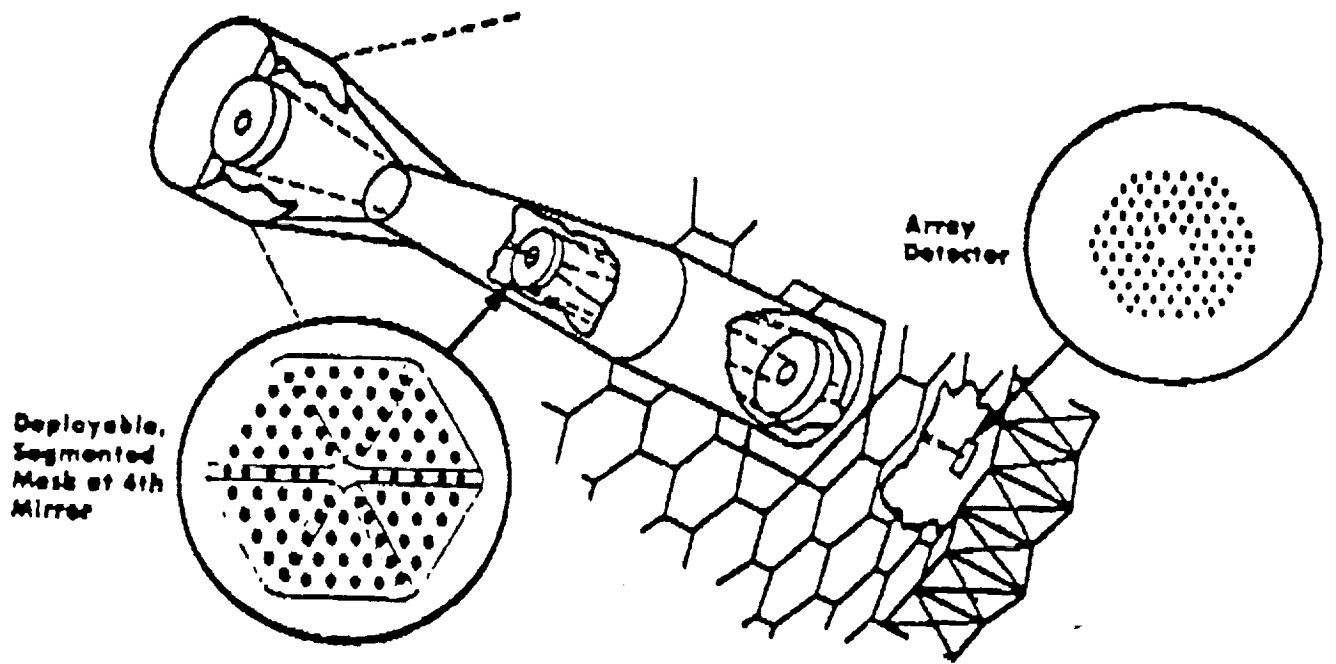


Figure 4. IN-LINE 2 STAGE LDR OPTICS

The major difference between this system and existing space systems is the size of the telescope and the use of a large number of segments. A major factor in its design is the requirement for chopping, done by nodding the quaternary mirror. The bottom line is that a complex multi-level control system is required, and its performance in maintaining a precise optical system, supported on a flexible structure, while disturbed by vibration sources, will be the subject of much new development work. Some of these issues are discussed further in the following section as an introduction to an outline of a strawman control system for LDR.

4.0 STRAWMAN LDR CONTROL SYSTEM

4.1 INTRODUCTION

As discussed in earlier sections, the LDR concept was chosen as a focus here because of the richness of its control requirements as well as its design possibilities. It also is preferable in that it is operationally closer to the optical wavelengths of the control devices of interest to this study, but sufficiently different that some of the larger wavelength issues are addressed as well. The configuration upon which the control is based relates most closely to the LDR concept of the ASILOMAR III, but always at this stage of a system evolution, the various controls are not necessarily refined and some overlaps and inconsistencies should be expected.

It is the intent in this section to present a preliminary outline for a "conventional" control system so that it becomes a strawman for the electro-optical computing alternates. The basic control systems are expected to include attitude and pointing control, structural mode control, vibration damping, optical form maintenance, and precision optical alignment. The first of these (attitude and pointing control) may use inertial or optical reference sensors, but they are not seen as advanced EO applications, and the actuators will be mechanical in nature; consequently this control system is of lesser interest and is dropped in favor of the remaining. These will be examined in terms of numbers of sensors/actuators, expected control bandwidth, range and resolution, and finally processor throughput.

4.2 OVERALL CONTROL SYSTEM APPROACHES

Since the primary structure surface (on which the mirror surface is supported) has a tolerance far larger than the mirror surface requirements listed in the table (Table 5), onboard sensors must measure the deviations of the optical system from its required configuration. It is prudent to do this with a primary wavefront error (WFE) sensor which measures the imaging performance of the overall telescope, and to augment this with secondary sensors which measure relative positions of individual mirrors and critical points on their supporting structures.

A specific rationale for further configuring the measurement and control systems is used in the following, with limited mention of alternates. This approach is a proper one for the purposes of this study, but it should be recognized that many other rationales not discussed here will be considered in the development of the LDR system.

The sources for errors in the figure of the optical system include, in addition to the initial structure configuration errors noted above, slow deviations such as are caused by aging and thermal changes, and structural vibrations. Structure vibrations are caused by the attitude control system, by any physical moving parts, such as refrigeration system components and communication antennas, by fluid transport or slosh, and can, as experienced in the Hubble Telescope, be initiated by small dimensional changes caused by abrupt changes in solar radiation.

The primary WFE measurement system will use a bright star as a reference object, and due to signal-to-noise limitations necessarily has a bandwidth well below the maximum vibration frequency components. Relatively long exposures are often required so vibrations must be controlled by other systems. The primary system also may have a narrow lock-in range, thus requiring some other system or mode of operation for coarse pre-alignment. In this approach, the primary system would be used intermittently, and during observations secondary systems would maintain the optics configuration.

The secondary system could also use a WFE system, but using on-board laser light with holograms on the primary mirror, assisted by auxiliary instrumentation to measure and control the non-common parts of the optical path. It is also possible that the secondary system does not measure WFE, but only measures positions of critical reference points in the system.

Data from a single star in one position in the field can in effect only correct one mirror, so if other mirrors are distorted or misaligned the optical resolution will be good only in the neighborhood of the reference star. Doing several runs with the reference star in several positions will check this, but separate instrumentation is generally required to maintain the positions and orientations of the smaller optical elements relative to the primary mirror. Methods to use data from more than a single star to achieve wide-field correction are complex and not required for this application.

A secondary WFE system could in principle have a wide enough bandwidth to provide inputs useful for controlling structural vibrations. The main problem is that the wavefront error along each light ray measured is a summation of errors contributed at each of a number of mirror reflections, and includes undesired components at the source and sensing end which are not parts of the functioning LDR telescope. If the entire system vibration model is known accurately enough, and if nonlinear and time-varying effects are small enough, it may be possible by data processing to separate the overall WFE measurements into the WFE components at each mirror, so that corrections can be made or the

vibrations can be damped out. However, even under these ideal conditions the measurements must include a time span related to the period of the lowest-frequency vibration, so the process tends to be limited in speed of response. The problem of knowing the system accurately enough is itself sufficient to justify depending on direct measurement of physical deflections for controlling vibration, rather than use indirect measurements by way of the telescope optical performance.

From these considerations, several approaches are considered for vibration control, and in essentially all large precision space systems a layered approach is considered. Individual continuous disturbances, such as motors and pumps, should be isolated at the sources. In addition, passive damping devices placed at many points in the structure are generally recommended. Much work has been done in deciding on the placement of passive and active damping components, in general concluding that members of the main structure that experience the largest vibration forces are good location candidates.

Active isolation and damping methods imply system complexity but may have significantly less weight. They also may be integrated with control of what should be the primary disturbance, which is the overall structural vibration remaining after repointing the LDR to a new observation direction.

It is generally recognized that we do not have sufficient knowledge about the micro-dynamics of structures being considered for large deployable precision space systems. The main body of modern control theory depends on representing the structure deformations as the summation of vibrational modes, whose force and deflections can be simply added to represent the overall system. The individual mode characteristics are obtained from linear finite element analysis, whose accuracy limits have been confirmed at convenient vibration amplitudes, and under stress conditions due to gravity in the laboratory. An overall integrated modern control system involving a large number of sensors and actuators can control (prevent or rapidly damp out) vibrations of a system with a large number of natural modes, provided that there are enough properly located sensors and actuators and that the system model used in the design of the controller is accurate. The problem is that, at the very small deflections which are critical for large optical systems, joints may behave differently from observations at larger deflections, so the system model is inaccurate, and the complex control scheme may not perform as required.

On the other hand, a distributed array of co-located sensors and actuators, primarily exerting local damping, do so rather independent of the overall structure, and so are "robust", in that performance does not degrade seriously

if the system varies from the model the controls designer used. This approach could be augmented by integrated control of the large-amplitude, low-frequency modes which are excited when repointing the system, since the low-frequency mode shapes will be best known. To further illustrate the problem, a sudden disturbance at a point on a large structure causes a wavelike motion to wash across a structure and then reverberate until damped. The description of this process for a modern-control controller requires treating it as the summation of hundreds of modes covering a wide band of frequencies, so that both the controller design and its performance assessment may be suspect when the structure model is not accurate, and if the real system at small amplitudes is nonlinear in a largely unpredictable way. The array of co-located sensors and actuators is much easier to design and to evaluate.

4.3 KEY DEVICES AND FUNCTIONS

Some specific sensors and actuators have been identified as candidates in the LDR work to date. These are included in the following strawman listings along with others likely to be employed.

4.3.1 SENSORS

- 1) Hartmann segment-slope sensor
128 x 128 detector array
- 2) Smartt interferometer
Assume 128 x 128 detector array, but this is conjecture, since, for example, it might have to operate at more than one wavelength to acquire control and reach 1 mm rms accuracy.

The above use a bright star as source, bringing the optics into precise alignment and figure. The following sensors assist in the precise alignment operation, and then during an observation, when a bright star is not available, must hold the figure without sensors 1) and 2).

- 3) Capacitance sensors between segment edges
relative piston displacements (2 per edge)
relative lateral displacement/rotation
- 4) Network of high precision ranging lasers
accuracy 0.1 mm two- or three-color to get absolute range 3 links, instrument package to tertiary 6 links, tertiary to

quaternary reference 6 links, quaternary reference to secondary multiple links (157), secondary to primary

- 5) Network of 3-axis accelerometers
 - 1 on instrument package
 - 3 on tertiary
 - 3 on quaternary reference
 - 3 on secondary
 - 15 on primary
 - 12 on sunshade
 - 6 on rear cylindrical equipment structure
 - 12 on solar arrays

4.3.2 ACTUATORS (SLOW-ACTING EXCEPT WHERE NOTED)

- 1) Tertiary mirror, 5-DOF (degrees of freedom)
- 2) Quaternary mirror reference, 3-DOF
- 3) Quaternary counterbalanced steering, 2 Hz motion, 2-DOF
- 4) Secondary mirror, 5-DOF (20 Hz bandwidth)
- 5) Each primary mirror segment
 - 7 deformable mirror actuators between mirror faceplate and the segment's backplane
 - 6 actuators between segment backplane and primary mirror support structure
- 6) Proof-mass active vibration dampers
 - 200 Hz bandwidth
 - 3-DOF, at each accelerometer
- 7) Structure main-strut extenders
 - 20 Hz bandwidth
 - very stiff, small displacement
 - 12 in sunshade trusses
 - 6 in primary support structure
 - 6 in rear cylindrical equipment structure
 - 6 in solar arrays
- 8) Reaction wheels
 - 6 sized for repointing and initial settling (locked during measurements)
 - 6 sized for fine control during measurements

4.4 MAJOR CONTROL SYSTEMS

The above sensor and actuator complement can be configured to operate in four interrelated control functions, treated separately as follows.

4.4.1 PRECISION OVERALL OPTICS ALIGNMENT

(Ignoring 3 non-critical DOF for each segment)

128 x 128 detectors in Hartmann sensor	
128 x 128 detectors in Smartt interferometer	
420 segment edge sensors	
30 ranging laser links	33218 sensors
84 x 3 segment position actuators	
84 x 7 segment figure actuators	
5 secondary mirror actuators	
5 tertiary mirror actuators	
3 quaternary mirror actuators	853 actuators

Convergence time can be many seconds or minutes. Data rate varies greatly due to extensive data averaging.

4.4.2 OPTICAL FORM MAINTENANCE

(Ignoring 3 non-critical DOF for each segment)

420 Mirror segment edge sensors	
30 ranging laser links	450 sensors
84 x 3 segment actuators	
5 secondary mirror actuators	
5 tertiary mirror actuators	
3 quaternary mirror actuators	265 actuators

Full-blown output controller per Ref. 3 would call for 238,000 operations/sample.

Since matrices are very sparse, actual processing load would be far less, much of it could be done at 1 Hz. Some (secondary mirror, for example) may be integrated into structure mode controller at 20 Hz rate. 2 Mflops are required.

4.4.3 STRUCTURE MODE CONTROL

55 3-axis accelerometers	165 sensors
6 3-axis reaction wheels	
30 main-strut axial-motion actuators	48 actuators
20 modes controlled using a general mode controller (Ref 3)	
	12580 Operations/sample

5 to 50 Hz modes controlled
6.5 Mflops required

500 samples/sec
(13 Mflops if estimator
used)

4.4.4 VIBRATION DAMPING

55 3-axis accelerometers	165 sensors
55 3-axis proof-mass active dampers	165 actuators
Bandwidth 0 to 200 Hz	
Individual small local controllers	(analog or digital)

4.5 SUMMARY

The above information provides a general indication of the magnitude and complexity of the control systems, making plausible assumptions, and omitting many significant aspects, in order to provide a strawman for determining applications and rough requirements for using new EO technology in future NASA missions. Clearly there is an accelerating trend toward requiring large numbers of sensors and for intelligent data processing and control systems.

5.0 ASSESSMENT OF TRADITIONAL TECHNOLOGY

The following section describes the state-of-the-art traditional processor, sensor, and actuator technologies used for flexible spacecraft control.

5.1 SOA ELECTRONIC PROCESSING TECHNOLOGY

Conventional computer processor technology is still rapidly evolving. In addition, processors can be tailored to very specific applications. These two factors make a comprehensive state-of-the-art survey difficult. Therefore, major features and trends will be highlighted and two specific processors being utilized by the government will be examined in detail. Following is a brief background discussion of "signal processors" adapted from a discussion found in Reference 1.

Signal processors were developed in the late 1960's as a result of military requirements for computer-based sonar and radar systems. Sylvania built the first programmable digital signal processor to replace a set of analog machines. The processors were more reliable, adaptable, and smaller than their analog predecessor. The second generation of signal processing equipment was developed by SPS, CSPI, and IBM in the early 1970's. These processors were more powerful and less costly than first-generation machines and the government was the main buyer. Processors of the 1980's are referred to as "signal processors" and "array processors." The digital signal processors of the 60's and 70's were usually stand-alone units which replaced more costly, less flexible, and less reliable analog devices. They performed calculations, usually multiplications and additions, strung together to form a difference equation. The calculations were typically on real-time data collected by A/D converters. Current "array processors" are usually peripherals used to increase the computational throughput of their host minicomputers or mainframes. With vastly increased memory and speed capabilities, several processors can now be utilized as integrated computer/processors.

To achieve high throughput rates, most processors now use some combination of parallel and serial processing to perform calculations. There are many different internal architectures for processors with as many design philosophies and performance capabilities as there are applications. Some processors are internally synchronous, other asynchronous. Some utilize numerous, independently programmable processing units, with separate registers, program counter, and memory, while others operate with a single master control unit and an arithmetic processing unit with global program and data memories. Some use independent data and program buses while others use a common program/data bus. All of these

factors must be evaluated when determining a processor for a specific application. Besides the standard issues of speed, size, and memory, space applications require environmental compatibility and high reliability (including fault tolerance).

The two processors examined in detail for this survey are the AC-100 by Integrated Systems Inc. and the MAST 1750A computer by SCI Technology Inc.. The AC-100 is presently being used by the Air Force in its SPICE ground-testing program and by the Boeing Aerospace Company. The MAST computer is being implemented at NASA Langley in its SS/CEM laboratory.

Following is a brief description of the AC-100. Further details can be obtained from the manufacturer in the Vendor List provided at the end of this section.

The AC-100 is an automatically-programmable real-time control system for both design and process control. The system consists of an engineering workstation connected to a high speed, real-time controller which runs ISI software (the MATRIX_x, AutoCode line). Autocode allows graphical specification and simulation of real-time systems. Implementation code in C or Ada can then be automatically generated. The Controller is a 80386-based multi-processor system with up to 10 computational processors performing parallel real-time computations at throughputs of up to 40 MIPS. Local and remote I/O options are available for either laboratory or production (space) applications.

The AC-100 allows designers to specify their system in terms of block diagrams or animated graphical representations, simulate performance, and implement the designs on a high performance, real-time controller. To use the multi-processor configurations, the user specifies the number of processors and their respective task assignments.

The AC-100 hardware consists of a design and monitor workstation, a real-time computer, and an optional I/O subsystem. Software design and real-time monitoring is performed on a VAXstation 3100 with a 19" color monitor running VMS. The real-time target computer uses a Multibus II backplane. The processor cards are based on an Intel 80386 processor with Weitek 3167 and Intel 80387 coprocessors. One Mbyte of random-access memory is available on the board for real-time code and data storage. The 40 Mbyte high-speed backplane allows high-speed parallel computations in a tightly coupled configuration of up to 10 processors. Table 6 compares the computational capability of the AC-100 to other processors and provides a set of specifications for operation of the AC-100.

Table 6. AC-100

Software Capability	Hardware Capability and Options
<p>The software integrated into the AC-100/AC-100A has the following capabilities:</p> <ul style="list-style-type: none"> • ISI AutoCode GPE Software: Block diagram modeling, simulation and automatic code generation • ISI MATRIX_x Software: Engineering analysis, control design, advanced system identification and signal processing, and simulation acceleration. For detailed description see the MATRIX_x and AutoCode brochures. • Interactive Animation: ISI software that allows for realistic application representations; animated simulation from design files; process monitoring and control. • ISI Multi-Board Implementation software. Handles all timing constraints, parallel tasks, topological specification, and other necessary information to allow AutoCode software to run in a parallel processor environment (AC-100) • C Compiler and Cross Compiler tools (AC-100) • Ada Compiler and Cross Compiler tools (AC-100A) 	<p><i>Base System</i></p> <ul style="list-style-type: none"> • Design Workstation <ul style="list-style-type: none"> - VAXStation 3100 with VMS Operating System - 19" Color Screen - 8 MB RAM - 2 105 MB Hard Disks - Cartridge Tape Unit • Real-Time Hardware <ul style="list-style-type: none"> - 80386 Processor Card with Weitek 3167 Coprocessor (AC-100) - 80386 Processor Card (AC-100A) - Multibus II backplane - High Speed 16-Channel Input/10-Channel Analog Output - 32 Parallel Digital - Ethernet Interface <p><i>Controller Board Options (AC-100)</i></p> <ul style="list-style-type: none"> • 80386 Processor (up to 10) <ul style="list-style-type: none"> - Weitek coprocessor - Multi-Board Implementation Software <p><i>I/O Options</i></p> <ul style="list-style-type: none"> • Optically Isolated Analog Digital Input/Output • Additional options as described in Table 2
<p>• AC-100A is a Ada Code implementation of the system</p>	

Processor Type	Relative Throughput
8086/8087 at 8 Mhz	1x
68020/68881 at 20 Mhz	3x
MicroVax	5x
AC-100 (one processor)	20x
VAX 8600	25x
AC-100 (ten processors)	150x

AC-100, AutoCode, and Multi-Code are trademarks of Integrated Systems Inc. MATRIX_x is a registered trademark of Integrated Systems Inc.

Multibus II is a trademark of Intel Corporation VAXStation 3100 is a trademark of Digital Equipment Corporation.

© 1988 Integrated Systems Inc. All rights reserved.

The Multi-processor Architecture Space Technology (MAST) 1750A computer, built by SCI Technology, Inc., is a general purpose computer designed for high reliability space and launch vehicle applications. It features a CMOS-SOS VLSI processor and radiation hardened Application Specific Integrated Circuits (ASIC's) as the core of its fault-tolerant design. The architecture uses the MAST Bus Interface (MBI) Standard Cell ASIC. Each processor, memory, or I/O module interfaces to the MAST System Bus through an MBI. The MBI is configurable to provide either a Bus Controller function or a Bus Responder function. The MAST architecture supports multiple processor modules which can allow for higher throughput and redundancy.

To provide fault tolerance, the computer uses extensive error detection and correction circuitry on all internal data buses and memories. Also included are multiple EDAC checking circuits, a watchdog timer, and two types of parity on the Memory Management Unit Page RAM. The specifications and features of the computer are listed in Table 7.

Table 7. MAST 1750A COMPUTER

FEATURES	SPECIFICATIONS
MULTIPLE PROCESSORS	PROCESSORS:
FAULT TOLERANT SYSTEM:	One to Eight MIL-STD-1750A CPUs with Memory Management Units Over 600 KIPS (DAIS Mix) per 1750A CPU 20 Megaflop Vector Processor Module
Bus Architecture capable of supporting Single, Dual or Multi CPU configurations	CLOCK RATES:
Single Error Correction/Double Error Detection on Memory and Data Buses	10 or 20 MHz
Isolated memory address spaces	INTERRUPT LEVELS:
Automatic page fault substitution (4K pages)	16 total (9 externally available, 7 internal)
Built-in Self Test	MEMORY
REAL-TIME OPERATING SYSTEM	(16-bit words): Up to 1 Megaword directly addressable 64K Radiation-hardened RAM Module 256K Non-radiation-hardened RAM/ROM Module 1K x 64 Trace Debugger Memory for real-time debugging on each CPU Module
RADIATION HARDENED:	PHYSICAL CHARACTERISTICS:
CMOS/SOS MIL-STD-1750A CPU Hardened ASICs and Page RAM	Size: 8.56" x 6.5" x 10.5" Standard 8.56" x 6.5" x 8.12" Mini Weight: 20 pounds (typical Standard configuration) Power: 25 watts single processor active nominal 5 watts sleep mode
MEMORY PROTECTION:	ENVIRONMENTAL:
Write Protection in 4K blocks Redundant MMU Page RAM with parity	Temperature: -55 to +70 C conductively cooled via baseplate Vibration: Random 14 gRMS all three axes Radiation: 1 x 10 ⁵ Rads (Si) total dose Meets MIL-STD-1540B requirements
INPUT/OUTPUT:	
Analog Input Module Discrete I/O Module Serial-digital Interfaces Module MIL-STD-1553B Interface Module SCI bus Fault-tolerant Serial Data Bus Module Dedicated Command/Status Interface RS-422 Serial Console Interface	
CONSOLE DEBUGGER:	
Supports Ada or JOVIAL Real-Time Debugging on Multiple CPUs	
GROUND SUPPORT EQUIPMENT:	
Performs automatic Functional Testing	

5.2 SOA CONVENTIONAL SENSOR TECHNOLOGY

Following is a description of each of the sensors summarized in Table 8. The intent here is not to fully describe the physics or operating principles behind each of these devices, but rather to give an overview of the technology where appropriate or highlight the features of each sensor. The most complete details on each device can be obtained from the manufacturers listed at the end of this section.

Accelerometers - High performance, inertial grade space accelerometers are extremely precise and exhibit good frequency response from dc to about 50 Hz bandwidth. They provide inertially referenced measurements with low drift and very small weight and size. While very precise devices are quite expensive, lower grade instruments are relatively inexpensive.

Capacitive Probes - These devices operate on the principle that the capacitance varies with the displacement between two plates. The drive electronics provide an output voltage proportional to displacement. The capacitive probe has good frequency response and linearity, no moving parts, is relatively inexpensive, and is very small and light. Measurement with capacitive probes is restricted to small amplitude vibration, thereby making them particularly useful for measuring length changes in individual bars of a structure.

Gyroscopes - Electromechanical (free rotor, tuned rotor, gimbaled, electrostatic) - The inertial grade space gyro has the same basic advantages and drawbacks of the inertial grade space accelerometer. Measurements are inertially referenced with low noise and drift. The more precise instruments are very expensive and contain a large number of moving parts, raising concerns about reliability and life.

Non-gyroscopic (ring laser gyros, fiber optics) - These devices utilize the difference in space or time it takes for a split light beam to traverse a distance. These sensors have a much higher bandwidth than conventional gyroscopes and are still relatively small and lightweight. Because these devices have fewer moving parts, they are highly reliable. They are generally expensive.

Interferometry - Laser interferometers provide very precise, non-contact measurements over a wide spectrum of operating distances. They have no moving parts but are quite expensive.

Table 8. CONVENTIONAL SENSORS

	BANDWIDTH	RESOLUTION	SIZE/MASS	COMMENTS	MANUFACT.
Accelerometers	<50 Hz	10^{-5}m/s^{-2}	2x2x1 in/.1-2kg	small, inexpensive, low drift	CSDL, Bell, Kearfott
Capacitive Probes	0-100 KHz	10^{-6}m	very small (10's of mm)/.5kg	good frequency response + linearity, no moving parts, inexpensive	ADE
Fiber Optics	>1 KHz	10^{-6}m	/.5kg	limited availability	
Gyroscopes Gyroscopic-free rotor, gimballed electrostatic	30 Hz	10^{-6}rad/s	1x1in/.1-1 kg	high cost, many moving parts	CSDL, Litton, Northrop, Kearfott
Ring laser, fiber optic	>1 KHz	10^{-6}rad/s	inches/1-3kg	expensive	Honeywell, Litton
Interferometry				high precision, non-contact, expensive, fragile, high power	
Jitter Measurement Unit	2-2000 Hz	$10^{-6}-10^{-9} \text{ rad}$	small	must couple with gyro to get low freq. output	
Linear Variable Differential Transformers (LVDT)	DC-500 Hz	10^{-7}m	very small (20x50mm typ)/.05kg	small, lightweight, inexpensive	Schaevitz
Ronchi Wavefront Sensor	>1 KHz	10^{-6}m			
Six-Axis Space Sensor (SASS)	.1-100 Hz	.001-1 μm .01- μrad			CSDL
Spatial High Accuracy Position Encoding Sensor (SHAPES)	.1-10 Hz	$10^{-4} \text{m}, 10^{-5} \text{ rad}$			

	BANDWIDTH	RESOLUTION	SIZE/MASS	COMMENTS	MANUFACT.
Strain Gages	> KHz	$<10^{-7}$ m	very small (mm)/1g	low cost, reliable, light small, thermally sensitive	
Surface Accuracy Measurement System (SAMS)	1 KHz	10^{-7} rad	/2kg	high precision, non-contact, electronically complex	TRW
Velocity Transducers	0-600 Hz	10^{-4} m/s	1-2cm x 8-100cm/20-1000g	small, light, lower precision, inexpensive	TransTek, Schaevitz
Optical Radar	>1 KHz	10^{-3} m	/heavy	complex electronics	
Piezoelectric Accelerometers	5-10,000 Hz	.02g	/1g	small, light, no moving parts, inexpensive, wide variety	PCB, Endevco, BBN Inst.
Force Transducers	0-300 KHz	.02g	/8g		PCB, Kistler

Strain Gages - These simple devices are extremely light weight and low cost. They contain no moving parts and are extremely reliable. They are sensitive to thermal variations and require temperature control and/or calibration. Strain gages also require periodic recalibration.

Surface Accuracy Measurement System (SAMS) - This optical measurement system was developed by TRW for measuring the accuracy of the shapes of space-deployable radar antennas. The system measures tangential excursions of an illuminated light-emitting diode with great precision. There are no moving parts and it is a non-contact method of measuring displacement in two dimensions.

Velocity Transducers - Velocity transducers operate on the principle that a permanent magnet moving through a coil of wire induces a voltage in the coil proportional to the velocity. The devices are small, light and relatively inexpensive. They have good frequency response to about 500 Hz and require no excitation power. Typical velocity transducers are not sensitive enough to measure very small amplitude vibrations, though seismic instruments can measure velocities as low as 3-10 micrometer/sec but are expensive.

Piezoelectric Force Transducers - This device is small, light, has no moving parts, and is inexpensive. It has a very broad frequency bandwidth and provides a relative measurement.

Ronchi Wavefront Sensor - These sensors utilize a series of transparent and opaque lines across the telescope's focal plane thus modulating the signals to sensors located beyond the ruling. The distance between the images is determined grossly by the number of lines between images and by comparing the relative phases of the modulated signals.

Spatial High Accuracy Position Encoding Sensor (SHAPES) - SHAPES provides a multipoint, three dimensional position sensor with sub-millimeter accuracy. It combines high speed EO technologies with CCD star tracker technology to determine the range to multiple retro-reflectors based on time-of-flight correlations of short laser pulses. The primary components of the ranging system consist of the laser diode, the retro-reflecting targets, and the streak tube camera with its CCD sensor and readout electronics. A second CCD is used to measure the angular displacement of the targets. Combining the information from both CCD's provides the angular location as well as the range along the line-of-sight.

Linear Variable Differential Transformers (LVDT) - LVDT's operate on the electromagnetic efforts between two surfaces to measure displacement. The RVDT

is a rotary version. LVDT's are small, light, relatively inexpensive, and have very good frequency response to 500 Hz.

Optical Radar - The radar signal is used as input to an acousto-optic modulator. The grating set up by the modulating acoustic wave modulates a beam of light which then can be processed optically.

Piezoelectric Accelerometers - These accelerometers are small, light, and relatively inexpensive. Frequency performance is good above 5 Hz or so, up to 100 kHz, making them much higher bandwidth than inertial accelerometers. There are no moving parts and the measurement is inertially referenced.

A summary of the conventional sensors is contained in Table 9.

Table 9. CONVENTIONAL SENSORS, OVERVIEW SUMMARY

	BANDWIDTH	RESOLUTION	SIZE/MASS	COST
Accelerometers	Low	High	Small/Light-Mod	High
Capacitive Probes	High	High	Small/Light	Low
Fiber Optics	High	Med-High	Light	Medium
Gyroscopes Gyroscopic Ringlaser, fo	Low High	High High	Small/Light-Mod Small/Mod-High	High High
Interferometry		High		High
Jitter Measurement Unit	High	High	Small	High
LVDT	Medium	Med-High	Very Small/Ext. Light	Low
Ronchi Wavefront Sensor	High	High		
Six-Axis Space Sensor	Medium	High		Proto- type/ High
SHAPES	Low	Med		
Strain Gages	High	High	Very Small /Light	Low
SAMS	High	High	Med/Heavy	Proto- type/ High
Velocity Transducers	Medium	Low-Med	Small/Light	Low
Optical Radar	High	Low-Med	Heavy	
Piezoelectrics Accelerometers Force Transducers	High High	High High	Small/Light Small/Light	Low Low

5.3 SOA CONVENTIONAL ACTUATOR TECHNOLOGY

Following is a brief description of conventional actuator technology. The intent here is not to provide a complete discussion of the physics or operating principles of each device but rather to provide a highlight of the benefits and disadvantages of each instrument. More detailed information can be obtained from the vendor list at the end of this section. The performance characteristics of the conventional actuators are contained in Table 10.

Control Moment Gyro - A control moment gyro is a single or double gimballed constant-speed spinning rotor in which control torque is generated due to the change in spin axis orientation as the gimbals are rotated. The control torque magnitude is proportional to both rotor angular momentum and gimbal rotation rate. Single gimbal CMG's produce large torques about an axis perpendicular to both the gimbal axis and the rotor spin axis, producing a torque vector that rotates with the rotor spin axis with respect to the spacecraft body. Typical implementations utilize several CMG's and partition the control actuation amongst them.

Electromagnetic/Electromechanical - This category encompasses all types of electric motors - rotary, linear, stepper, torque, moving coil, moving iron, etc. For most aerospace applications, dc motors are preferred over ac motors because of power supply considerations. DC torque motors operate in continuous motion, while dc stepper motors move in discrete angular jumps, i.e. stepping angles. Stepping angles have a range that varies from a few degrees to as much as 90 degrees. There is typically an upper limit to stepping rate. The bandwidth of a dc motor varies with the moment of inertia of its load, and is limited by the fundamental torsional frequency of the load/shaft/armature combination. A motor is usually used in conjunction with a gear train or lead screw arrangement. For optimum performance, motors require ample cooling which is difficult to provide in the space environment. In addition, motors consume a large amount of power.

Reaction Momentum Wheels - Reaction and momentum wheels are motor-driven inertia or flywheels whose spin axis is fixed to the spacecraft body. A momentum wheel is controlled to spin at a constant spin rate to provide a momentum bias. A reaction wheel applies torque to the spacecraft about the spin axis in a direction opposite to the torque applied by the motor to spin up the inertia wheel.

Thrusters - These devices are available in a variety of sizes ranging from thrusts of a fraction of a newton to hundreds of newtons. Cold gas thrusters involve the physical expansion of a single gas. Hot gas, monopropellant

Table 10. CONVENTIONAL ACTUATORS

	BANDWIDTH	RESOLUTION	RANGE	FORCE LIMIT	COMMENTS	MANUFACT.
Control Moment Gyros	>1 KHz					
Electromagnetic Moving Coil	1 KHz	$<10^{-6}m$	$10^{-3}m$	30N	designs for very large range of applications	Bendix, Honeywell
Moving Iron	200 Hz	$10^{-5}m$	$10^{-2}m$	120N	high power	
Electromechanical Rotary	10 Hz	$5 \mu rad$	continuous	1N-m	low power	
Linear	10 Hz	$10^{-7}m$.2m	1000N	readily available relatively inexpensive	
Fluidic	1 KHz	$10^{-6}m$.2m	>5000N		
Hydraulic	150 Hz	$10^{-7}m$.2m	250N	relatively heavy	
Piezoelectric Crystal	0-10 KHz	1N-m	$10^{-6}m$	4.5kg	small (cm), .5kg, high voltage	Burleigh
Inchworm		$10^{-6}m$	$10^{-3}m$	1.5kg	2kg	Burleigh
Peristaltic		13 N-m	$10^{-2}m$	10N	2 kg, small size	Perkin-Elmer
Reaction/Momentum Wheels					can be tailored to specific app.	Bendix, RCA, GE, TRW
Thrusters	NA				nonlinear (on/off)	TRW, Martin, Rocket Research
Voice Coil	1 KHz	$10^{-7}m$	$10^{-5}m$	50-150N	high power	Kimco

thrusters involve a hot chemical reaction of a single gas with a solid catalyst. Hot gas, bi-propellant thrusters involve a hot chemical reaction between two gases; a fuel and an oxidizer. Electric thrusters involve the ionization of a solid fuel by means of an electric arc. Compared with other torque actuators, a thruster pair can provide greater torque for the same cost. A reaction thruster typically has limits on switching rates and fuel supply. Most thrusters are non-linear devices: either on or off, thereby complicating control laws. Thrusters and their associated support equipment are moderately expensive.

Hydraulic - These actuators work on the principle of a pressurized fluid. Typically the bandwidth is moderate with good resolution. In general, these devices are heavy and on-orbit operation is difficult due to fluid flow concerns.

Piezoelectric Crystal - The single crystal consists of a quartz crystal which elongates when a voltage is applied to it. Deflections in both directions can be obtained by preloading the crystal and applying a bias voltage.

Inchworm - The inchworm actuator is comprised of a shaft which travels through three connected piezoelectric sleeves. The two outer sleeves are capable of gripping and releasing the actuator shaft. The inner sleeve is only capable of elongation. The three sleeves are independently switched on and off in sequence so as to feed the shaft in one direction. Reversing the switching sequence causes motion in the other direction.

Peristaltic - The peristaltic actuator consists of ten narrow, grip/release sleeves fitted adjacent to one another along the actuator shaft. Like peristaltic muscles in the human body, the piezoelectric sleeves grip and release the shaft in sequence, starting at one end and working towards the other. Two sleeves grip the shaft at any given time. Poisson elongation of the shaft material results in the shaft being fed slowly in one direction.

Piezoelectric actuators - The piezoelectrics provide extremely high resolution, excellent frequency response, and high reliability at a moderate cost. Inchworms and peristaltic actuators are capable of extra long travel. Drawbacks of these devices include high voltage operation resulting in the need for heavy switching mechanisms and power supplies. Many of these devices are limited in their speed or load-bearing capacity. Hysteresis effects may drastically reduce their accuracy.

A summary of the actuator technology is shown in Table 11.

Table 11. CONVENTIONAL ACTUATORS - OVERVIEW SUMMARY

	BANDWIDTH	TORQUE/FORCE LIMIT	COST
Control Moment Gyros	High	High	High
Electromagnetic (Moving Coil)	High	Medium	Low
Electromagnetic (Moving Armature)	Medium	Medium	Low
Electromechanical (Rotary)	Low	Low	Low
Electromechanical (Linear)	Low	High	Low
Fluidic	High	High	Medium
Hydraulic	Medium	High	Medium
Piezoelectric Crystal Inchworm Peristaltic	High	High	Low
Proof-Mass	Medium	High	High
Reaction/Momentum Wheels	Low	Medium	High
Thrusters	High	High	High
Voice Coil	High	Low	Low

VENDOR LIST

<u>Vendor</u>	<u>Products of Interest</u>
ADE Corporation 77 Rowe Street Newton, MA 02166 (617) 969-0600 Contact: Mary Thwarta	Capacitive Probes
Burleigh Instruments, Inc. Burleigh Park Fishers, NY 14453 (716) 924-9335 Contact: Timothy Van Slambrouck	Piezoelectric Actuators, inchworm motors/actuators, interferometers
Integrated Systems, Inc. 2500 Mission College Boulevard Santa Clara, CA 95054-1215 (408) 980-1500 Contact: Douglas Case	Processors
Kistler Instrument Corporation 75 John Glenn Dr. Amherst, NY 14120 (716) 691-5100 Contact: Richard Cadille	Piezoelectric force, pressure, and acceleration measurement devices
PCB Piezotronics, Inc. 3425 Walden Ave. Depew, NY 14043-2495 (716) 684-0001 Contact: Dave Jaros	Accelerometers, piezoelectric force and pressure transducers
Schaevitz Engineering 7905 North Route 130 Pennsauken, NJ 08110-1489 (609) 662-8000 Contact: Robert Yaffe	LVDT's, RVDT's, RVIT's, accelerometers, magnetostrictive linear displacement transducers
SCI Technology, Inc. 2109 West Clinton Ave. Huntsville, AL 35805 (205) 882-4202	Processors
Trans-Tek Incorporated P.O. Box 338 Rt. 83 Ellington, CT 06029 (203) 872-8351 Contact: William Padin	LVT's, LVDT's

6.0 ASSESSMENT OF ADVANCED OPTICAL PROCESSING MATERIALS, DEVICES, AND APPLICATIONS.

The following section contains a survey and assessment of advanced optical technologies. The section begins with a discussion of electro-optic materials including photorefractive crystals, semiconductors, and nonlinear optical polymers. The discussion details the current capability as well as the future potential of these materials for implementation in NASA spacecraft control applications. Several advanced technology electro-optic devices are then introduced; spatial light modulators, optical computers, optical correlators, neural architectures, as well as state-of-the-art charge-coupled devices (CCD's). Their application to NASA control implementation is discussed. In general, photonic materials and devices can still be considered to be in the basic research stages of development. The technologies are starting to emerge from the laboratory. Their demonstration in "real" systems will greatly assist in their development and will help promote their characterization and refinement.

6.1 MATERIALS

It has been expressed in the photonics community that there is a need for a material similar in function to what silicon is for the electronics industry. This material has been referred to as an "optical silicon"; a single material in which sources, threshold arrays, volume holographic optical elements, and optoelectronics integrated circuits can be developed. To date, no single material has been developed which can serve these needs. Three promising materials areas that are described in the following sections are photorefractive materials, nonlinear organic polymers, and semiconducting materials such as gallium arsenide and indium phosphide. To date, each material area has shown promise for various applications, but no one material has emerged which is a "clear-cut" choice for fulfilling the needs of "real-world" applications.

Inorganic crystals are presently the most widely used nonlinear optical materials, representing 77% of the total market [2]. The compound semiconducting materials such as gallium arsenide are used as photonic devices because of the technology leverage from the microelectronic industry as well as the ability of such semiconductors to operate in the infrared spectral region. Operating in the infrared spectral region allows the materials to operate with semiconductor injection lasers; a desired characteristic. More important is the ability of the compound semiconductors to operate with nanosecond response times; orders of magnitude faster than the photorefractive crystals.

The performance deficiencies (slow response time, low diffraction efficiencies) of photorefractive crystalline materials have spurred the development of organic materials. Because of their high nonlinear response coefficients (greater than 35 pm/V) and potentially high optical qualities, organic materials have received increased attention over the last several years. The organic materials are expected to be in commercial use by 1995 and are expected to earn a considerable market share thereafter [3].

6.1.1 PHOTOREFRACTIVE CRYSTALS

There has been a considerable amount of research given to the development of photorefractive materials. Photorefractive crystals such as bismuth silicon oxide (BSO) and barium titanate (BaTiO_3) have been actively researched for several decades and the majority of real-time proof-of-concept systems have been demonstrated with these materials. Despite the experience gathered using these photorefractive materials, there has yet to emerge a well characterized, stable, producible, fast, and large magnitude of response material. Despite the attention given to materials such as BSO and BaTiO_3 , each has limiting performance characteristics such as the magnitude of response (as is the case with BSO) or speed (BaTiO_3). Both are difficult to process and control, their performances are sensitive to environment, and it is difficult to tailor their characteristics for a desired response. Theoretically the storage capacity of these materials is on the order of $10^9 - 10^{12}$ bits/cm³, which corresponds by means of the thick holograms' properties, to a theoretical ability to store several hundred holograms in a single one cubic centimeter crystal.

The photorefractive crystals can be separated into two groups of materials; the ferroelectric crystals which include BaTiO_3 , SBN, KNbO_3 , and LiNbO_3 , and the cubic crystals and non-ferroelectrics, which include BSO and bismuth germanium oxide (BGO). A list of the characteristics of the ferroelectrics is shown in Table 12 [4]. A list of the properties of the cubic and non-ferroelectrics is shown in Tables 13a and 13b [4]. Due to their large electro-optic coefficients, resulting in a large photo-induced index change, the ferroelectric materials have a large magnitude of response. From the table, it can be seen that BaTiO_3 has an EO coefficient of 1640 pm/V and LiNbO_3 of 32.6 pm/V. In order to obtain large value electro-optic coefficients in these crystals, special processing must be performed. This can include poling the material first by heating it above its Curie point and then allowing it to cool to room temperature. In addition to a large magnitude of response, only some ferroelectrics have storage times on the order of days or months. The primary drawback of the ferroelectric materials is their slow response in reaching steady state. They thus are slow to form holograms. This is due to their high DC dielectric constants (3600 for

<u>SUBSTANCE</u>	<u>SYMMETRY</u>	<u>WAVELENGTH</u>	<u>e-o COEFFICIENTS</u>	<u>INDEX OF REFRACTION</u>	<u>DIELECTRIC CONSTANT</u>
BaTiO ₃	4mm	0.546 μm	r ₅₁ = 1640 r _c = 108	n _o = 2.437 n _a = 2.365	ε ₁ = 3600 ε ₂ = 135 ε ₃ = 135
BaSrNbO ₆	4mm	0.633 μm	r ₁₃ = 67 r ₃₃ = 1340	n _o = 2.3117 n _a = 2.2987	ε ₃ = 3400
LiNbO ₃	3m	0.633 μm	r ₁₃ = 9.6 r ₂₂ = 6.8 r ₃₃ = 30.9 r ₃₅ = 32.6 r _c = 21.1	n _o = 2.286 n _a = 2.200	ε ₁ = 78 ε ₂ = 32 ε ₃ = 32
KNbO ₃	2mm	0.633 μm	r ₄₁ = 6.6 r ₅₂ = 6.0 r ₆₃ = 6.0	n ₁ = 1.840 n ₂ = 1.984 n ₃ = 1.960	
LiTaO ₃	3m	0.633 μm	r ₁₃ = 8.4 r ₃₃ = 30.5 r ₂₂ = 0.2 r _c = 22	n _o = 2.176 n _e = 2.180	ε ₁ = 51 ε ₂ = 45 ε ₃ = 45
		3.39 μm	r ₃₃ = 27 r ₁₃ = 4.5 r ₅₁ = 15 r ₂₂ = 0.3	n _o = 2.060 n _e = 2.065	

Table 12. FERROELECTRIC NON-LINEAR MATERIALS

Table 13a. CUBIC NON-LINEAR MATERIALS

<u>SUBSTANCE</u>	<u>SYMMETRY</u>	<u>WAVELENGTH</u> <u>m</u>	<u>e-o COEFFICIENT</u> <u>r_{1k} (10⁻¹²m/V)</u>	<u>INDEX OF REFRACTION</u> <u>n_i</u>	<u>DIELECTRIC CONSTANT</u>
Bi ₁₂ GeO ₂₀	23	0.666	r ₄₁ = 3.22	n = 2.54	
Bi ₁₂ SiO ₂₀	23	0.633	r ₄₁ = 5.0	n = 2.54	

Table 13b. SEMICONDUCTOR - NON-LINEAR MATERIALS

<u>SUBSTANCE</u>	<u>SYMMETRY</u>	<u>WAVELENGTHS</u> <u>m</u>	<u>ELECTRO-OPTIC COEFFICIENTS</u> <u>(10⁻¹²m/V)</u>	<u>INDEX OF REFRACTION</u>	<u>CONSTANT</u>
CdTe	43m	1.0	r ₄₁ = 4.5	n = 2.84	- 9.4
		9.39	r ₄₁ = 6.8		
		10.8	r ₄₁ = 6.8	n = 2.60	
		23.95	r ₄₁ = 5.47	n = 2.58	
		27.95	r ₄₁ = 5.04	n = 2.53	
GaAs	43m	0.9	r ₄₁ = 1.1	n = 3.60	- 13.2
		1.15	r ₄₁ = 1.43	n = 3.43	
		3.39	r ₄₁ = 1.24	n = 3.30	
		10.6	r ₄₁ = 1.51	n = 3.30	

BaTiO₃ and 78 for LiNbO₃). Response times for BaTiO₃ are on the order of 100 milliseconds. The ferroelectrics are also difficult to process and are therefore not available in very high optical quality (free of defects) or in large sized crystals. SBN (another ferroelectric material) doped with various elements, has been shown to possess a higher photorefractive response than BaTiO₃ and may, with further development, be capable of operating below the response time of BaTiO₃. High optical quality SBN crystals, 1 cm on a side, have been manufactured by Rockwell International.

A desirable photorefractive material has the largest refractive index, Pockels constant (r), broadest spectral response, and the smallest dielectric constant. A figure of merit for these materials is the EO (Pockels) coefficient, r , divided by the dielectric constant, ϵ . A good example is BaTiO₃, the EO coefficient is 1640 and the dielectric constant is 3600 resulting in an r/ϵ ratio parameter of 0.45.

The non-ferroelectric materials exhibit different characteristics than the ferroelectrics. Materials such as BSO and BGO can respond and reach steady state within milliseconds, though their magnitude of electro-optic response is not nearly as large as that of the ferroelectrics. As can be seen in Figure 19 [4], the Pockels coefficient of BSO is 5 and the dielectric constant is approximately 56, giving a r/ϵ ratio of near 0.1, much lower than that of BaTiO₃ (0.45). To improve the magnitude of response, BSO is typically operated with an applied electric field range from 6-12 kV/cm.

The steady-state index as a function of grating period for BaTiO₃ is shown in Figure 5a and is shown for BSO in Figure 5b [4]. As can be seen in the figures, the steady-state index in BaTiO₃ is approximately 50 times larger than that in BSO. The response times for BaTiO₃ and BSO for an intensity of 1 w/cm² are shown in Figures 6a and 6b respectively [4]. As can be seen in the figures, the response time for BaTiO₃ increases with the magnitude of the diffraction grating and the response for BSO decreases with the magnitude of the grating. This is due to the different recombination rates in the two crystals. BSO is about 1000 times faster than BaTiO₃ due to its larger absorption coefficient, smaller recombination coefficient, and smaller dielectric constant. Figure 7 [4] shows the sensitivity or index change per unit volume input to the crystal. For small grating periods, BaTiO₃ is more sensitive than BSO but at grating periods greater than 1 μ m BSO is more sensitive. A number of variables affect the performance of the photorefractive crystals. These variables are listed below:

VARIABLES AFFECTING OPERATION OF PHOTOREFRACTIVE CRYSTALS

PROCESSING:

- Crystal cut
- Doping concentrations
- Size of crystal
- Temperature of processing
- Poling
- Defect density

CONFIGURATION:

- Angle of incidence
- Temperature of operation
- Applied bias
- Input power intensity
- Wavelength
- Grating index

The growth and processing of the photorefractive crystalline materials have continued to remain an art. The temperature of processing, the optimal crystal cut, the optimal processing and operation applied biases, and the poling technique all contribute to the quality and the operating characteristics of the devices.

The main attributes to be considered for selecting photorefractive crystals for application in advanced optical signal processing are summarized in the following list:

PHOTOREFRACTIVE MATERIAL PERFORMANCE ATTRIBUTES

- Photorefractive sensitivity
- Photorefractive recording and erasure time
- Refractive index change
- Spatial frequency response
- Laser wavelength
- Crystal quality
- Dark storage of information

A desirable photorefractive sensitivity ($100\mu\text{J}/\text{cm}^2$) is obtained by materials with large drift or diffusion lengths of the photocarriers. The crystal is an efficient photoconductor if the quantum efficiency of the charge

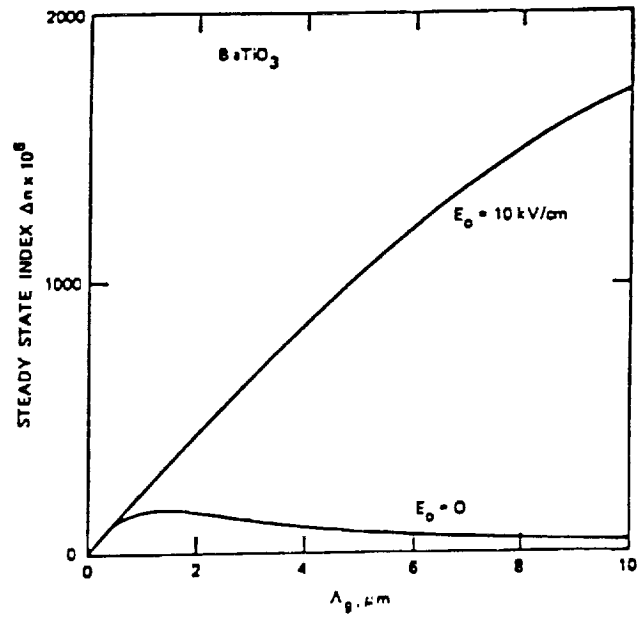


Figure 5a. STEADY STATE INDEX CHANGE IN BaTiO₃ AS A FUNCTION OF GRATING PERIOD FOR APPLIED FIELDS, E₀ = 0, 10 kV/cm

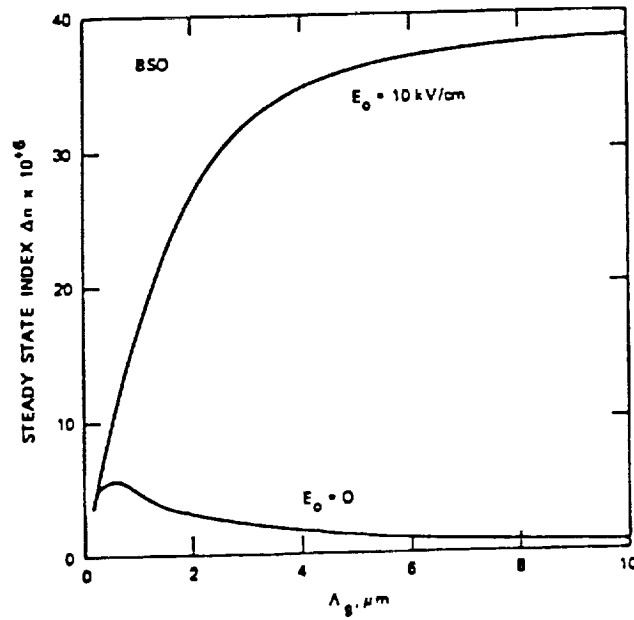


Figure 5b. STEAD-STATE INDEX CHANGE IN BSO AS A FUNCTION OF GRATING PERIOD FOR APPLIED FIELDS, E₀ = 0, 10 kV/cm

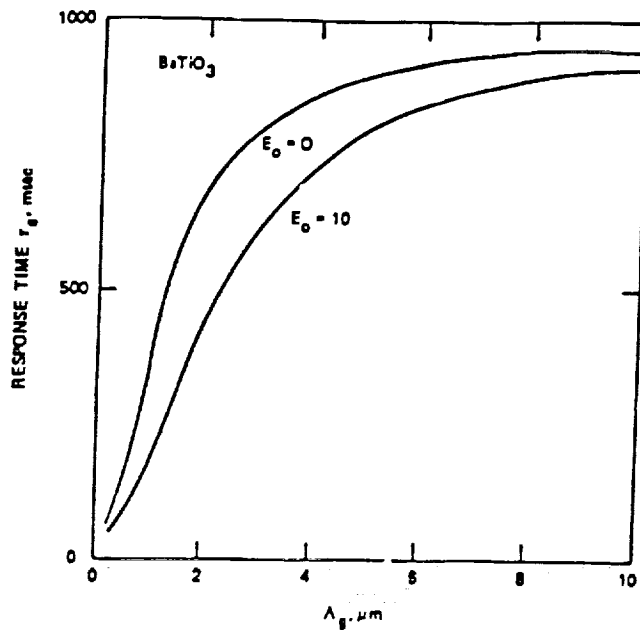


Figure 6a. RESPONSE TIME OF BaTiO3 AS A FUNCTION OF GRATING PERIOD FOR APPLIED FIELDS, $E_0 = 0, 10$ kV/cm, AND MEAN IRRADIANCE $I_0 = 1\text{w/cm}^2$

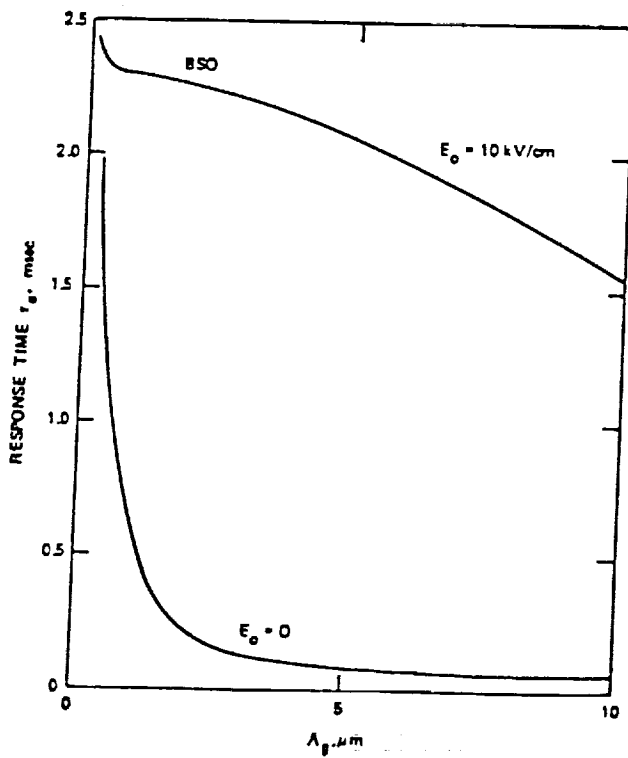


Figure 6b. RESPONSE TIME OF BSO AS A FUNCTION OF GRATING PERIOD FOR APPLIED FIELDS, $E_0 = 0, 10$ kV/cm, AND MEAN IRRADIANCE $I_0 = 1\text{ w/cm}^2$

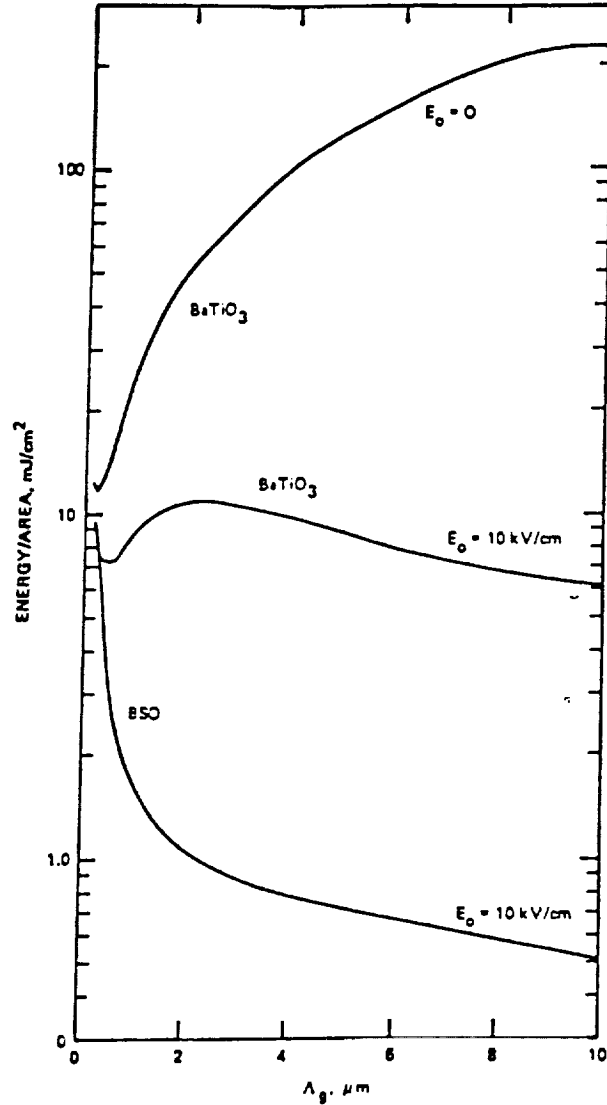


Figure 7. ENERGY PER UNIT AREA TO WRITE A 1% DIFFRACTION EFFICIENCY GRATING IN BSO AND BaTiO₃ AS A FUNCTION OF GRATING PERIOD FOR APPLIED FIELDS, $E_0 = 0$, 10 kV/CM. NO CURVE IS GIVEN FOR BSO WITH $E_0 = 0$ BECAUSE A 1% DIFFRACTION EFFICIENCY CANNOT BE REACHED IN A 1 mm PATH LENGTH

generation is close to unity and the crystal absorption coefficient is sufficiently high ($1-3\text{cm}^{-1}$). These factors result in an optimal grating time constant. Materials which exhibit such characteristics include BSO, BGO, and GaAs. High values of photo-induced index change are obtained in materials with high electro-optic coefficients. In crystals with low electro-optic coefficient (BaTiO_3 , KnbO_3 , SBN), the grating change can be increased with an externally applied electric field.

All the photorefractive crystals have a high spatial frequency response. The spatial frequency can be controlled with the amplitude of the applied bias. As can be seen in Figure 7, grating spacing of $.1\mu\text{m}$ can be efficiently recorded.

Crystalline materials have displayed adequate performance for reasonably high-speed beam modulation (as in communications) however their performance is questionable for fulfilling two-dimensional modulation requirements. Part of the problem associated with photorefractive crystals can be attributed to the lack of sufficient sources for the materials in the United States. Three universities: MIT, Stanford, and University of Southern California each study a different photorefractive crystal, and Hughes, Rockwell (SBN), and Sanders Associates (BaTiO_3) are industrial sources of photorefractive materials for research activities. DARPA is funding several of these sources to develop processes so that materials will be available to the community. The DARPA program office, however, has stated that it has in general been disappointed with the progress of the research and development of photorefractive crystals. The difficulty of tailoring the response of these materials, growing volume high quality crystals, and the lack of a clearly superior crystal for a majority of applications, has hindered the development and continued funding of research of the photorefractive crystals. Several alternate candidates have emerged in the last several years that show promise of filling the need for producible, controllable, photonics materials. The III-V compound semiconductor family, quantum well and superlattice structures, and organic polymers have all shown promise as possible photonics materials of the future.

6.1.2 NLO POLYMERS

In recent years, there have been demonstrated several organic materials that are capable of very large electronic second and third order responses. Nonlinear organic polymers have been promoted for achieving the electro-optic performance requirements without many of the drawbacks of the inorganic crystals. The polymers are the subject of intense research because their response can be tailored, through their molecular structures, to achieve desired operating characteristics. There are several optical device groups working on device

architectures using NLO polymers. These include Lockheed, 3M, Kodak, University of Arizona, University of Southern California, RADC, and AFWL/ML. Because the electro-optic and dielectric properties of the devices are decoupled, and the dielectric constants are characteristically low, the NLO materials are capable of extremely fast switching. A property of the material may be enhanced without sacrificing the performance of the device in other respects. Polymers offer response times ranging over fifteen orders of magnitude. The mechanisms for the variety of response times include the large nonresonant electronic nonlinearities (fsec-psec), thermal and motional nonlinearities (nsec-msec), configurational and orientational nonlinearities (μ sec-sec), and photochemical nonlinearities [5]. Another attractive attribute of the NLO polymers is the ease with which they can be processed. Non-vacuum techniques are being developed to deposit optically clear films.

In second order polymers, a large electro-optic constant, greater than 30 pm/V, is possible. The dielectric constant is on the order of 3. While the switching time of the polymers is several orders faster than lithium niobate or the semiconductor devices, the power per bit is in the range of 1 watt, considerably higher than the other optical switching technologies. Despite the high power per bit, the turn on/turn off time for the polymers is on the order of femtoseconds and the absorption coefficient is 1/10,000 that of gallium arsenide. The performance of the devices, therefore, compensates for their power requirements. The polymer materials currently being researched are listed in Table 14 [5].

Despite the encouraging potential of NLO polymers, laboratory verification of performance, environmental stability, and device performance predictions have not been performed. Much more research is necessary to determine the potential of utility for these materials. Application of the NLO polymers will likely be first seen in the communications industry for extremely fast switching devices.

6.1.3 SEMICONDUCTORS

Of the III-V semiconductors, gallium arsenide has seen the most research activity because of its use in microelectronics applications. Gallium arsenide has been developed in many optical processing contexts. Combined detector, processor, and source devices have been fabricated using GaAs. In addition, SLM's, acousto-optic devices and volume holographic devices have been produced. Moreover, because of its important role in advanced computer architectures, such as the newest CRAY computers, technological leverage from the microelectronics industry has been achieved with materials derived from GaAs technology.

Table 14. NLO POLYMER CLASSES

<u>Class</u>	<u>Examples</u>	<u>NLO Function</u>
Isotropic	Glasses Alloys Composites	$\chi^{(2)}$, $\chi^{(3)}$
Bond-Alternation	Ladder Polymers PTL, PQL Polyacetylene Polythiophene	$\chi^{(3)}$
Liquid Crystalline Polymers (LCP)	Side Chain LCPs	$\chi^{(2)}$
Rigid Rod Aromatic Heterocyclics	PBT LCPs PBO BBL	$\chi^{(3)}$
Polydiacetylenes		Mostly $\chi^{(3)}$ Some $\chi^{(2)}$

The nonlinear response of the semiconductor compounds is related to optical excitation inside the material. Excitons are formed in a semiconductor when photons of light just below the energy gap are absorbed. A free-exciton is a bound state of an electron and a hole. The excitonic nonlinearity originates from saturation of the excitonic absorption and the corresponding change in the index of refraction. Another nonlinear mechanism is the "band filling" effect where states just above the band-gap energy are filled, preventing absorption of those energies. The absorption spectrum thus appears to be shifted, and at the energies just below the band gap, large nonlinearities occur.

III-V semiconductors, such as GaAs offer important advantages over the crystalline oxides. Their photorefractive responses occur within tens of milliseconds, about 100 times as fast as that of the oxides. Relaxation times for many GaAs devices can occur in subnanosecond time domains. The electro-optic coefficient of GaAs is 1.51 pm/v and the dielectric constant is 13.2. This is equivalent to a r/e ratio of 0.11, comparable to that of BSO. GaAs devices operate in the infrared and are compatible with semiconductor injection lasers. They have the attractive property of providing adequate absorption (absorptivity lengths ($\alpha L = 1$)) in very short lengths ($1\mu\text{m}$). Another III-V compound, InP, has been the subject of materials research in several laboratories including those at the Air Force RADC facilities [6].

The III-V semiconductor family of materials and the superlattice materials are emerging as the most likely "optical silicon" for the optical processing technologies. Scientists at AT&T Bell Laboratories recently announced the development of the world's first multi-purpose photonic IC, a 2-kilobyte GaAs/AlGaAs chip that can be configured as logic and memory [7]. NEC last year announced the development of a similar 1-Kbit memory device. These devices are to be the building blocks of the first all optical general purpose computer [8].

The capability to exploit the processing and device manufacturing experience of GaAs and the ability of the III-V devices to form multiple device hybrid photonic/electronic circuits, makes the compound semiconductors a desirable material for increased research. To augment the opto-electronic III-V research, more experience is needed in using the semiconductors for volume holographs and in four wave mixing applications. Photorefractive beam coupling is possible in GaAs crystals with even low coupling coefficients. The tensor nature of the electro-optic coefficients of GaAs crystals allows beam coupling among different polarization components of two beams. Under certain conditions, beam coupling creates no net energy transfer, but polarization rotation only. A polarization modulation can be converted into intensity modulation using a cross polarizer.

6.1.4 SUMMARY OF MATERIALS

Of the three photonic materials discussed, crystalline photorefractive, NLO polymer, and semiconducting, each has its own particular advantages and disadvantages. Photorefractive materials are difficult to grow, they have closely coupled performance characteristics, and they are difficult to characterize, but they are capable of volume holographs and phase-conjugation. Nonlinear organic polymers offer a tremendous potential for large second and third order responses that can be tailored molecularly for a given application, yet there are serious questions as to their long-term environmental stability and there is a lack of experience in their characterization for these applications. III-V materials and superlattices offer a large payoff in the technology leverage achieved from the microelectronics industry and for their ability to operate as detectors, waveguides, emitters, and light modulators, though their EO performance is limited.

6.2 SPATIAL LIGHT MODULATORS

A major limitation of optical processing applications has been the lack of high speed, large format spatial light modulators (SLM's). Spatial light modulators are seen as the fundamental building blocks for all optical processing systems. In response to market needs, SLM technology has experienced tremendous growth in recent years. A spatial light modulator is a real-time reconfigurable device capable of modifying the amplitude (or intensity), phase, or polarization of an optical wavefront as a function of position across the wavefront [9]. They are used in such processing areas as: I/O real-time programmable masks, optical logic operators, high density optical storage, real-time projection, optical crossbar and feedback networks. The great diversity in the SLM designs results from modulating different variables of the optical wavefront (amplitude/intensity, polarization, phase, spatial frequency spectrum) and choosing different modulation mechanisms (mechanical, electrical, magnetic, thermal). A SLM imposes information on a carrier beam of light by creating a pattern of variation in either intensity or phase. The information-bearing control signals for the SLM can be electrical or optical, leading to two major classes of SLM's: Optically addressed spatial light modulators, which generally change state due to the intensity or phase of the incident light; and electrically addressed spatial light modulators, which are electrically addressable by pixel. Individual pixels are turned on by activating the address lines of that pixel. A chart classifying the SLM technologies is shown in Figure 8. SLM operating parameters are shown in Figure 9.

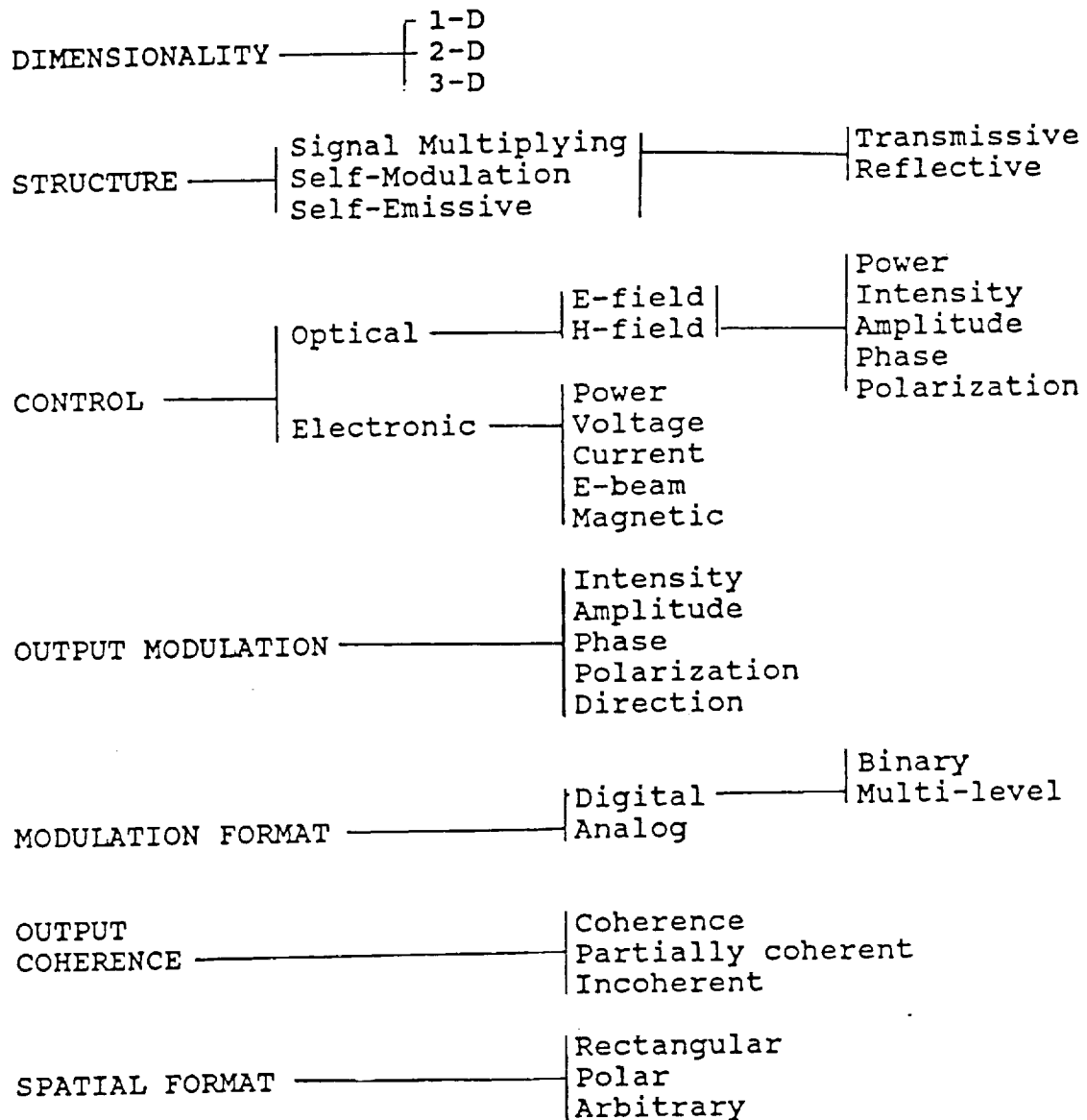


Figure 8. SLM CLASSIFICATION

Space-bandwidth product, pixel number
Cost, fabrication ease
Signal-to-noise, contrast, integrated sidelobe level
Dynamic range, grey scale levels, bits
Diffraction efficiency, modulation depth
Insertion loss, scattering level
Optical quality, dynamic distortion
Response time, cycle time, modulation bandwidth
Throughput rate
Storage time, memory drop-out rate, latency
Spatial resolution, pixel size, spread function, MTF
Sensitivity to drive signal
Linearity/nonlinearity
Spatial format
Complexity, maintainability, temperature sensitivity
RFI susceptibility
Optical power limitations
Acceptance angle, wavelength range
Packaging, size, weight, power consumption
Special features

Figure 9. SLM PARAMETERS

An optical processor has the potential to operate at greater than 10^{21} operations per second (OPS). Currently, the throughput rate of available SLMs does not exceed 10^{14} OPS. It is obvious that an improvement in the performance of SLM devices will provide a major impact of the viability of optical processing. The 1000 x 1000 element liquid crystal displays operating at 60Hz, which is a goal of the DARPA High Definition TeleVision (HDTV) program, will provide a good basis from which the SLM technology required for optical processing technologies can be developed. An example of the state-of-the-art SLM technology are the emerging high resolution, large format, fast frame-rate LCD displays that are capable of operating with a track ball mouse. Such a display is packaged with the new Apple laptop computers. A list of commercially available SLMs and their performance characteristics is shown in Table 15.

Electrically addressed SLMs, usually of ferromagnetic materials are used for matrix computations, switching, and information storage. As can be seen in the list of available SLM technologies, the electrically addressed SLMs can be switched at fairly fast rates (app. 100 frames/sec). The switching speed is limited in some designs by local heating, caused by the switching mechanism, which may cause a change in the properties of the materials. In newer electrically addressed SLM devices, the frame rate has been limited by the computer used to drive the addresses. 128 x 128 SLMs from Litton have been operated at over 200 frames a second and are theoretically capable of operating at 1000 frames a second. The 128 x 128 ferroelectric SLM from DISPLAYTECH, Inc. offers a 128 x 128 format, with a 150:1 contrast, and a 100Hz frame rate. The DISPLAYTECH SLM can process information at 1.6 Mbits/sec. The company is under contract to develop a 512 x 512 matrix format at 10 kHz.

Shown in Figure 10 is the principle of operation of the Semetex "Sight-Mod" [10]. The Sight-Mod is a magneto-optic SLM that is made of a monolithic crystal of magneto-optic garnet, grown through liquid phase epitaxy on the surface of a clear optically inactive garnet substrate. The epilayer exhibits a magneto-optic effect that rotates the polarization plane of linear polarized light by a constant angle. These states can be designated ON or OFF. The light passing through the material in the OFF state is extinguished by placing a polarizer in the path of the exiting beam and orienting it perpendicular to the polarization angle of the exiting beam. Light passing through the MOSLM material in the ON magnetization state is rotated in the opposite direction and is therefore partially transmitted by the polarizer.

To create a usable device from the magneto-optic material, the epilayer is first etched into discrete pixels of the desired size. Control wires are then embedded between each row and column of the array. The address wires are used

ELECTRICALLY ADDRESSED

<u>MANUFACTURER</u>	<u>TYPE</u>	<u>DIMENSION</u>	<u>PIXEL SIZE</u>	<u>SWITCHING SPEED</u>	<u>TRANSMISSION</u>
SEMETEX	MAGNETO-OPTIC	256x256	56 μm^2	100 $\mu\text{s}/\text{sec}$	@790 nm 23% (ON)
DISPLAYTECH	FERROMAGNETIC LIQUID CRYSTAL	128x128	185 μm^2	100 $\mu\text{s}/\text{sec}$	75% (ON)
LITTON	MAGNETO-OPTIC LIGHTMOD	128x128			
HUGHES	DEFORMABLE MIRROR DEVICE	128 x 128	51 μm^2	100 $\mu\text{s}/\text{sec}$	

00000

OPTICALLY ADDRESSED

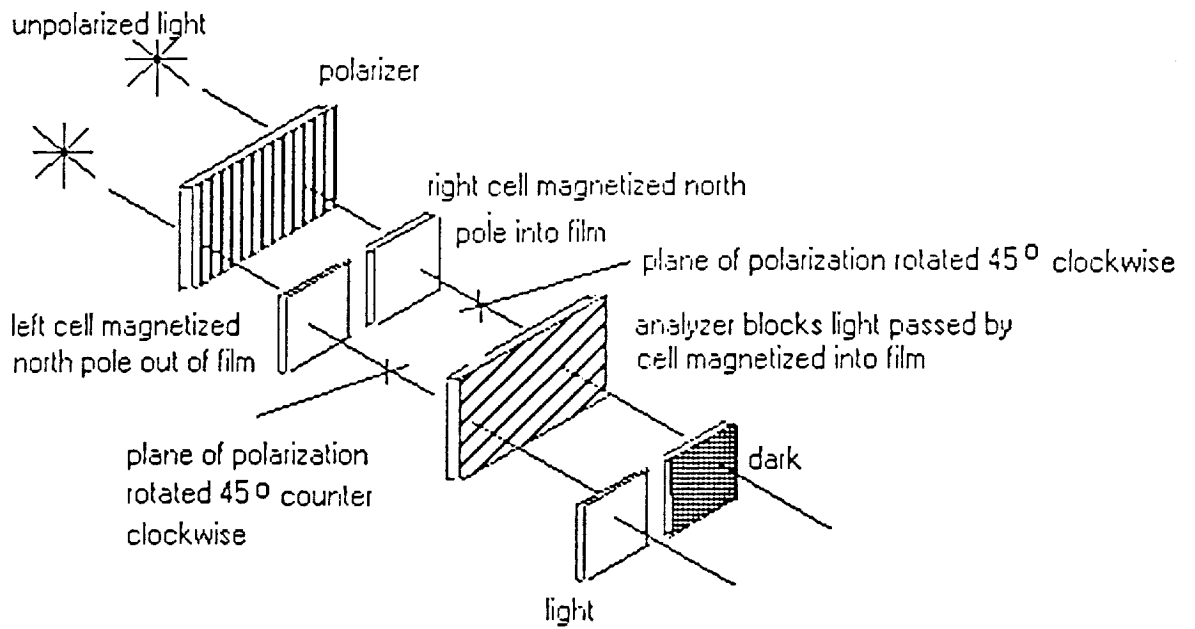
		<u>RESOLUTION</u>	<u>FRAME SPEED</u>	<u>SENSITIVITY J/CM²</u>
HUGHES*	LIQUID CRYSTAL LIGHT VALVE	30 lp/mm	25ms	8
MIT	MICROCHANNEL SLM (LITHIUM NIOBATE)	10 lp/mm	30ms	3.10 ⁻⁶
ITEK	PROM (BSO)	6 lp/mm	<0.2ms	5
LOCKHEED	GaAs NEMATIC LIQUID CRYSTAL	37 lp/mm	10ms	
SOVIET	PRIZ (BSO)	10 lp/mm	<0.2 ms	5.10 ⁻⁶

* VERY SHORT STORAGE TIME

00000

Table 15. SPATIAL LIGHT MODULATOR TECHNOLOGY

Figure 10. PRINCIPLE OF OPERATION OF SEMETEX "SIGHT-MOD"



to produce the magnetic field for each pixel. The 128 x 128 element Sight-Mod is capable of 130 Hz frame rates and has exhibited a 60,000:1 contrast ratio. The ON state transmission of the device is approximately 25% at 780 nm. Anti-reflective coating and prism polarizers can increase the ON transmission value.

An optically addressed gallium arsenide liquid-crystal spatial light modulator developed at Lockheed is shown on Figure 11 [11]. The write light illuminates the photoreceptor, which activates the electro-optic material. Modulation of the readout light is achieved by successive passes through the electro-optic element in a retro-reflective scheme. Since the output is optically isolated, the readout can be performed with a high intensity beam and the device can therefore increase the gain of the input information. The SLM was shown to have a limiting spatial resolution of about 37 lp/mm. High diffraction efficiency is possible in a write/erase mode at 100-Hz frame rate.

The deformable-mirror device (DMD) shown in Figure 12 was developed by Texas Instruments [12]. The DMD is a line addressing and monolithic device. Each element of the DMD consists of four cantilever-beam deformable mirrors. The elements are fabricated on 2-mil centers. Underneath the array of deformable mirrors is an array of electrodes connected to the floating surfaces of similarly arrayed MOS transistors. Each set of four deformable mirrors and their underlying electrodes form an air-gap capacitor. The electrostatic attraction between the capacitor plates causes the deformable mirror to be deflected downward. The deformation of the mirror modulates the incident light. The DMD allows for the addressing of the 16K (128 x 128) pixels from a single analog line at a data rate greater than 20 MHz. Although the device is limited by a small active area and the small deflection angle of the pixels, the devices offer a significant potential to provide high contrast phase-modulation.

Another type of SLM device that acts as a bistable switch is the SEED device that is becoming available in arrays, and can be used for optical computing. In December of 1989, AT&T Bell Laboratories announced the development of a high-capacity electro-optic integrated circuit [13]. The integrated circuit is a 2-Kbit array of symmetric self-electro-optic-effect devices (S-SEEDs) fabricated in GaAs. The entire array can be accessed simultaneously, allowing for parallel processing at the chip level. The device can act as a static or dynamic memory or as a switch for a logic function. The 32 x 64 element array has a switching speed of under 1-ns and requires a switching energy per device of 2.5 pJ. The holding power for long-term memory is 1 mW for the entire array. The SEED device operates by the application of light increasing the absorption of light at the operating wavelength. The absorption of that light results in a positive feedback that switched the transmission from a high to a low value.

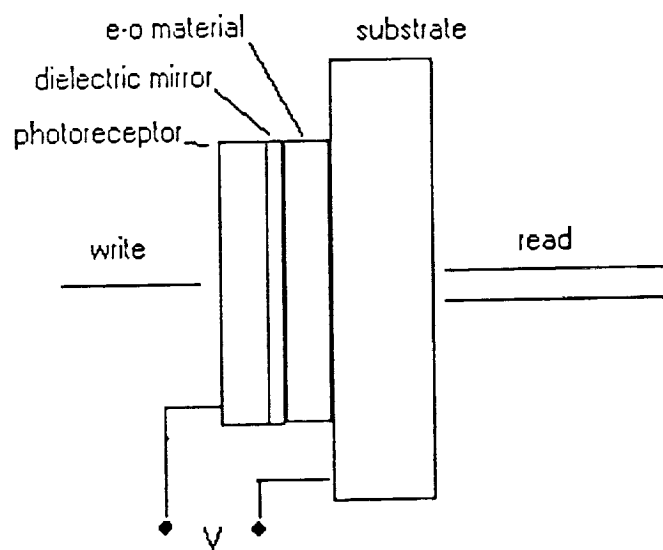


Figure 11. REFLECTIVE-READOUT PHOTOADDRESSSED SPATIAL LIGHT MODULATOR

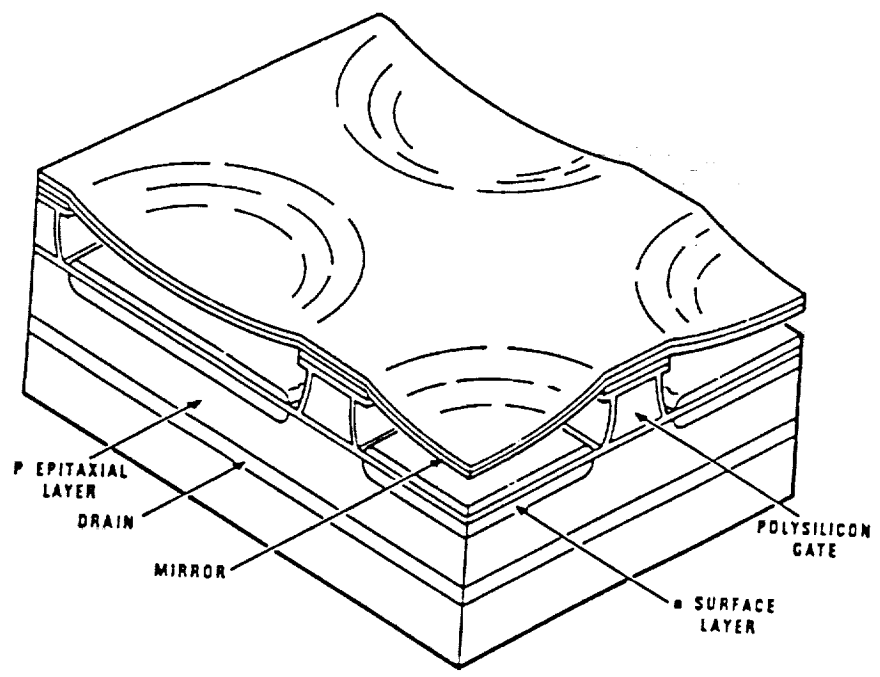


Figure 12. DEFORMABLE MIRROR DEVICE

The change in the absorptivity is caused by a change in an applied electric field that is brought about by the generation of free carriers. The principles of the SEED device are shown in Figure 13.

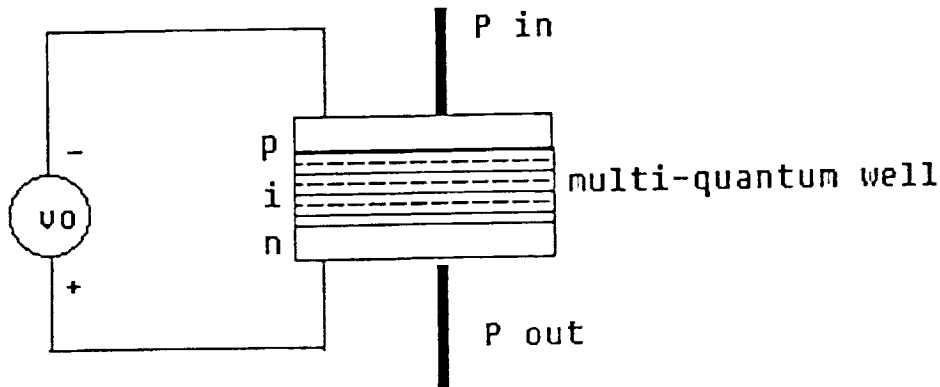


Figure 13. PRINCIPLE OF SEED DEVICES

SEED devices operate in a reverse fashion from many other etalon devices. Optical logic etalons increase transmission with increased incident optical power. A Fabry-Perot etalon consists of two partially reflecting mirrors transmitting light only when it is an integral number of wavelengths optically thick. For bistable operation, the wavelength of the light beam is detuned to one side of the Fabry-Perot peak so that the device is operating in a region where the transmission is low and thus the device is off. As light intensity increases, the index of refraction is shifted closer to the transmission peak. Positive feedback occurs until a critical point is reached, and the device is activated and the device transmits. Increasing the light at this point causes little effect in total transmission. This effect is shown in Figures 14a and 14b. The shifting of the peak can result in these devices performing logic operations such as NOR, NAND, XOR, OR, and AND, depending upon the initial detuning of the peak.

6.3 OPTICAL COMPUTERS

The potential for creating very high resolution spatial light modulators capable of performing logic operations has engendered research in the field of optical computing. There have been several optical computing architectures reported in journal literature. As is the case in conventional electronics, optical computing research falls into two categories: analog and digital. Although the analog nature of optics makes them readily adapted to analog computer designs, with the magnitude of the numbers defined as proportional to

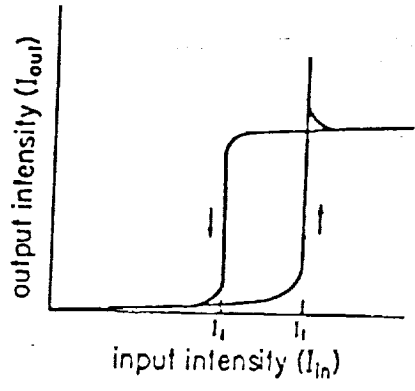


Figure 14a. INPUT INTENSITY vs. OUTPUT INTENSITY FOR OPTICAL BISTABLE DEVICE

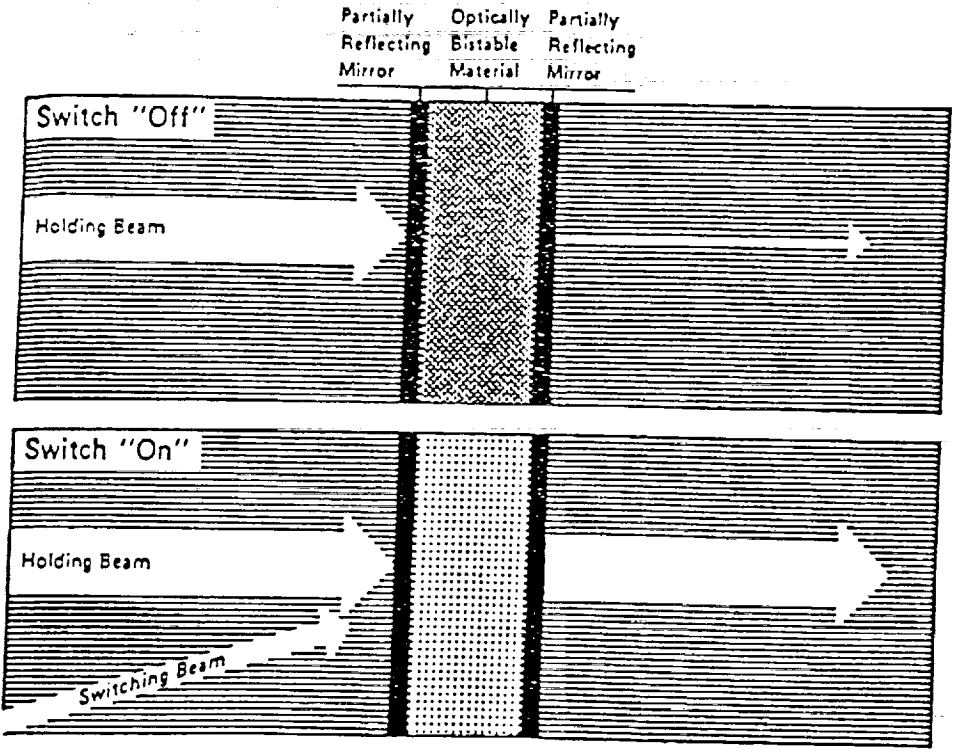


Figure 14b. BISTABLE OPTICAL DEVICE

the magnitudes of the signals used to represent them, the accuracy of analog optical computing systems tends to be low. Light intensity levels may be produced, controlled, and detected in about 500 discrete levels. This corresponds to about 8 bits of numeric accuracy. Eight bits are seldom sufficiently accurate, especially for problems with many steps in which inaccuracies accumulate. This has led many optical computer designs to be implemented in digital format. Digital optical computers, although somewhat slower than analog optical computers, offer increased accuracy and flexibility.

The implementation of optical digital computers offers potential EMI immunity, high degrees of parallelism, power, and cost advantages over conventional digital electronic computers. Moreover, optical computing systems need not obey the nearest neighbor interconnect law. With demonstrated gate densities approaching 10^9 elements and clock speeds of 10^8 , optical systems show potential gate interconnect bandwidth products in excess of 10^{17} . Advanced electronic neural processors under development at companies such as Siemens promise to offer approximately 10^{14} gate interconnect products.

The key to the development of optical computers is the ability to develop mathematical methods and transformations of signals so that representative values can be implemented in optics. In theory, a control algorithm should be developed and optimized for the computer architecture chosen for implementation. However, in most cases, an algorithm is developed in a high level language, and the implementation of the algorithm in the computer hardware is performed by a compiler. This process is satisfactory for most control applications designs utilizing conventional processors. The non-trivial nature of implementing algorithms in hardware has received exposure recently from the development of multi-processor parallel processing systems and other non-Van Neumann architectures. Segmentation of problems, efficient distribution of work, and manipulation of data require attention when implementing algorithms on these parallel systems.

The implementation of control systems in optical computers is further complicated by the limited accuracy of optical designs and the inability of optics to perform carry branching operations easily. These factors, combined with the limited maturity of most of the optical processing devices, have resulted in very few of the proposed optical computer designs being demonstrated in the laboratory and even fewer developed to solve real-world problems. Most optical computer designs to date have been of the applications-specific benchtop variety and their designs have been very application specific.

There is a great need to the community to develop and demonstrate

mathematical methods and transformations of controls problems that can be adapted to optical computers. Of the few optical computer concepts, many designs are hybrid optical/digital electronic architectures. A digital electronic computer is commonly used in these designs to download portions of an algorithm to the optical computer for solution. They are also used to store the information presented to the optical SLMs. This type of hybrid design is likely to represent many of the initial optical computer designs. The digital computer will be used to segment the matrices to store data, and the optical computer will be used to process the data.

6.3.1 OPTICOMP COMBINATORIAL PROCESSOR

Peter Guilfoyle with Opticomp, located in Lake Tahoe, Nevada, has developed an optical processor that is transparent to the SUN RISC computer programming environment [14],[15]. The optical processor understands instructions from the SUN RISC computer without the user's knowledge of its operation, much like a coprocessor. Guilfoyle uses a combinatorial logic based approach in his design to implement an unlimited set of nonlinear functions. The architecture forms systollically interconnected programmable logic arrays (PLA's). The system demonstrates the 3-D global interconnect capability of optics, uses detectors as OR gates not as integrators or threshold devices, uses computer generated holograms to broadcast light, and uses feedback. The system has the potential of offering the computing power of a supercomputer at a fraction of the cost.

Opticomp utilizes the natural AND-OR-INVERT capability of optics to perform the digital logic primitives from which most digital circuits are designed. Two-level combinatorial logic has been developed and implemented in PLA designs. Using the optical processor, a virtually unlimited set of nonlinear functions can be implemented. Because the combination sets are only generated once, they are formed in the electronic computer. The logic functions that need to be performed numerous times are performed in the optics. These designs represent sequential logic functions as Finite State Machines implemented by a combination and a storage component.

One of the key components of the Opticomp design is that the detectors are not used to detect threshold levels of analog signals. They are used only to detect the presence of light. This greatly improves the accuracy and reliability of the system. To avoid the problems of digital multiplication by analog convolution, Guilfoyle developed a combinatorial approach in which the combinations were created and then used over and over by the acousto-optic cell as all terms are multiplied. By utilizing various interconnect methods and global broadcast methods, highly precise and fast processing functions can be

performed. The current size of the word is limited by the size of the acousto-optic devices to 4-5 bit lengths. For problems requiring larger words, the problem is folded into the three dimensions that the optics afford. The result of the work at Opticomp was a demonstration of the first general purpose optical computer. As stated above, the initial demonstration in 1988 provided an optical processor that was invisible to the SUN RISC programming environment. Although the initial demonstration provided no significant speed advantages over conventional processors, the processor or processing methods were not optimized. Future designs should offer the power of a supercomputer. The system does offer cost and reliability benefits over conventional processors. A hardware implementation of the system is shown in Figure 15.

6.3.2 BIMODAL OPTICAL COMPUTER

Work in bimodal optical computers (BOC's) originating at the University of Alabama [16] and now studied at Carnegie Mellon [17], [19] is aimed at reducing the residual error of linear and nonlinear algebra using parallel optical implementations.

The BOC hardware shown in Figure 16 has three major parts. The optical system, the electronic circuit, and the digital processor. The optical system consists of a fully parallel matrix-vector multiplier. The lights from the LED's represent the input vector components. The light from the diodes is spread vertically by planar waveguides onto the columns of the matrix mask. The transmitted light is summed by rows using another set of planar waveguides and detected by photodiodes that represent the output vector b . The electronic circuit acts as a feedback loop to correct for the input light of the LED's until a solution is reached. The digital computer is used to generate the matrix A and store the approximate solution x . The residue vector r is calculated and if the residue vector is not small enough the optical processor solves for the system of linear equations of the error of the approximate solution. A new residue is found for the new approximate solution. The process is iterated until a 16-bit accuracy is obtained. The solution x will then be read and stored by the digital processor. A graph of the log of the error versus the number of iterations is shown for an example problem in Figures 17a and 17b. The solution in this case was obtained within 6 iterations. The process uses a fast low accuracy processor to obtain a first guess at the norm of the solution vector. It then uses a slow accurate processor to evaluate the residual. By manipulating the matrices and by integrating several times, a convergence can be obtained for even ill-conditioned problems, independent of the vector x . The BOC obtains $O(1)$ temporal complexity, a constant algorithm for all problems, and solutions independent of x and $E(P)$.

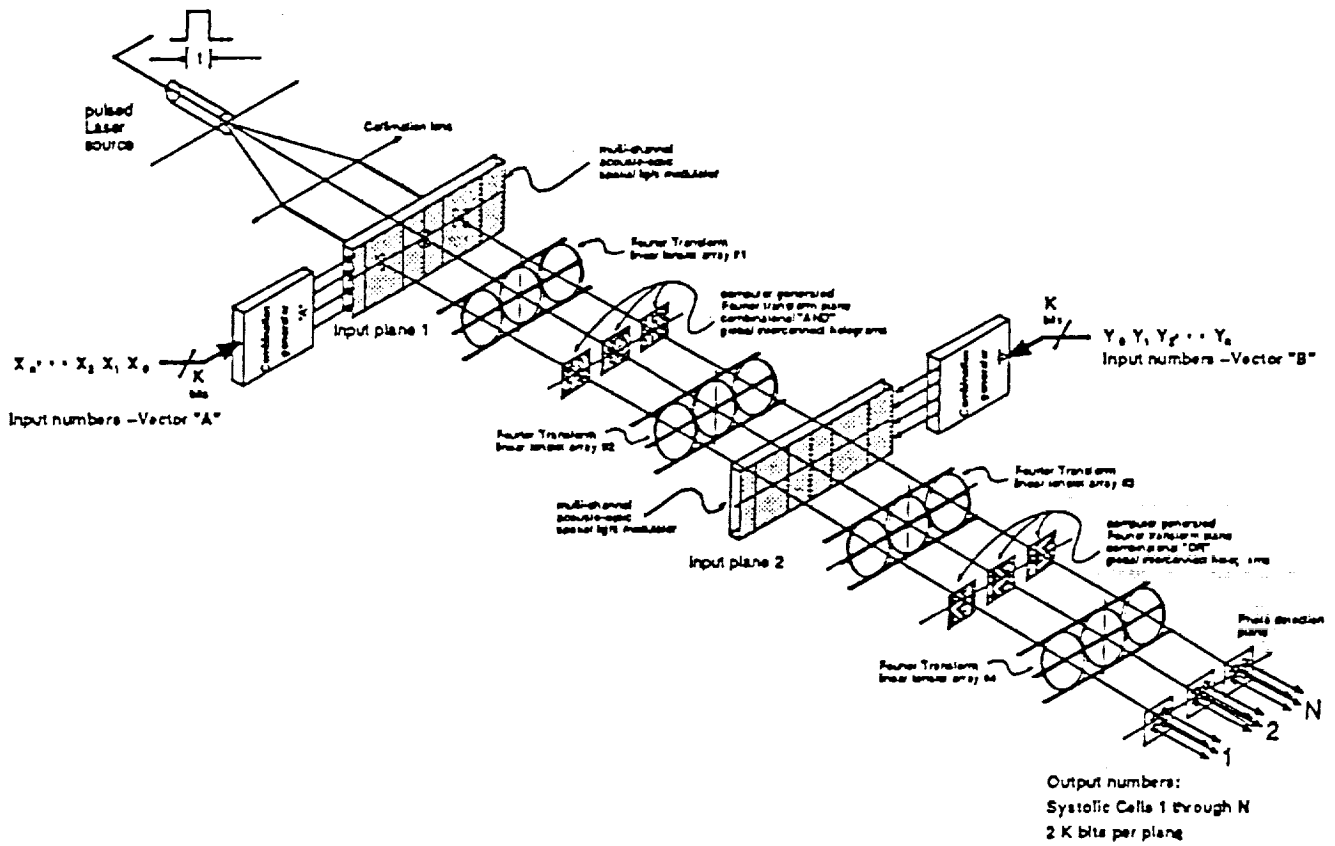


Figure 15. OPTICOMP OPTICAL COMPUTER HARDWARE FOR GENERAL PURPOSE PROGRAMMABLE COMBINATORIAL LOGIC PLA COMPUTATION ELEMENTS

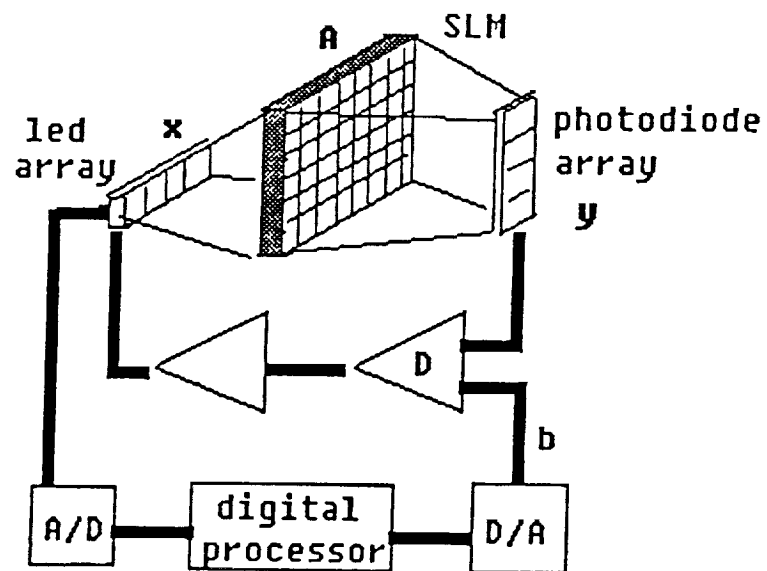


Figure 16. THE BIMODAL OPTICAL PROCESSOR

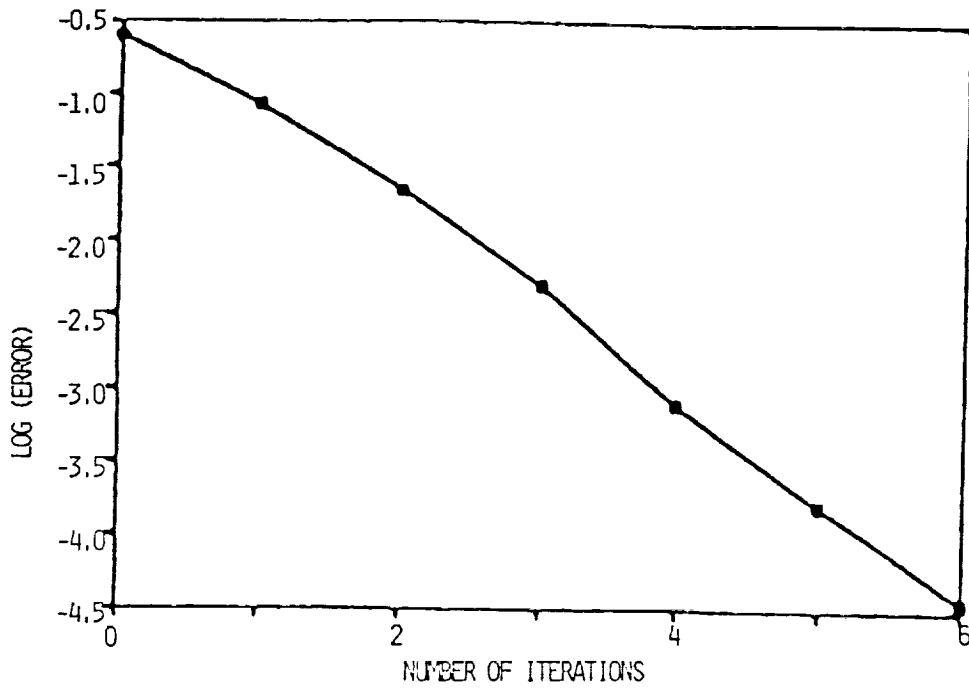


Figure 17a. THE LOG(ERROR) AS A FUNCTION OF THE NUMBER OF ITERATIONS. THE BOC STARTED WITH 30% ERROR [17]

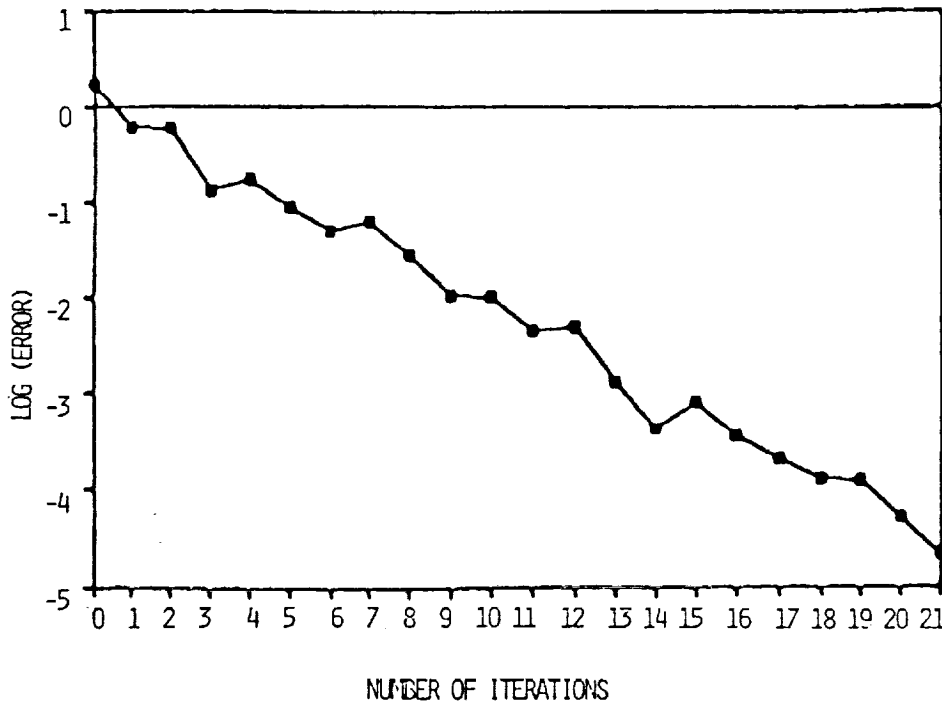


Figure 17b. THE LOG(ERROR) AS A FUNCTION OF THE NUMBER OF ITERATIONS. THE BOC STARTED WITH 100% ERROR [17]

A research activity at the University of Alabama, Huntsville, implemented a system of nonlinear equations on the BOC and proposed two algorithms [18]. One algorithm solved the problem approximately and the other solved the system of equations exactly. The BOC system solved a system of nonlinear equations $f(\mathbf{x}) = 0$.

If J_k is the Jacobian matrix for a system of nonlinear equations represented by $f(\mathbf{x})=0$, where f_i s are nonlinear functions of \mathbf{x} , then

$$J_k C_k = f_k,$$

which is a system of nonlinear equations to be solved for C_k . Using Newton's method, an algorithm for solving the system of nonlinear equations would be as follows:

- a - Assume a solution of \mathbf{x}_0
- b - Compute the $n \times 1$ vector f_x and the $n \times n$ matrix J_k
- c - Solve the linear system of equations $J_k C_k = f_k$ for C_k .
- d - Compute the refined solution $\mathbf{x}_{k+1} = \mathbf{x}_k - C_k$
- e - If the norm $[f_{k+1} - f_k]$, allowable error (e), stop. Otherwise go back to step b.

The interactive algorithm above requires on the order of n^3 [$0(n^3)$] operations when used with a conventional digital computer. John Caufield and researchers at the University of Alabama in Huntsville demonstrated the solution of the system of nonlinear equations using a hybrid analog optical computer and a hybrid bimodal optical computer (BOC). The analog optical computer was used to solve the equation for c approximately using the following algorithm.

- a - Use a digital processor to guess an initial solution \mathbf{x}°
- b - Use the digital processor to compute both the vector f_k and the matrix J_k
- c - Use the analog processor to solve the system J_k matrix $J_k^\circ C_k^\circ = f_k^\circ$ for C_k° approximately. (The $^\circ$ denote inaccuracies in the optics or electronics).
- d - Use the digital processor to read C_k° and compute the refined solution $\mathbf{x}_{k+1} = \mathbf{x}_k - C_k$
- e - Check if the norm $[f_{k+1} - f_k] < e$. If not, go back to step b.

Although the optical computer is used only to solve the system of nonlinear equations, it is this step in the algorithm that is the most expensive in an electronic digital computer. For the BOC the following algorithm was developed

to solve the problem exactly, with the specified accuracy.

- a - Use the digital processor to guess an initial solution x^0
- b - Use the digital processor to compute both f_k and the matrix J_k
- c - Use the BOC to solve the system $J_k c_k = f_k$ exactly for c_k
- d - Use the digital processor to read c_k and to compute the refined solution $x_{k+1} - x_k = c_k$
- e - Check if the norm $< e$, otherwise go to step b.

A comparison was performed by the researchers at UAH of the two optical processors and a digital electronic computer. The time required for a digital computer to solve the system of equations (T_d) is given by

$$T_d = (n^3/3) + 2n(n+1)T_{d1}N_D, \quad 1)$$

where T_{d1} is the time required for one digital operation and N_D is the number of iterations needed for the system to converge. On the analog hybrid computer the total time (T_A) to solve the system of equations is given by

$$T_A = [n(n+2)T_{d1} + T_{a1}]N_A, \quad 2)$$

where T_{a1} is the time required for the optical analog processor to solve the system of linear equations and N_A is the number of iterations required for the solution to converge.

For the hybrid BOC processor the time required to solve the system of nonlinear equations (T_B) is given by

$$T_B = [2n(n+1)T_{d1} + T_{a1}]I_B N_D, \quad 3)$$

where I_B equals the number of iterations needed for the BOC to solve the system accurately.

Of interest in these demonstrations was a determination of the point at which the optical processor is faster than the digital processor. For the hybrid analog computer this point can be arrived at by setting equation 1 equal to equation 2. This results in the equation given by

$$[[n^2(n/3+1)/(N_A/N_D)] \times [T_d/T_a] \gg 1 \quad 4)$$

For the hybrid BOC the break even point is given by

$$[n^3/3-2n(n+1)(I_B-1)/(N_B/N_D)] \times [T_d/T_a] \gg 1 \quad 5)$$

The first terms of these equations are problem dependent and are much larger than 1 for large values on n. However, the second term in both equations $[T_d/T_a]$ depends on the speed of the analog processor for solving a system of linear equations, which can be in the range of microseconds. Because the matrix J_k needs to be updated every cycle, the system is limited by the speed at which the SLM can be updated. Today's SLM technology requires at least several milliseconds for a frame of data to be written. This limits the second term $[T_d/T_a]$ to be less than 1. Shown in Figures 18a and 18b is the $\text{Log}(A_n)$ and $\text{Log}(B_n)$ plotted in terms of system size, n, where A_n is the first term of equation 2 and B_n is the first term of equation 3. For a $[T_d/T_a]$ ratio of 10^{-3} , a speed advantage for $n > 50$ for the analog processor and for the hybrid BOC processor $n > 120$, can be achieved. If the write time to the SLM can be reduced, the ratio $[T_d/T_a]$ can be reduced and the break even point for both processors reduces.

6.3.3 OPTICAL LINEAR ALGEBRAIC PROCESSOR

Shown in Figure 19 is an example of a multi-channel high-accuracy optical linear algebra processor developed at Carnegie Mellon [17].

To handle large problems using the optical processing hardware, the researchers at Carnegie Mellon developed a unique diagonal partitioning method [19]. An example of the partitioning of a matrix is shown in Figure 20. The best matrix partitioning methodology can be determined by analysis of the problem, the algorithm, and the system architecture. Partitioning reduces the storage and housekeeping required by breaking the matrices into small blocks. Improved accuracy has been obtained by bit partitioning. The processor has been used to solve computational fluid dynamics. The algorithms that were used were optical realizations of the Newton-Raphson method for nonlinear equations and an optical implementation of an LU direct decomposition.

6.3.4 RESIDUE MATHEMATICS

Residue mathematics have been developed for implementing numeric operations on optical digital computers. Westinghouse, Boeing, Litton, as well as Georgia Tech, and the University of Huntsville have performed work in this area [16], [18]. Residue mathematics represents integers using several prime numbers as bases. Opto-electronic chips with 3-10 GOPS capacity are being developed using this technique. In residue, arithmetic numbers are represented by writing down their remainder (residue) after division by a chosen set of mutually prime moduli. Parallel, carry-free modular addition, subtraction, and multiplication

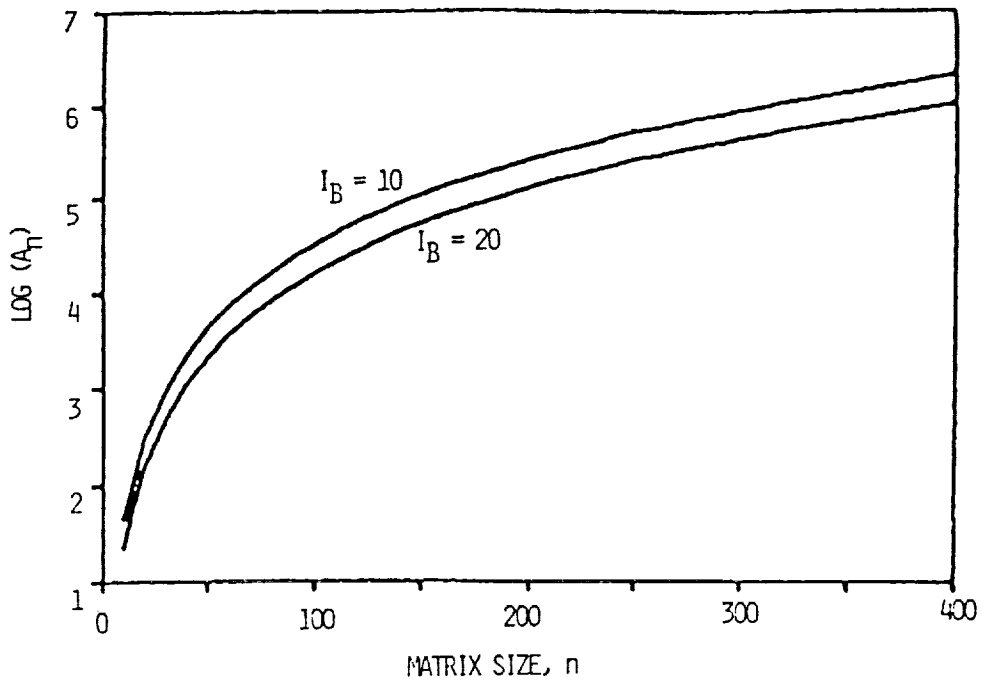


Figure 18a. PLOT OF LOG OF THE RATIO A_n IN TERMS OF THE SIZE OF THE MATRIX [19]

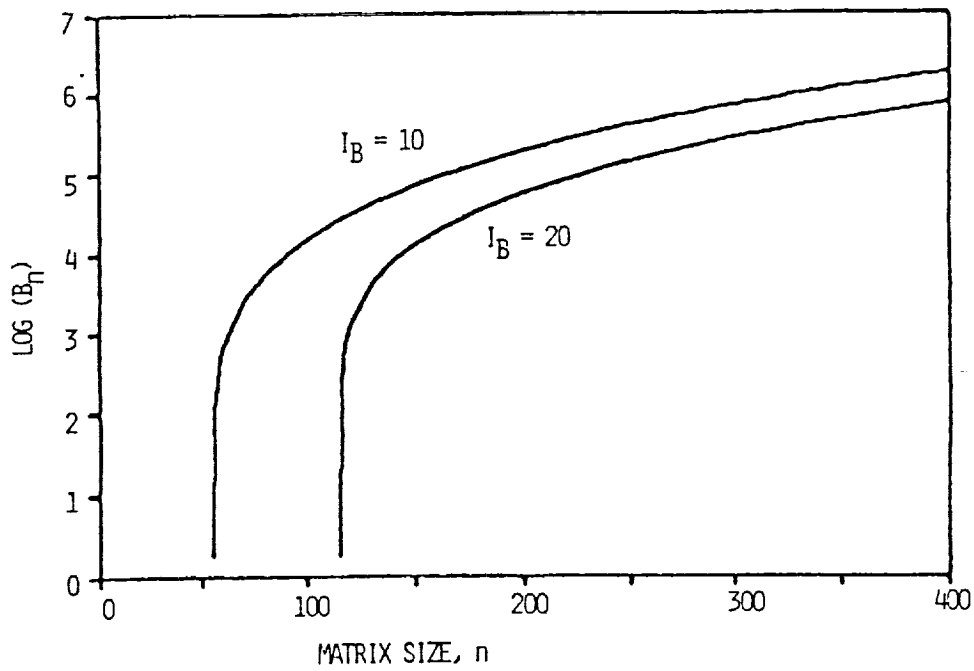


Figure 18b. PLOT OF THE LOG OF THE RATIO B_n IN TERMS OF THE SIZE OF THE MATRIX [19]

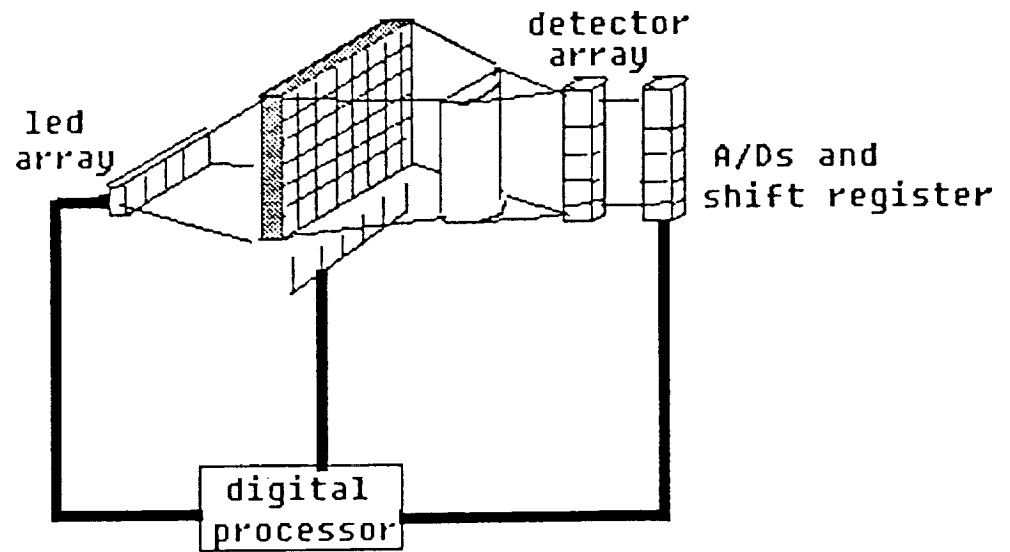


Figure 19. OPTICAL LINEAR ALGEBRAIC PROCESSOR

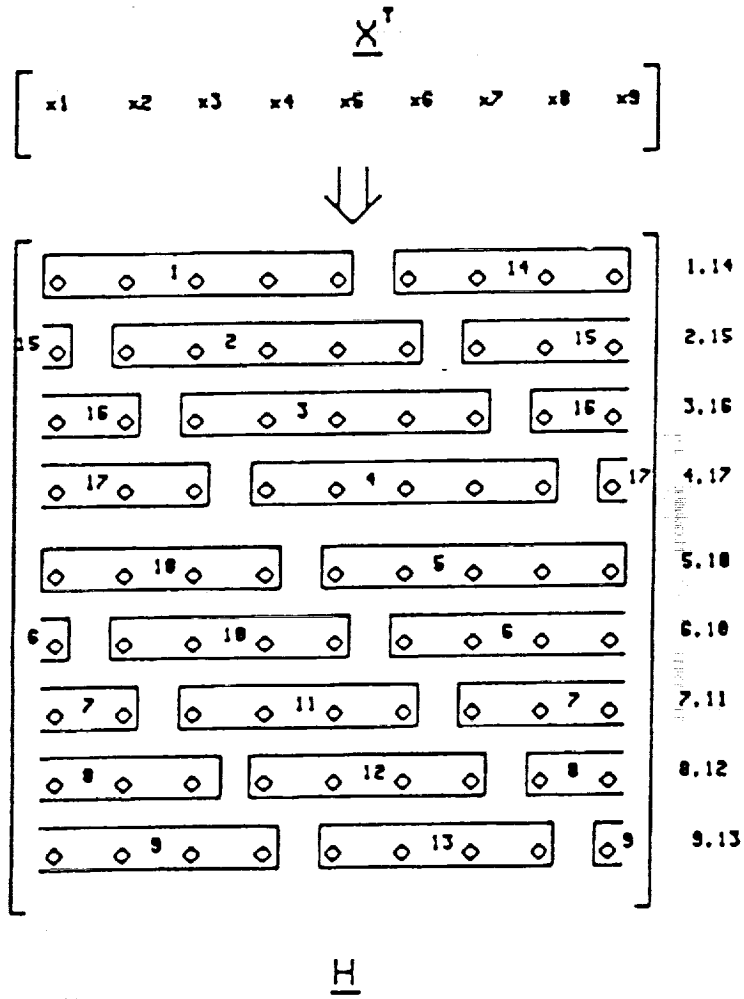


Figure 20. DATA FLOW ARRANGEMENT FOR PARTITIONING MATRIX [20]

can be performed separately for each residue. An example of residue mathematics is shown in Figure 21 using base 3 and 5 to form the residue. Numbers up to 64 can be represented using the bases 3 and 5.

Base 10 Digital	Base 3 Residue	Base 5 Residue	Base 3, 5 Residue
0	0	0	00
1	1	1	11
2	2	2	22 * 22
3	0	3	03 * 03
4	1	4	14 --
5	2	0	20 * 25 → 20

$$\begin{array}{r}
 3 \\
 + 2 \\
 \hline
 5 \rightarrow \text{base 3,5 residue 20}
 \end{array}$$

Figure 21. ADDITION PERFORMED USING BASE 3,5 RESIDUE MATHEMATICS

The key component of most of the optical computer designs is the spatial light modulator. It seems reasonable to assume that a 1000 x 1000 element SLM operating at 1MHz will be commercially available within the near future. There are however many problems which must be overcome before these devices can be applied to an architecture design. The cascability and interconnection of elements should be analyzed in great detail so as to exploit the potential of the optical devices. More importantly, representative problems should be identified and applied to the optical hardware. The implementation of practical algorithms onto optical computers is an area of study that has not been developed.

The ability of optical systems to perform massively parallel processing, to be massively interconnected, and to perform at the speed of light has made optical technologies the focus of interest for many image processing, computing, and automatic target recognition concepts.

6.4 OPTICAL NEURAL NETWORKS

The characteristics of optics have made them attractive for the implementation of neural network concepts. Addressing the problem of decision making under variable conditions, neural network concepts have been researched to provide systems with a better ability to react appropriately in a varying

environment.

Optical neural networks are the offspring of two parents: optical information processing and neural network theory. Optical processing techniques have been applied to exploit the vast interconnectability of optics and the ability of optics to perform massively parallel processing.

Neural networks have been the area of considerable research in developing systems which can perform "characteristically biological" functions such as pattern recognition, generalization, abduction, intuition, problem finding, and language, faster than a digital computer. The motivation for such efforts is the failure of conventional algorithms implemented on digital computers to solve them. Most neural network systems today are simulations performed on digital computer architectures. These systems are inadequate for real-time application because of the limitations of the architectures to perform the parallel process.

The key ingredient of neural networks is the interconnection of the neurons. Like a biological neuron which is capable of firing only several times per second but is connected to tens of thousands of other neurons, an optical cell can receive inputs from tens of thousands of pixels in the previous frame and distribute that information to tens of thousands of pixels in the next frame. This characteristic allows optics to be used to perform parallel reasoning processes. In general, the more highly connected a process is, the more complex problems it can handle. A hybrid opto-electronic implementation of a neuron is shown in Figure 22. The figure illustrates the fan-in/fan-out capability of the optical implementation.

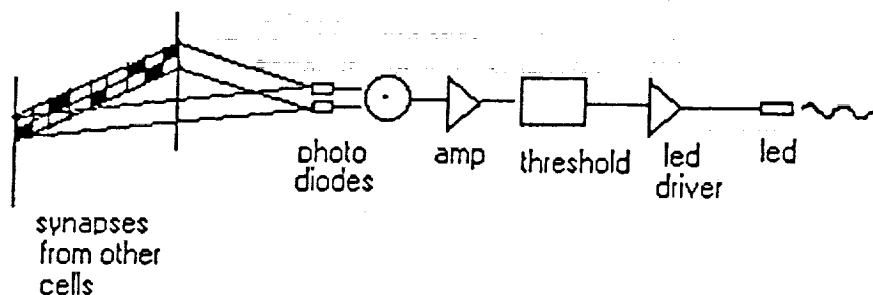


Figure 22. OPTO-ELECTRONIC ANALOG OF A NERVE CELL

In the future, the neural cell receives input from a number of other neural cells. This information is represented as values on the SLM. Information is shown in binary form as white and black segments in the figure. The information from the other neurons is imaged onto photodiodes which represent the synapse of the modelled nerve cell. The information of all the nerve cells imaged onto the

synapse of the cell of interest is integrated and a pulse corresponding to the sum of all these inputs is processed by a threshold function in the body of the cell. A pulse of light is produced which simulates the firing of the nerve cell.

There are currently ten universities actively involved in optical neural network research. They are: California Institute of Technology, Clark University, New Mexico State University, Stanford University, University of Alabama, University of California at San Diego, University of Colorado, University of Dayton, University of Pennsylvania, and University of Southern California. Industrial laboratories exploring optical neural networks are: AT&T Bell Labs; Bellcore; Hughes Research; micro-electronics Computer Consortium; Northrop; and Rockwell International Science Center. The Naval Research Laboratory is the only government lab active in the area.

Compared to electronic devices, optical devices are inherently parallel and are not limited by wire interconnections and cross-talk. Table 16 shows the figure of merit for the human brain, an optical computer, and a VLSI computer [6].

$$F = F(N, I, S)$$

N = # of neurons

I = # of interconnects

S = speed of neuron update

$$F = (N I) \times (N I S) = N^2 I^2 S$$

SYSTEM	N	S	I	NxI	F
Brain	10^{12}	10^3	10^3	10^{15}	10^{33}
Optical Neurocomputer	10^6	10^9	10^3	10^9	10^{27}
VLSI fully connected	10^3	10^9	10^3	10^6	10^{21}
VLSI nearest neighbor	10^6	10^9	0(1)	10^6	10^{21}

Table 16. FIGURE OF MERIT FOR HIGHLY CONNECTED PROCESSORS

The human brain has between 10^9 - 10^{12} neurons, and each one is connected to 10^3 and 10^4 other neurons. As can be seen in the chart, it is not the speed of update that makes the computational power of the brain, but the number of interconnects. Because of their ability to perform weighted interconnections in three dimensions, and to use light to carry information, optical processors can

approach the processing power of the brain. VLSI designs are limited by the requirement of electronic interconnects which limits VLSI designs to two dimensions. Moreover, because most electronic computers use around 10^8 kT per fan-in and fan-out, (k = Boltzmanns constant and T = absolute temperature), the typical 10^4 kT of the optical computers offers potential power savings.

A simple model of a neuron is shown in Figure 23. A potential is developed at the synapse of the cell from stimulation from other neurons. The potential of the excitatory or inhibitory signals from the other neurons and the state of the cell v_i determine whether the cell "fires" or not. The signals e_{ij} are passed along the axons and are gated by the long term memory traces z_{ij} before they can perturb their target cell v_j .

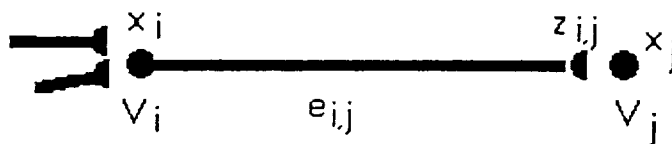


Figure 23. MODEL OF A NEURAL CELL

The long term memory (LTM) trace is the component of the model that allows the neuron to learn. As more signals are passed along the neuron, the value of Z_{ij} is increased. The ability of a signal to fire the neuron thus becomes easier. The ease of firing is therefore enhanced both by the number of times that signals have been generated in the neuron and by the number of stimuli that are present at the synapse of the neural cell.

Biological and technological networks are usually arranged in layers. The outputs of one layer becomes the inputs of another layer or vice versa. Lateral neural interconnects are allowed as well. The weights of the interconnects provide the methods for adaptation.

Several neurocomputers are emerging on the market in the form of chips, boards, and development tools. Fujitsu Laboratories is developing a 1,024 floating-point digital signal processor architecture capable of generating a billion connection updates per second. Siemens is developing a 900,000 transistor waferscale systolic array which is capable of a billion connections per second. Neural Semiconductor Inc., has announced a set of neural ICs. Neural Semiconductor claims its 32 x 32 neuron chips offer recognition speed of up to 100,000 patterns per second.

Shown in Figure 24 is an example of an optical implementation of a Hopfield neural network first demonstrated by Psaltis and Farhat in 1985 [21]. It consists of a linear array of N light emitting diode sources that enter an N bit binary digital vector into the processor. An optical lens system images each LED onto a single row of an N^2 transmission matrix. Each pixel has a programmable transmission value T_{ij} . At the output end of the optical processor is placed a linear array of N photodiodes, each arranged to scan the output of a single column of the transmission matrix. Thus, every input data line is connected to every output data line, with the mask providing N^2 individually adjustable weighting functions. The thresholding functions and feedback of the Hopfield model are provided electrically. The Hopfield model assumes in its mathematical description that both positive and negative values can be handled, both for the input data and the stored weights. In the optical implementation, the intensity of the light is always positive. One solution is to use two-channel operation with one channel containing positive values and the other containing negative. This increase is twice as many sources and detectors and a fourfold increase in the number of weights. An alternative approach is to bias the optical system to operate about a mean level of unity.

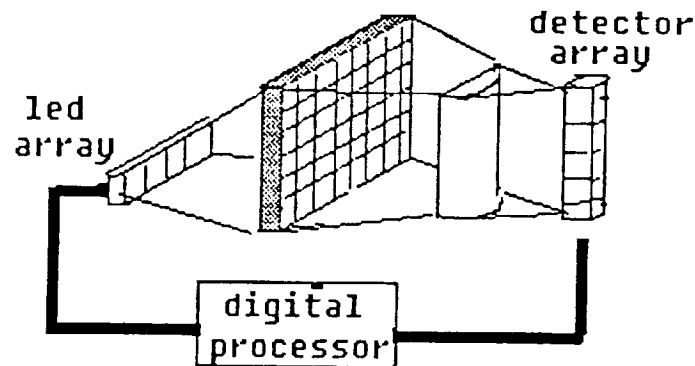


Figure 24. OPTICAL PROCESSOR SHOWING COMPONENT OF HOPFIELD NEURAL MODEL

The Hopfield neural model is designed to recognize a partial or distorted input pattern, or code state vector, as being one of its previously memorized state vectors and to output the perfect and complete memorized versions. In the neurological model, a series of neurons are highly connected by synapses having various interconnection strengths. Each neuron examines the signals at its input via the weighted synapses at a random time, and changes its state according to some probabilistic response algorithm and the sum of its inputs. The input state vector is a series of initial potentials on the neuron nodes and the output state vector is the final stable series of neural potentials into which the network settles after the asynchronous random updating. The neurons at any particular time have a certain probability of changing their state depending upon their

inputs.

The T_{ij} matrix is able to adjust the weights at each of the N^2 data points. This represents an $N:N^2:N$ system. A volume hologram can be used to wire a complex three dimensional system to a three dimensional output pattern to achieve a $N^2:N^4:N^2$ system.

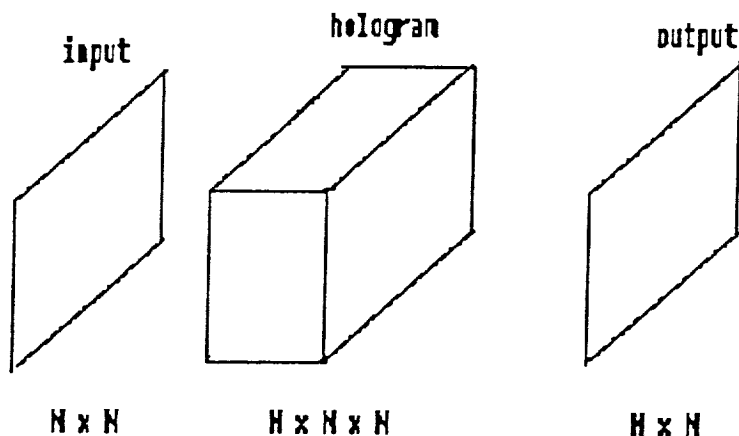


Figure 25. VOLUME HOLOGRAM CONNECTING $N \times N$ INPUT AND OUTPUT FRAMES

To quantify the upper limit to the complexity of interconnection possible in this manner, consider a plane source of area $A \text{ cm}^2$. If the wavelength of the light is $L \text{ cm}$, then the number of resolvable points within the area is A/L^2 . Using light of $1 \mu\text{m}$ wavelength with a 1 cm^2 image, 10^8 points can be resolved. Thus, a holographic element connecting 10^8 points of an input image to 10^8 points of an output image appears to provide 10^{16} independent connections. This apparent scaling, however, is likely to be false. If the dimensions of the elements of Figure 25 are scaled by a factor F , the holographic image would necessarily have to scale by a factor of 4 ($\text{input}^2 \times \text{output}^2$). However, the $N \times N \times N$ hologram can only scale as a factor of 3, in proportion to the volume of the hologram. It follows that the linear packing density of source points that can be allowed if truly free interconnection is to be possible, must at best scale as $F^{3/4} \times F^{3/4} = F^{3/2}$ and the total number of interconnections scales as F^3 as required. For an implementation using barium titanate the maximum index change typically achieved is $dn/n = 10^{-2}$. Thus for a sample of thickness 1 cm , one hundred 100 cycle unit slices will result, each with a 0° or 180° phase thickness state. Each can be considered as a discrete written data point which can be read and tested optically. A hologram 1 cm thick can thus store 10^{10} digital states or resolvable connections which can by the rules developed above connect 10^5 output points. The 10^8 (A/L^2) resolvable points of the input need therefore to contain only 10^5 input points. Spreading these across a $1 \text{ cm} \times 1 \text{ cm}$ input or output plane would require $30 \mu\text{m}$ centers. $30 \mu\text{m}$ centers is compatible with modern

photolithograph fabrication techniques.

If we consider a single point in the input plane and a single point in the output plane and a thick hologram in the far field region between them, then the holographic pattern needed to interconnect them is a three-dimensional plane grating tilted at such an angle as to act as a Bragg reflecting [22]. If cross-talk is to be avoided, a unique set of mirror planes for each input-output point is required. The nature of the Bragg grating is such that light at the same wavelength and angle to the grating normal will be reflected regardless of azimuthal direction. Shown in Figure 26 is an example of this effect. A circle centered around the direction of the normal will connect all possible pairs of points. As can be seen, having selected an input point and an output point, no other point should be located in that circle. The weighting of the interconnect is obtained by varying the strength of the grating index.

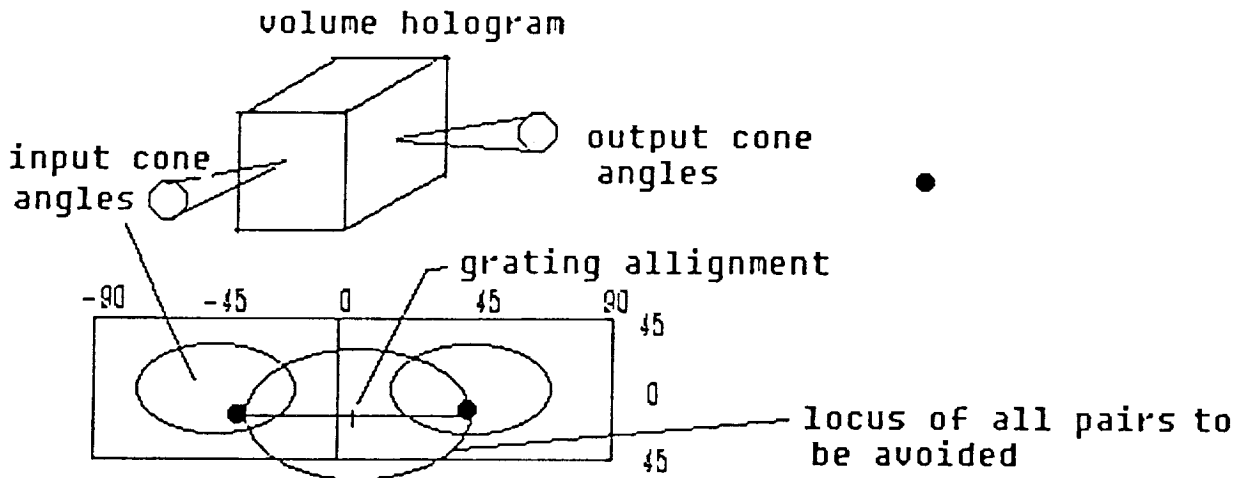


Figure 26. INPUT/OUTPUT CONSIDERATIONS FOR GRATING FORMATION IN VOLUME HOLOGRAMS

Considering both the nature of the holographic element and the information theory presented earlier, careful consideration must be given to placement of input and output data points. The speed of light is about 30 psec/cm. In a 10cm optical path length the light can traverse the distance in well under 1 ns. Liquid crystal spatial light modulators have response times of approximately a millisecond.

6.5 REAL-TIME CORRELATION

In 1964, VanderLugt proposed using a Fourier plane mask for pattern

recognition. His system performed a correlation between functions, f_1 and f_2 , based upon the autocorrelation theorem and the Fourier transform property of a lens and coherent light. VanderLugt used photographic film to record a matched filter, the Fourier transform of the reference image, which was inserted in the Fourier plane of the input image. The correlation of the Fourier transform of the input image and the conjugate of the Fourier transform of the reference image was present at the correlation plane of the system [23]. Such a correlator is shown in Figure 27.

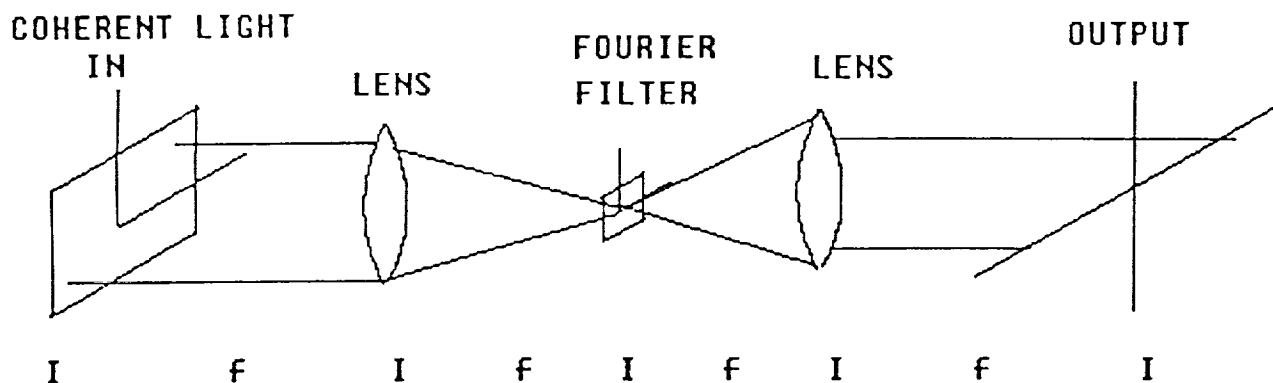


Figure 27. VANDURLUGT OPTICAL CORRELATOR

Goodman and Weaver later proposed another optical correlator, the Joint Transform Correlator (JTC). The JTC presents both the reference and the object image in the input plane and records the Fourier transform of both [24]. The inverse Fourier transform is then taken of the joint transform and thus a matched filter correlation between the signals is achieved.

A coherent optical correlator concept is shown in Figure 28 [25]. To date, a large portion of the laboratory data reported has involved using images on photographic film for an input scene and holographic film spatial filters to store reference images. The real-time image correlation system shown in the figure uses a spatial light modulator to convert the incoherent input scene to modulated coherent light. The incoherent-to-coherent converter is read out using laser light. The resulting coherent image is passed through a programmable spatial filter which contains information about the reference image(s). An extensive amount of research has been performed on identifying the optimal type of filter to be used for correlation. Binary, phase-only, amplitude-only, as well as circular harmonic filters have been used at the filter plane [26],[27],[28]. The choice of which filter to use is application dependent. The correlation signal is detected using a two-dimensional detector array and sent to a computer for analysis. An optical correlator similar in concept to that outlined in the figure, has been demonstrated by the Army Missile Command

and will be flown in a submissile dropped from a heliborn test rig in FY90.

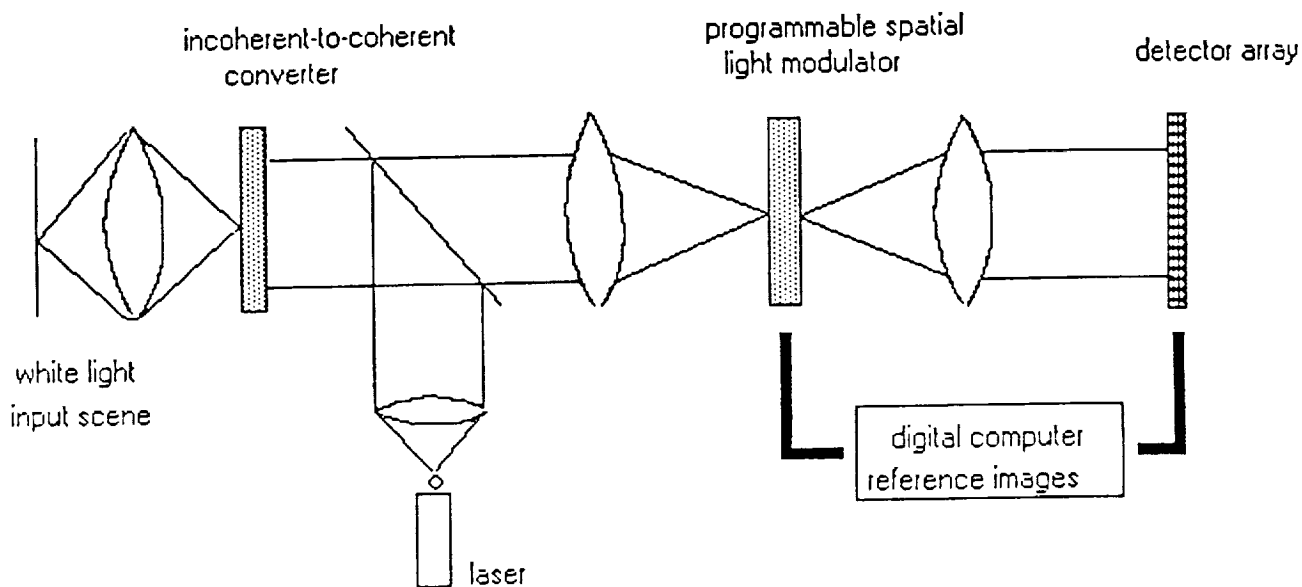


Figure 28. REAL-TIME OPTICAL CORRELATOR

6.6 DETECTOR ARRAYS

A majority of the optical sensing concepts require sensors to convert the optical information to electronic information for processing. Present day solid-state sensors come in three different technologies: photodiode arrays, charge injection device (CID) arrays, and charge-coupled device (CCD) arrays. All three types of sensors work on a similar charge storage technique of photo integration. What differs between the three is the readout technique. The diode array uses a digital multiplexer to combine each signal onto a common video line. The CID array injects charge into the sense node, and the CCD sensor shifts the signal charge in series to an output sensing node. Each technique has its advantages and disadvantages to certain system applications. A list of commercially available detectors is shown in Table 17.

Because of the requirement for a MOS device for the readout of each sensing element, the photodiode arrays typically have on the order of 100 μm centers. This makes high density packaging difficult. Detector arrays are currently available in video formats (app. 512 x 512) with a typical dynamic range of 3000:1.

Charge injection devices were developed by General Electric in the 1970's. CID sensors employ an intracell transfer and an injection of current to sense the photo-generated charge at each sensing element. The sites are addressed by an

<u>MANUFACTURER</u>	<u>FORMAT</u>	<u>PIXEL SIZE</u>	<u>TRANSFER MECHANISM</u>	<u>MAX. FRAME RATE</u>
KODAK	1320 x 1035	6.8 m ²	SHUTTER	10 fr/sec
THOMPSON	1000 x 1024	19 m ²	SHUTTER	30 fr/sec
TEXAS INST.	1000 x 500	12 m ²	FRAME TRANSFER	30 fr/sec
TEXAS INST.	1148 x 488	11 x 13 m	INTERLINE	30 fr/sec
TEXTRONIX	2048 x 2048	27 m ²	SHUTTER	5 fr/sec
FORD	2048 x 2048	20 m ²	SHUTTER	10 fr/sec

06478

Table 17. LARGE FORMAT CCD ARRAYS

x-y coincidence-voltage technique. The ability to randomly access the individual sensing sites by controlling the addressing makes it possible to readout only portions of the array. This makes CID technology practical for high speed applications in which the area of interest covers only a portion of the sensing array. Because of the readout technique it is also possible to perform a non-destructive readout of the CID arrays, in which charge is sensed but not removed from the detecting element. Thus large integrations can be obtained while maintaining readout.

In their simplest implementation CCD's consist of closely coupled capacitors. The signal charge from these photosensitive capacitors is transferred by manipulating the potential of the MOS potential wells. CCD technology is available in several types of readout implementations. Frame transfer, in which the full frame of information from a photosensitive portion of the array is transferred to a portion of the device and is thus non-photosensitive, and is then readout. Interline transfer, in which charge from the elements is transferred from each column of photosensitive elements to an adjacent column of masked elements which are subsequently read out. The last is shuttered: in which the device is shuttered from optical energy until the information can be read out from the device.

4000 x 4000 element CCD area arrays of approximately 5-10 μm^2 elements exist. As the size of the array increases the time required to read out the device scales as the square of the scaling factor. This usually requires multiple readout lines.

Although silicon detectors and CCD imagers are at an advanced stage of development, these devices cannot meet the bandwidths desired in some applications. The additional speed of GaAs technology may be useful. Bandwidths approaching 1 GHz can be approached with GaAs technology. Another attribute of GaAs detector technology is that it is capable of operating at low cryogenic temperatures. The charge transfer efficiency of silicon deteriorates below 70°K. By contrast GaAs CCD's operate nearly as well or in some cases better at temperatures as low as 14°K.

7.0 DEVELOPMENT PLAN FOR THE IMPLEMENTATION OF ADVANCED OPTICAL PROCESSING TECHNOLOGIES FOR THE CONTROL OF LARGE FLEXIBLE SPACECRAFT

7.1 INTRODUCTION

A development plan is presented in the following section. This plan addresses the optical technology areas of materials, devices, and applications which will advance the state-of-the-art of optical technologies and will have the highest payoff for NASA large structural control applications. First a brief overview of the current areas of research interest are presented. Following this, a development plan for electro-optic materials, including ferroelectric photorefractive crystals, NLO polymers, and III-V materials, is presented. The approach for materials development concentrates on identifying and developing a selection of materials which will be able to meet application requirements as well as to meet qualification standards. Next is presented a development plan for optical devices/applications including: neural networks, phase-conjugation, optical computing, SLM technologies, pattern recognition and wavefront sensing and correction devices. Each plan includes specific objectives and a block diagram of plan implementation.

Most promising for spacecraft applications are the areas of neural networks, optical computing and pattern recognition. Neural networks offer the potential for control systems which "learn" about the plant. This would provide a very robust control design with the capability to adapt the controller to a structure which is not mathematically well-known a priori. It would also allow for deviations from the assumed characterization of the structure. This is especially important for large flexible spacecraft where extremely nonlinear and hard to characterize joint behavior dominates. Pattern recognition has been intensely researched for speech and image applications. This technology could be adapted for structural mode identification or matching and optical alignment. Alignment would be necessary both locally as in LDR segment alignment and especially useful in long global optic trains such as in COSMIC, the 100 meter TAT or JPL's SOI. Optical computing would allow very large matrix manipulation for the control of larger plants. This is vitally important in large flexible spacecraft where the plant and controller may need to include thousands of state variables so that the structure and control frequencies do not interfere or overlap.

In the materials area, the III-V compounds appear to be the most promising. Focusing on extending performance and utilizing these in applications such as 4-wave mixing, will be highly beneficial.

The development of the optical technologies must take into consideration not only performance but also the characterization, stability, and the integration of the materials in practical system designs. The areas of research should then be applied in proof-of-concept designs to solve controls problems. From these demonstrated efforts, the devices required for improving the performance of the systems will be identified and an effort should be undertaken to demonstrate and improve their performance.

Optical technologies for the control of spacecraft will provide opportunities for two categories of space systems. The first opportunity is one in which optical processing will perform better than traditional electro-mechanical technology, perhaps faster, lighter, cheaper, etc., with relatively little or no impact on the rest of the system design. An existing mature spacecraft design concept is enhanced with optical technologies. This is the case with the LDR example. The second opportunity is further in the future, where the spacecraft is designed taking into account optical processing and sensing. Both the structural and control system configuration would be influenced by optical technologies, perhaps appropriate surfaces would need to be shielded or exposed for sensing, for example. This second opportunity will be very important once optical processing technologies are demonstrated in the laboratory. Examining overall structural configuration is beyond the scope of this preliminary study.

7.2 CURRENT RESEARCH INTEREST

NASA Langley Research Center has established a basic research activity aimed at developing optical processing technologies for spacecraft control applications. The activity has three prime goals. One is basic technology development, which involves improving the material qualities, processing techniques, and material characterizations. Another is developing laboratory experiments which integrate the optical technologies in a closed-loop optical control system. The third involves an analytic evaluation of control system concepts using the new optical technologies in realistic spacecraft applications. The following section is aimed at addressing the first of these objectives: developing a technology plan to further materials and optical processing technologies. The demonstration plan focuses on laboratory experiments, the second goal of the optical processing activities. This phase is described in the next section, with a detailed series of experiments which integrate the optical technologies in control systems.

7.3 DEVELOPMENT OF MATERIALS

The requirements for large flexible spacecraft control are shown in Table 18. The performance expectations of the advanced optical processing materials and devices are also shown in Table 18. As can be seen in the table, the bandwidth for the sensing requirements for control: 2 KHz for vibration, 500 Hz for mode control, 20Hz for optical form, and 10Hz for precision overall, is above the obtainable bandwidth requirements for the ferroelectric photorefractive crystals, which display an upper limit of approximately 10Hz cycle time. Little progress has been made at increasing their speed or optical purity over the last 20 years. If improvement in materials could be made so that response speed were to increase 10 to 50 times, then a broad range of NASA control applications becomes possible.

The III - V and II - VI semiconductors, semiconductor heterostructures, and the multi-quantum well devices offer GHz operating speeds in many switching applications. Their performance in holographic sensing applications is similar to that of the non-ferroelectric BSO and BGO. They are capable of lms response times but the magnitude of the photorefractive response is about ten to a hundred times less than the ferroelectrics.

NLO polymer materials have been the subject of intense research recently because of the ability to tailor their molecular structures, which have inherently fast response times and large second and third order molecular susceptibilities. As can be seen in Table 18, the speed of the devices for grating response is on the order of Khz. Switching times for the devices exceeds GHz operation. The polymers offer synthetic and processing options that are not available to other materials. Groups at Lockheed, University of Arizona, and University of Southern California are developing devices using NLO polymers. Second order NLO polymers now perform as well as inorganic crystals. Third order materials are just starting to be refined for device implementations. Further research is needed on stability, molecular structure modeling and fabrication of these materials.

A list of the applications for these advanced optical materials is shown in Figure 29.

A summary of the performance relative to controls requirements, is given in Figure 30 for each of the photorefractive candidates discussed in this section.

CONTROL FUNCTION:CONTROL REQUIREMENTSOPTICAL TECHNOLOGY PERFORMANCE

	<u>SAMPLE/</u> <u>SEC</u>	<u>RESOLUTION</u>	<u>RANGE</u>	<u>DEVICE</u>	<u>CYCLES/SEC</u>	<u>RESOLUTION</u>	<u>SPATIAL</u> <u>SIZE</u>
SENSING:							
VIBRATION	2000	.1 μm	10μm	FERROELECTRIC	10	.2 μm	1cm ³
MODE	500	.1 μm	1 mm	CUBIC	1,000	.2 μm	1 cm ³
OPTICAL FORM	20	.3 μm	200μm	SEMI CONDUCTORS	> 1,000	.2 μm	> 1 cm ³
PRECISION OVERALL	10	.3 μm	200μm	NLO POLYMERS	> 10,000	.2 m	> 1 cm ³
				OPTICALSLM	> 100	15μm	
				ELECTRICALSLM	100	30 μm	256 x 256

COMPUTING :

	<u>OPERATIONS/SEC</u>	<u>ELEMENTS</u>
VIBRATION	DEDICATED LOCAL	165
MODE	13 MFLOPS	165
OPTICAL FORM	2 MFLOPS	450
PRECISION OVERALL	24 MFLOPS	33,218

OPTICAL
HYBRID COMPUTERS:OPTICOMP - 819.x.10⁸ BINARY OPSBOC-OUT PERFORMS DIGITAL
ELECTRIC COMPUTERS ABOVE APP. 100
ELEMENTS

- LIMITED BY SLM TECHNOLOGY

Table 18. LDR CONTROL REQUIREMENTS COMPARED TO OPTICAL
TECHNOLOGY PERFORMANCE CHARACTERISTICS

COMMUNICATIONS

- Modulators
- Multiplexors
- Logic
- Repeaters

SERIAL SIGNAL PROCESSING

- Waveguide devices
- Modulators

PARALLEL SIGNAL PROCESSING

- Tuneable filters
- Degenerate FWM
- Phase conjugation

DIGITAL OPTICAL COMPUTERS

- Bistable devices
- Switches

ANALOG OPTICAL COMPUTERS

- Switches
- Neural networks
- Spatial light modulators

Figure 29. SEVERAL OF THE OPTICAL APPLICATIONS OF MATERIALS

MATERIAL

PERFORMANCE FOR NASA CONTROLS

- | | |
|----------------|---|
| Ferroelectric | - response time (100ms) not sufficient for control requirements (>10 Hz) |
| | - crystals of insufficient size (1cm) or of optical quality for system integration |
| | - sensitive to environment |
| Non-FE/cubic | - response time (1ms) fast enough for control (<1KHz). |
| | - diffraction efficiency too low (<10%) for practical implementations |
| | - sensitive to environment |
| Semiconductors | - response times (<ms) are fast enough for controls applications (10 ⁹ Hz) |
| | - magnitude of photorefractive response similar to BSO |
| | - can be monolithically fabricated as detector, processor, emitter |
| | - technology leverage from microelectronics industry |
| | - processing fairly easy |

Figure 30. SUMMARY OF STATUS OF ADVANCED OPTICAL MATERIALS

Of the three materials areas discussed, each has particular advantages and disadvantages. Ferroelectric photorefractive materials are difficult to grow, they have closely coupled performance characteristics, and they are difficult to characterize, but it has been demonstrated that they can make volume holographs and can do phase-conjugation, albeit with either magnitude or time response compromises. Nonlinear organic polymers offer a tremendous potential for large second and third order responses which can be tailored molecularly for given applications, yet there are serious questions as to their long-term environmental stability and a lack of experience in their characterization for these applications. III-V materials and superlattices offer a large payoff in the technology leverage achieved from the microelectronics industry and for their ability to operate as detectors, waveguides, emitters, and light modulators.

The following is a description of technical objectives which should be addressed to insure that producible, well characterized, environmentally stable, high performance materials will be available for a broad range of NASA applications. The proposed objectives represent a balanced development plan which includes materials engineering, performance enhancement, and reliability.

7.3.1 PHOTOREFRACTIVE CRYSTALS

There is considerable doubt as to whether the existing inorganic photorefractive crystal will be able to meet the requirements of control for flexible spacecraft. As discussed above, BaTiO_3 will not meet bandwidth requirements and other photorefractive crystals, such as BSO, do not have sufficient magnitude of response for control applications. Because of fundamental physical constraints, there has been little progress at converging on a material or an enhancement that satisfies both requirements. Significant development is needed to produce crystals of the quality or size for implementation in a working system, and even more effort will be required to demonstrate an enhancement to the crystals that would allow for their application in spacecraft control designs. They are, however, the most commonly used materials for real-time proof-of-concept demonstrations and are capable of generating volume holographs. The suggested development plan for the photorefractive materials is to continue to utilize the materials for proof-of-concept demonstrations, and to continue to monitor or fund at a moderate level, efforts to enhance the material's performance and quality. In parallel, alternative materials should be developed to meet the requirements that the inorganic crystalline materials will not meet. A development plan is shown in Figure 31.

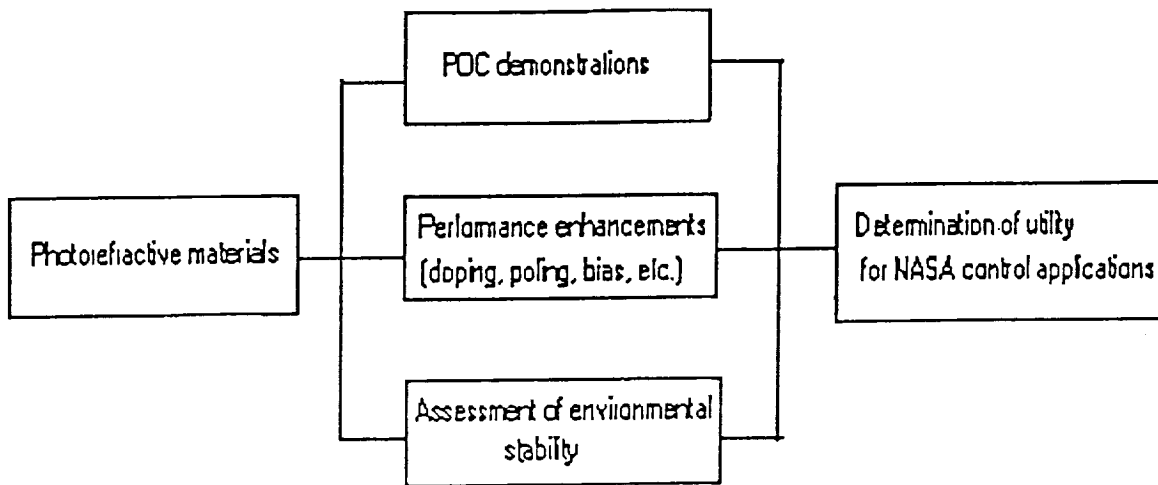


Figure 31. DEMONSTRATION PLAN FOR PHOTOREFRACTIVE CRYSTALS

The following objectives outline this development plan:

- 1) Continue to develop optical technology proof-of-concept devices and systems utilizing photorefractive crystal technology.
 - This will allow advanced optical processing concepts to be demonstrated. It will provide needed feedback for device and materials growth efforts, and will provide a performance indication and a foundation for later system developments aimed at fielding systems based on these or other materials.

- 2) Undertake an effort to enhance the performance of the devices by doping, process modifications, poling, etc..
 - It is necessary to improve the speed of BaTiO₃ and LiNbO₃, and the magnitude of response for SBO, all the PR materials need enhancements to extend their performance into the near-infrared so that they can be utilized with semiconductor sources.

- 3) Determine environmental stability of PRC materials.
 - The limitations of the materials for given applications will be determined and knowledge will be obtained so that architectures can be developed to minimize the materials to environmental susceptibilities.

4) Determine applications of photorefractive crystals for NASA control applications.

- Having determined the physical limits of the technology and the environmental stability, a determination of the utility of photorefractive crystals for NASA controls applications can be made and systems designed to exploit them.

7.3.2 NLO POLYMERS

Nonlinear organic materials offer potential for future optical processing applications. The very large nonlinear response of the materials at very high speeds will allow for the polymers to be exploited in modulators, logic, neural networks, spatial light modulators, and bistable switches. The research into NLO polymers has been very intense over the last several years. In order to assure the success of the material for electro-optical applications, an effort must be undertaken to develop molecular models and an understanding of the chemistry of the materials so that stable large response devices can be fabricated. The ability to independently tailor the performance characteristics of the organic polymers will be extremely useful for system designers. The materials should be processed and integrated into device architectures so that their performance and environmental stability can be better understood. Figure 32 illustrates a development plan to develop the NLO polymer materials for NASA control applications.

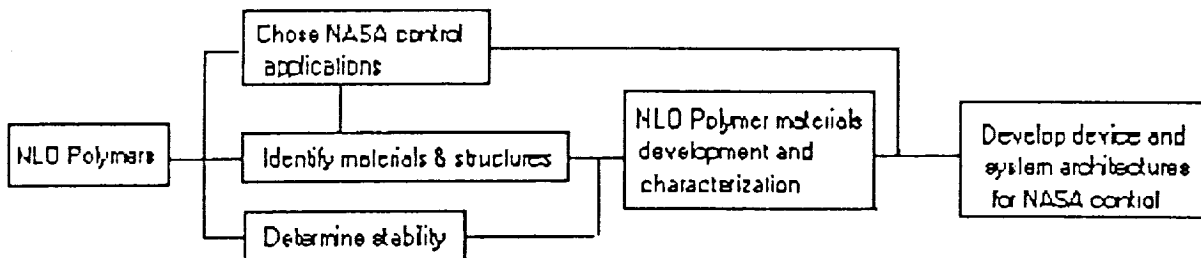


Figure 32. DEMONSTRATION PLAN FOR NLO POLYMERS

The objectives for the development of NLO polymers are:

1) Identify NASA control applications which would benefit from NLO Polymers.

- Because the NLO Polymers can be molecularly tailored for response and are easy to process, it would be beneficial to identify a mission derived specification which a material can be developed to

meet. This would demonstrate the versatility of the material.

- 2) Identify materials and molecular structures of interest for the NASA applications.
 - There is a range of organic polymers which could be used for a variety of second and third order response architectures. Applications should be chosen and materials identified, specified, and produced to meet those applications.
- 3) Characterize the NLO polymer materials and determine their environmental stability.
 - Although progress has been made on understanding the molecular structures of the materials and in their processing, an effort is needed to determine their environmental sensitivities. The long term stability of the materials, the thermal stability of the poled states, and the electrochemical effects of electrodes have not been studied and would provide much needed feedback for the development of the material technology.
- 4) Demonstrate and refine NLO polymers in proof-of-concept architectures.
 - Despite chemical synthesis, theoretical calculations, and orientation processing, successful transfer of NLO materials to practical applications depends on reliable measurements and performance characterization in device configurations.
- 5) Demonstrate the material in system architectures.
 - The large nonlinear response, the speed of response, and the ease with which the device can be tailored will enable it to be applied on optical neural networks, optical modulators, spatial light modulators, logic, and phase conjugation.

7.3.3 III-V MATERIALS

As mentioned above, the III-V semiconductors, primarily GaAs, have received considerable attention because it is possible to manufacture integrated sources, detectors, switching devices, and processing elements on the material. As was demonstrated with the announcement of the AT&T photonic IC based on S-SEED technology, GaAs and GaAs heterostructures will be utilized in future optical

processing designs. In addition to the SEED devices, various commercially available SLMs have been designed with GaAs. Having been demonstrated for photonic IC's and for switching devices, the technology still has to make headway into the holographic and beam coupling applications. There would be a tremendous payoff for the technology if the magnitude of photorefractive response could be increased and four-wave mixing and beam coupling demonstrated. The response of the material is similar to that of BSO (BSO has an EO coefficient of 5, GaAs is 1.5). If the photorefractive response could be improved through modifications to the structure or in the composition, the material would be a front runner for implementation of a majority of applications. Figure 33 illustrates a development plan for the III-V semiconductors with GaAs the primary focus.

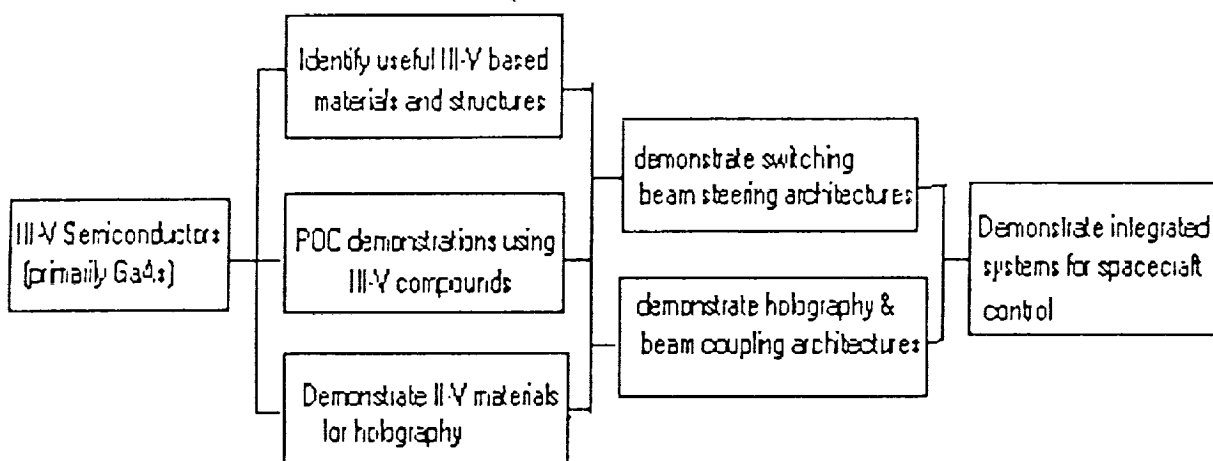


Figure 33. DEMONSTRATION PLAN FOR III-V SEMICONDUCTOR MATERIALS

The III - V semiconductor materials development objectives are:

- 1) Identify sources of materials for switching devices, holographic applications, and for use in the infrared.
 - Because III-V materials and III-V quantum well devices are emerging as the technology of choice for optoelectronics devices, structural, and doping modifications should be explored to enhance the holographic utility of the material, to extend the response into the infrared, and for monolithic emitter, detector, and processing elements.
- 2) Demonstrate proof-of-concept architectures for NASA control with III-V materials.

- Proof-of-concept demonstration with GaAs will provide a basis for future system architectures. Integrated and monolithic devices based on GaAs technology should be demonstrated. As new devices such as laser diode arrays or SEED arrays are announced, they should be integrated in system designs.
- 3) Demonstrate the photorefractive response of the III-V semiconductors and derivatives.
- Although GaAs has been utilized for switching and for SLMs, application of GaAs for holography and beam coupling has not been the subject of as intense research. JPL has done some work on demonstrating the capability of GaAs for image transfer.
- 4) Integrate emitter arrays, waveguide devices, SLMs, and detector arrays in system architectures.
- Integrating entire 3-dimensional architectures with III-V based technologies for beam switching, logic, and computing will provide a basis for all optical computing designs and will provide the foundation for a reliable, producible, optical architecture.
- 5) Integrate the II-V materials in sensing and processing system architectures.
- Integrating holographic, interferometric, and beam coupling III-V devices into system architecture will provide the foundation for advanced photonic wavefront sensing and optical processing applications.
- 6) Integrate and demonstrate all of the functions of the materials.
- Materials such as GaAs and its derivatives can be used as switching devices, as SEED digital memory, as SLMs, as holographic elements, emitters, detectors, as well as for analog and digital electronics. Exploiting all of the potentials of the technology will lead to the development of a future all optical control system.

7.4 DEVELOPMENT OF EO DEVICES AND APPLICATIONS

With the exception of spatial light modulators and optoelectronic

integrated circuits, there have been few advanced device architectures based upon optical technologies. This has been for several reasons. One reason is that the materials technology has not been mature enough, or with necessary performance, to support device architectures. Another reason is that there has not been a concentrated effort to develop devices based upon the specifications of a chosen architecture. There has thus been no directive to develop optical processing devices or innovations. A good example of application spurring innovation is illustrated in the development of real-time optical correlators. The Army Missile Command has developed an optical correlator based on the Hughes liquid crystal light valve, a technology that is over a decade old. To accommodate the slow response and the low sensitivity, the correlator was mounted on a large telescope. The recent development of such optical correlators demanded faster and higher resolution spatial light modulators. The industry has responded in recent years to these needs by producing several high resolution and fast SLMs and consequently optical correlators which are promoting a wide variety of optical processing technology areas. The demand for high definition television is another application that has demanded the development of advanced display technologies. The following discussion will detail several application areas that may enhance NASA's ability to control large flexible spacecraft. The primary objective is to apply these developing concepts to solve a "real life" problem so that insight into the performance and limitations of the optical processing technologies can be gained.

The following section outlines a series of objectives for a NASA study of applications of concepts to utilize optical processing technologies, and may be applied for the control of flexible spacecraft. The objectives outline application areas to be explored. The primary objective is to implement the concepts, solving a real life problem, so that insight can be gained into the performance of the optical technologies in a configuration applicable for control system designs.

7.4.1 NEURAL NETWORKS

An area of interest in optical processing technology which could have extremely high payoffs for NASA controls designs is that of optical neural processing. Addressing the problem of decision making under variable conditions, neural network concepts have been researched to provide systems with a better ability to react appropriately in a changing and variable environment. Electronic neural implementations have just recently been achieving headway in various applications, including pattern and speech recognition. As was discussed previously, the vast three-dimensional interconnections and parallelism of optics makes it a very good candidate for implementing neural systems. A suggested

development plan for NASA controls implementations would be to demonstrate single neural node and single plane neural networks to validate the use of optical technologies for these applications. The second stage of development would be to implement optical neural systems for NASA control system designs. Figure 34 illustrates the demonstration plan for neural applications of NASA controls.

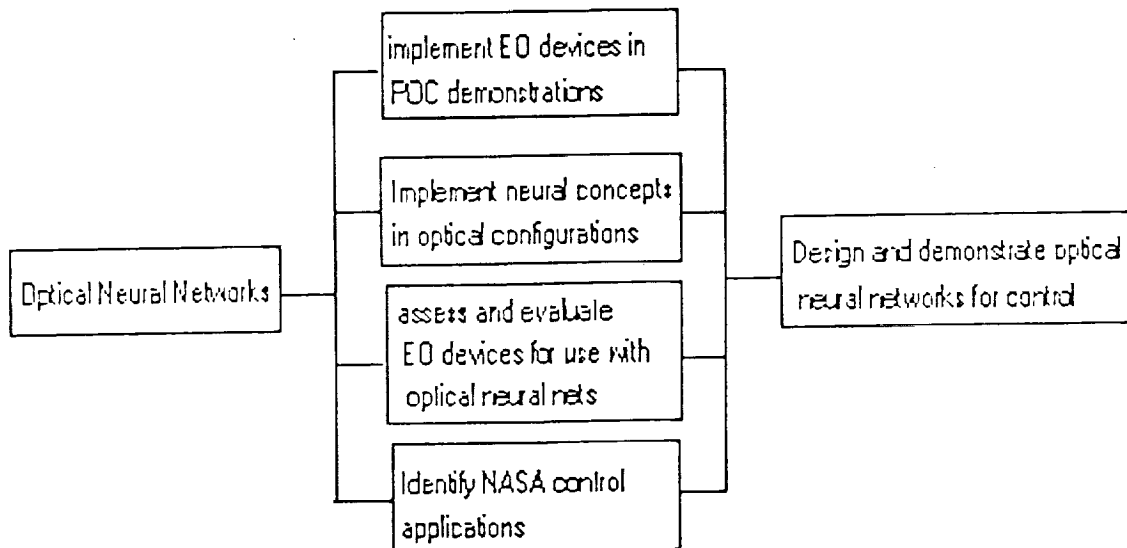


Figure 34. DEMONSTRATION PLAN FOR OPTICAL NEURAL NETWORKS APPLIED TO NASA CONTROL SYSTEM DESIGNS.

The objectives for a demonstration plan to apply optical neural concepts to NASA control applications are:

- 1) Identify NASA applications that would benefit from optical neural technologies, ie. mode shape identification and control, robust control for incompletely characterized structure.

- Because of their ability to learn and to operate under variability, neural architectures could significantly enhance methods of structure control. Neural concepts for spacecraft control should be identified and developed.

- 2) Implement neural concepts in optical configurations.

- Various neural structures (Hopfield, Adaptive Resonant Theory, etc.) should be developed in optical architectures so that they may be utilized in system designs. Because of the vast number of interconnects and parallel nodes, most neural concepts can only be

simulated on supercomputers.

- 3) Assess and evaluate optical devices to be implemented in neural networks.
 - Large parallel switching arrays, holographic devices, beam coupling, and nonlinear devices which are currently being developed should be implemented in neural network designs to demonstrate their utility and performance for the application.
- 4) Implement devices and neural models in proof-of-concept demonstrations of the components of a neural control system.
 - Paradigms and algorithms for implementing the control problem in a neural architecture should be developed. The demonstration of the neural architecture will outline areas of the technologies that need development and will provide validation of the concept.
- 5) An optical neural network should be designed and demonstrated for the control of flexible spacecraft.
 - The concepts and paradigms demonstrated in the previous tasks, and the experience and knowledge gained from them, should be implemented in a neural network for spacecraft control. Implementation of the neural concepts provides feedback containing information related to the performance, performance sensitivities, and limitations of materials and devices and will prove the utility of optics for neural designs.

The following is a list of devices which may be utilized in an effort to develop optical neural networks for control: volume holographs, spatial light modulators, phase conjugate devices, emitters, detectors, beam modulators, and degenerate four-wave mixing.

7.4.2 OPTICAL COMPUTING

A majority of the work in optical computing is supported by DARPA or RADC. The key to the development of optical computers is the ability to invent not only the devices necessary, but also the mathematical methods, so that algorithms can be implemented in optics. Examples of algorithm manipulation for implementation on optical computers were given in the state-of-the-art assessment portion of this report. Because aspects of computing such as carry and branching operations

cannot readily be performed in digital optics, whereas large spatially parallel operations can, alternative methods must be developed to optimize problems for implementation in optics. An illustration of the development plan for optical computing concepts for spacecraft control is shown in Figure 35.

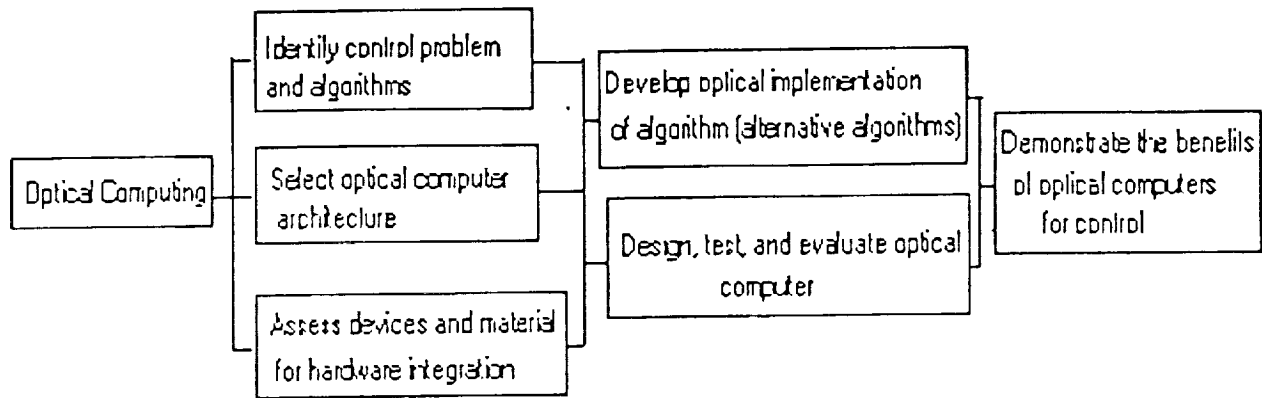


Figure 35. DEVELOPMENT PLAN FOR OPTICAL COMPUTING CONCEPT IMPLEMENTATION FOR THE CONTROL OF FLEXIBLE SPACECRAFT

The objectives for the demonstration of optical computing concepts are:

- 1) Identify NASA mission's control system design and algorithms for implementation in optical processor designs.
 - A majority of CPU time is spent solving systems of algebraic equations. Optics can beneficially impact control system designs by reducing the number of state variables or by handling the large matrix computations. Large flexible space structures may require modal models with thousands of states. Control problems with a large number of elements should be identified so that optical implementation benefits can be demonstrated.
- 2) An optical processor design should be chosen.
 - An optical processing or a hybrid optical processing design should be identified for the NASA controls problem. The choice of system should reflect the nature of the control problem.
- 3) Assess devices and materials for implementation in the optical computer design.
 - Based upon the nature of the problem, the size of SLMs, the speed of

operation, the switching mechanism, etc. should be identified and the proper device or material should be chosen for the computer design.

4) Mathematical methods or matrix transformations which could solve the problem optically, ie. residue, symbolic substitution, etc., should be developed for the control application and for the optical computer hardware design.

- Because many algorithms have been developed for the speed and accuracies of conventional digital electronic technologies, a study must be performed on the control system and control laws using an optical processor. A simulation of the system should be performed to determine how many bits of accuracy are required, what the impact of input errors has on the system, and the speed of convergence of the system.

5) Design an optical computer for a closed-loop NASA control system.

- Having identified the devices for implementation and having developed algorithms for implementation on the optical computer, a hardware design can be developed and tested.

6) Demonstrate the optical computer and the control algorithms in a laboratory closed-loop control system.

- Developing the optical computing hardware, the mathematical methods, and the control system architectures, to solve a real-life NASA controls problems would provide a very valuable indication of the performance, the benefits, and the limitations of optical computing designs. The cost, performance, reliability, and size and weight benefits can be determined.

7.4.3 PATTERN RECOGNITION

Real-time pattern recognition techniques have been demonstrated for a broad range of applications. The MICOM demonstration of an optical correlator for targeting will provide one of the first demonstrations of advanced optical technologies in a real-time system. Pattern recognition concepts can be utilized for mode identification, structural control, and optical alignment. If modal responses can be "recognized", then appropriate actuation can be applied for structural control. The concepts have to be developed, and the devices

identified and developed, which would allow for pattern recognition systems to be used for control system design. An illustration of a development plan for pattern recognition concepts to be utilized in spacecraft control systems is shown in Figure 36.

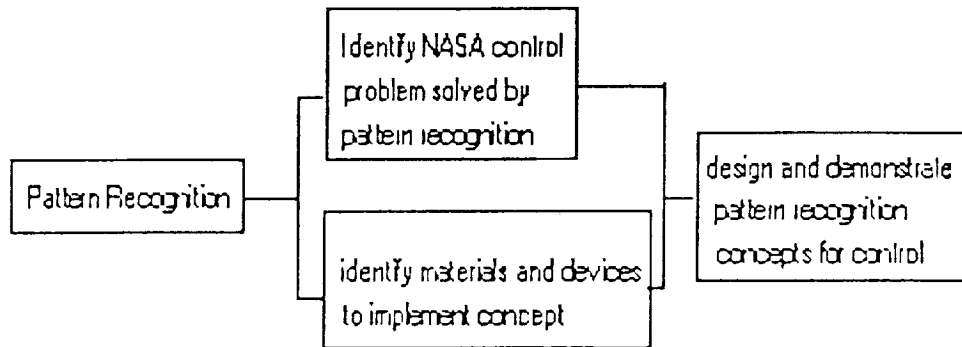


Figure 36. DEVELOPMENT PLAN FOR UTILIZING REAL-TIME PATTERN RECOGNITION AND CORRELATORS FOR SPACECRAFT CONTROL.

The development plan for utilizing pattern recognition for spacecraft control consists of:

- 1) Identify NASA controls problems which may be enhanced by optical pattern recognition techniques.
 - Optical correlators have been demonstrated in real-time systems. Applications of optical correlation to such problems as mode recognition or figure control should be identified for a NASA mission.
- 2) Identify materials and devices for pattern recognition for control implementations.
 - Devices and materials should be developed so that real-time correlators and pattern recognition concepts can be realized. Devices such as SLMs and volume holograms must be made in larger formats and with larger bandwidths for many controls applications.
- 3) Perform a proof-of-concept demonstration of the optical correlation technique to the chosen application.
 - Demonstration of the correlation technique will provide feedback as

to the performance of the technology for control implementations and will highlight optical processing technology areas that need development support. The concept potentially will greatly reduce the number of state elements which must be sensed, reducing the computational load on the main control processor. It may also allow for local processors to be utilized which would distribute the burden of the control.

7.4.4 WAVEFRONT SENSING AND WAVEFRONT CORRECTION DEVICES

The demonstrated utility of optical materials for non-destructive testing of objects has proven the effectiveness of real-time wavefront sensing to examine the state of a structure. To date, many of the interferometric measurements made with holographic materials have not had sufficient bandwidth for NASA control application. A majority of the wavefront correction techniques require a double-pass scheme to correct for optic or atmospheric distortions. The ability of holographs to store three-dimensional images makes interferometry based on advanced optical technologies desirable. However, the strict laboratory setups required for these measurements and the slow response of the holographic mediums has precluded such devices from implementation in system designs. A development plan is illustrated in Figure 37 and discussed in the following text.

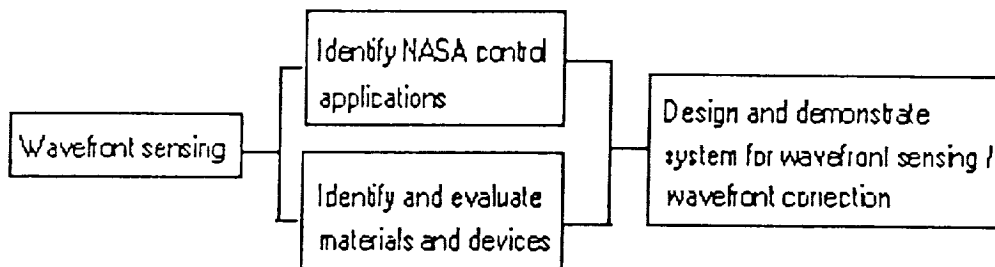


Figure 37. DEVELOPMENT PLAN FOR THE DEVELOPMENT OF WAVEFRONT SENSING APPLICATIONS FOR NASA CONTROL SYSTEMS

The objectives of the interferometry and wavefront correction development plan are:

- 1) Identify NASA mission requirements for interferometry and wavefront correction.

- There have been numerous laboratory demonstrations of interferometry and of wavefront correction. What is needed is an identification of a NASA mission-driven set of requirements and a system developed to

perform to these specifications. It is felt that many of the systems demonstrated to date are not fast enough for practical application. The mission requirements may, therefore, demand that new materials be utilized in such designs.

2) Identify materials and devices which would allow for faster and larger response interferometric images to be formed in real-time.

- Materials do not exist with a fast enough response for practical interferometry to be performed in a majority of NASA missions. There needs to be a development of materials for such applications to become practical. The devices and materials needed for practical implementations need to be identified and developed.

3) Design and demonstrate interferometric and wavefront correction systems for implementation in NASA control applications.

- Interferometric and wavefront correction systems need to be designed and demonstrated for practical NASA mission control requirements.

8.0 A PROPOSED DEMONSTRATION PLAN

8.1 INTRODUCTION

Proposed large flexible space systems, such as optical telescopes and antennas, will require control over vast surfaces. Most likely distributed control will be necessary involving many sensors to accurately measure the surface. Some proposed control schemes use many conventional electrical and/or electro-mechanical sensors placed at strategic locations to determine the system response. Information from these myriad sensors must be processed rapidly. After an appropriate complex control algorithm determines actuator commands, a similarly large number of conventional actuators must act upon the system. Potential bottlenecks to this type of control system include too large of a processing time due to both the number of components and the transmission delay times and excessive weight, cost, and complexity due to the large number of components. Recent advances in optical technologies may provide lightweight and rapid sensors and processors. Also, optical technologies most likely will have reduced power requirements, increased reliability, lower cost, reduced complexity, and an improved ability to calibrate. Because optics are capable of processing information in parallel, are capable of massive connectionism in three-dimensions, are immune to electromagnetic interference, and operate at the speed of light, they are ideally suited to advanced processing and neural concepts in which conventional electronics either fail or have significant drawbacks. In addition, a possibility exists to correct system errors due to structural flexibility solely in the optical domain. Therefore, the use of advanced optical components may be either enhancing or truly enabling for future NASA missions.

In general, photonic materials and devices can still be considered to be in the basic research stages of development. Many concepts are still experimental with a lack of device maturity. Materials quality and characterization is not fully defined. Many have long response times and alignment problems. Other problems include optical distortions and inaccuracies and environmental sensitivities. Also, these devices have not been demonstrated for use in structural control of spacecraft where an integrated sensor/processor/computer/control package will be required. Subcomponent electro-optical proof-of-concept demonstrations have been performed but no integrated e-o experiment has been shown to date. Experiments are required to establish material and device environmental stabilities, focus material and device developments, identify technology long poles, and define the state-of-the-art in integrated designs. The proposed experiment would provide such a demonstration and also yield a testbed with which to develop and test new

technologies and devices such as holographic materials, phase-conjugate devices, etc.

8.2 POTENTIAL APPLICATIONS

The use of electro-optical technologies in large flexible spacecraft appears most promising in distributed sensing, parallel processing, integrated sensing and computing, and wavefront control. Many proposed missions will either require or would benefit from one or all of these technology areas. For example, the Large Deployable Reflector (LDR), a precision optical system, will be a dedicated astronomical space observatory operating in the spectral region between 30 micrometers and 1 millimeter. The baseline concept consists of a Cassegrain telescope with a segmented, actively controlled 20 meter primary reflector composed of 37 segments. Active control of the optics is anticipated with potential candidates including edge sensors, wavefront error measurements, or directed laser range finding to control the position and orientation of each optical segment. In addition, active pointing and structural vibration control will be required. This system would most likely require all four areas of technology where optics would be either enhancing or enabling. Sensing of all the segments will require distributed sensors. Parallel processing would speed computation and such a large flexible system might require a controls and plant model with hundreds or thousands of state variables to assure no structural control interaction. Integrated sensing and computing might yield faster response. Wavefront control will be essential.

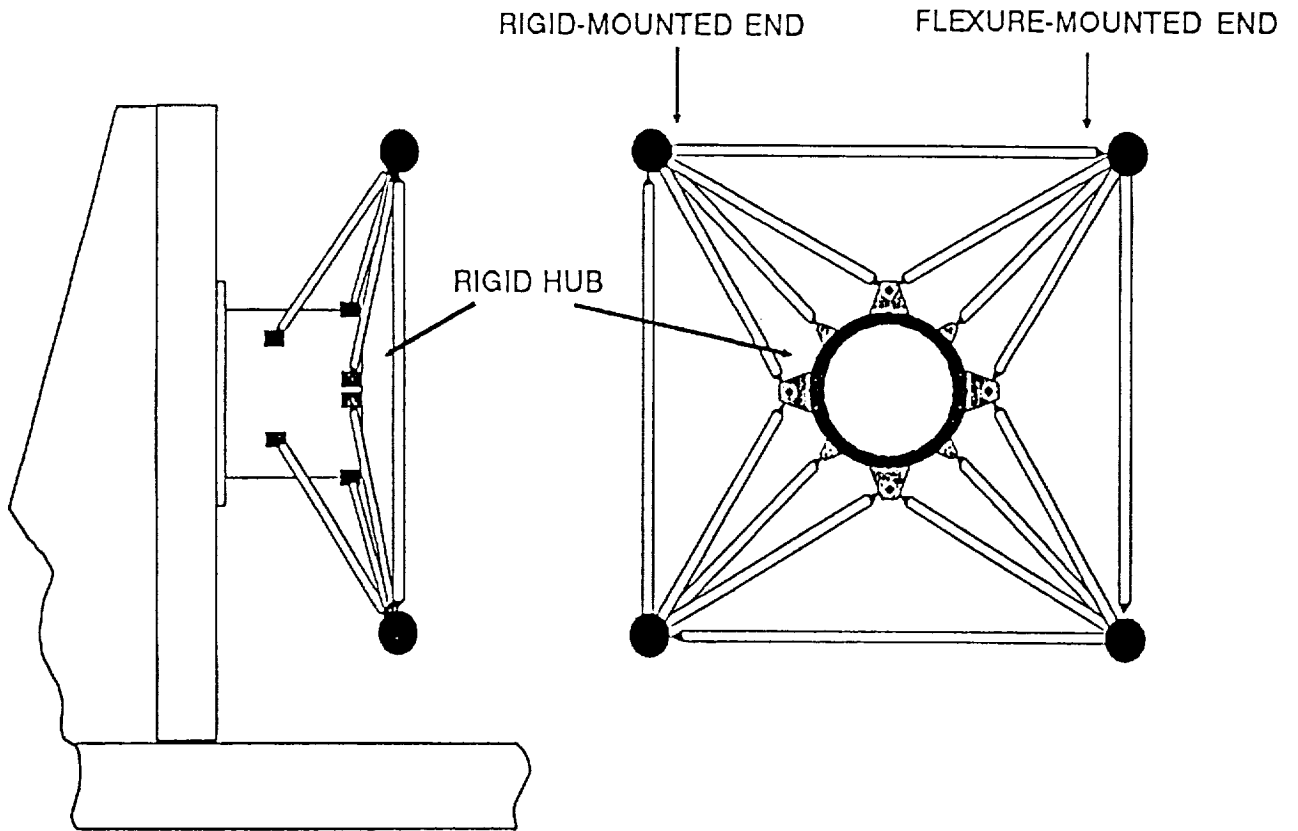
The use of electro-optical technologies would yield numerous advantages in large space systems. Distributed sensing using photonic devices would require fewer sensors than traditional electrical or electro-mechanical sensors. Fewer parts would increase reliability and probably lower weight and power requirements. Massive parallel processing would allow very large scale problems to be solved. Mathematical detail could be included in plant and controller models and designs. Integrated sensing and computing would provide very fast solution with no time delay and the ability for high data rates plus reduce the number of moving parts. The use of optical devices for wavefront control could result in designs without mechanical devices.

8.3 ELECTRO-OPTICAL STRUCTURAL CONTROLS EXPERIMENT

8.3.1 EXPERIMENT OVERVIEW AND CONFIGURATION

Our proposed approach would utilize a two-dimensional ring structure with corner reflectors as shown in Figure 38. The test article configuration

Figure 38. PANCAKE TRUSS ARRANGEMENT



would be highly traceable to several NASA missions which require a relatively small spacecraft bus which supports a large experiment sensor such as a large antenna or telescope. Such a generic space system structure would be traceable to such missions as the Advanced Communications Technology Satellite, Large Deployable Reflector, Coherent System of Modular Imaging Collectors (COSMIC), Thinned Aperture Telescope (TAT), and large interferometers such as the Spaceborne Optical Interferometer (SOI), and the Infrared Interferometer (II). This structure could also represent a portion of a large platform system such as the reflector on the Geostationary Platform.

This configuration is directly traceable to a large primary mirror such as found in the LDR. The truss elements must support compression. Element cross-sections must be appropriately sized since even slight curvatures can significantly affect stiffness. It is very important to achieve a flexible truss with good, well understood properties. Stiff tubular truss elements are required to avoid structural bending modes. Rigid attachments will be needed for displacing mass points to avoid mass rotation modes. In order to achieve the appropriate flexibility, special end-weakening techniques will be used. Either masses at the center of the flexible end plate on the strut tube will be attached at the base end of the truss element and some mass ends or multiple slots in the strut tube wall near one end will be implemented. Figure 39 provides examples of these truss element modifications. Actuators can be integrated with either end-weakening approach.

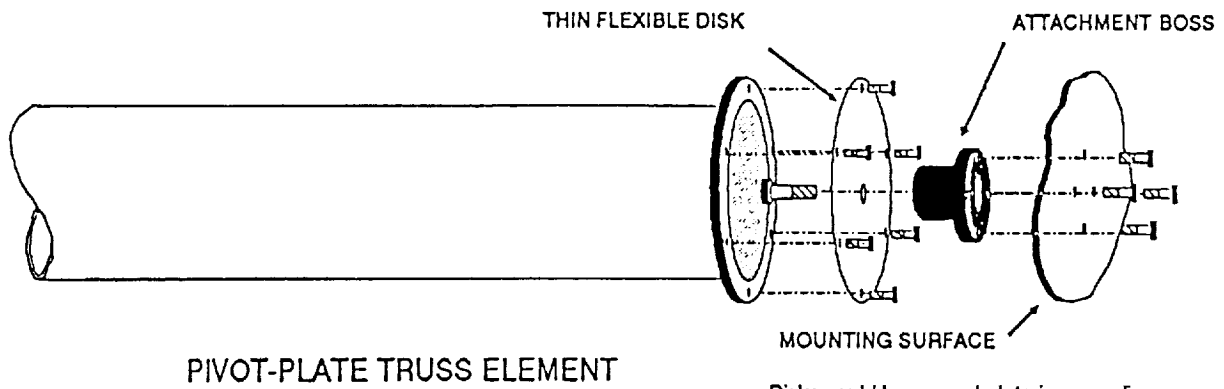
8.3.2 OBJECTIVE

The principal objective of the experiment plan will be to demonstrate a series of major optical sensing milestones leading to an optical processor capable of identifying and quantifying a number of the modes in the structure. The second objective will be performing a closed-loop control of one or more modes.

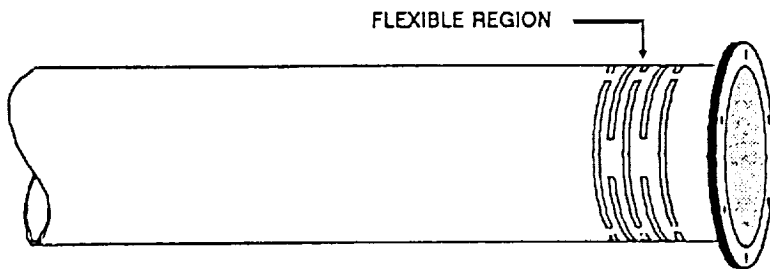
8.3.3 APPROACH

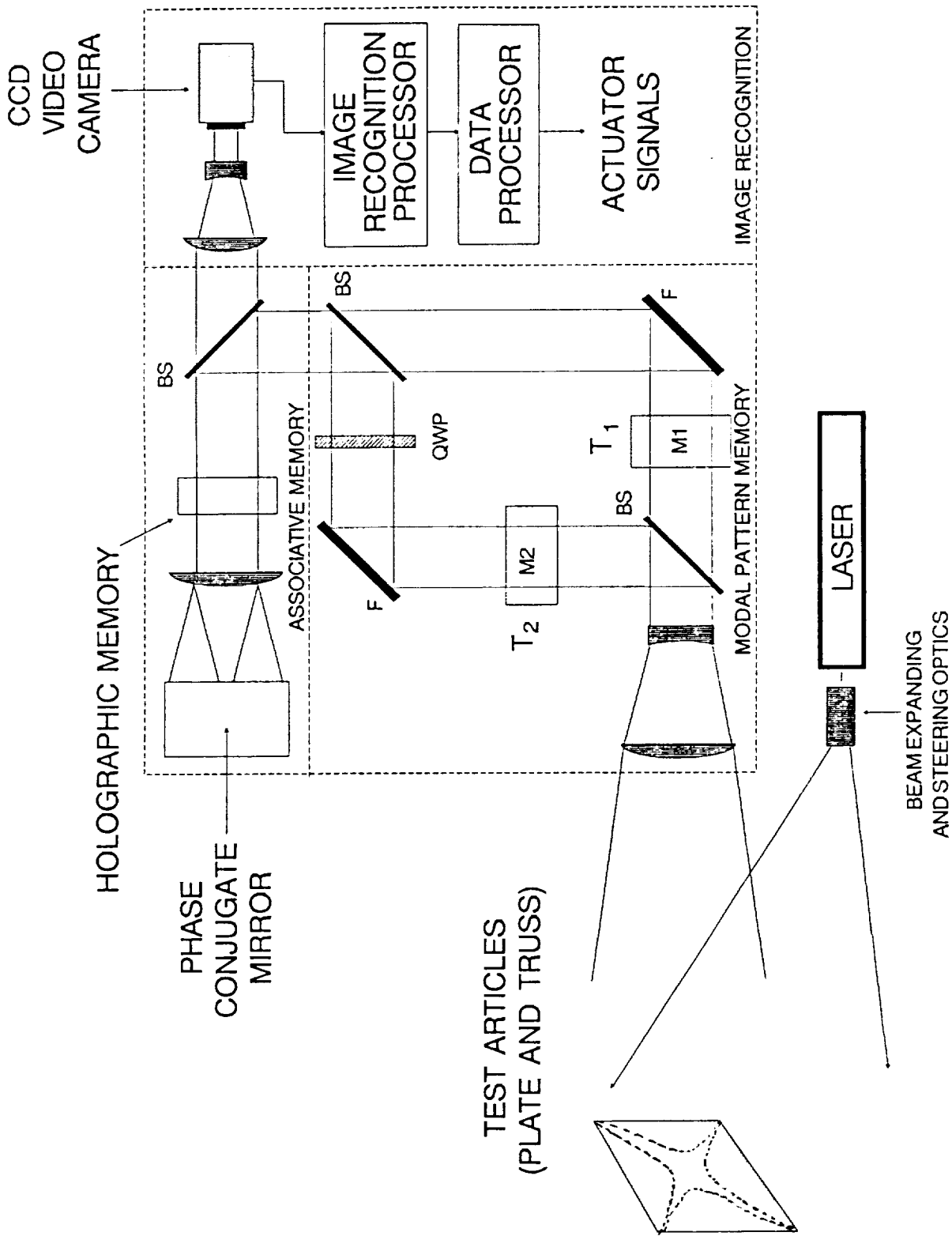
The experiment approach is to develop a modal pattern recognizing system as illustrated in Figure 40. We would use the current NASA Langley optical memory setup as shown in Figure 40 as a modal pattern memory. Photo-refractive memories M_1 and M_2 are latched at times T_1 and T_2 , respectively, to record a time lapsed holographic record of the flexible structure modal pattern displacements. This is a Mach-Zehnder interferometer configuration which provides a difference output which can be interpreted by an associative memory. It is proposed to assemble and demonstrate the associate memory system separately at first, then later integrate it with the modal pattern memory.

Figure 39. TRUSS ELEMENT CONFIGURATION EXAMPLES



Disks could be cascaded to increase linear range but then lateral force is a problem.





TEST ARTICLES
(PLATE AND TRUSS)

Figure 40. MODAL PATTERN RECOGNIZING SYSTEM

The associative memory, shown in detail in Figure 41, consists of a half-silvered mirror, a holographic memory element and a phase-conjugate mirror. The associative memory can recognize two images with common features. Multiple modal images are stored in the memory element at different reference beam angles. The input to the associative memory comes from the Mach-Zehnder modal pattern memory. The output of the associative memory is the undistorted modal pattern or patterns which best match the stored patterns. Modal identification and quantification is achieved by using image recognition techniques applied to the associative memory output. Thus, the complete sensing-processing system in Figure 40 consists of three major subsystems: the modal pattern (difference) memory, the associate memory and the image recognition subsystem. Output from the image recognition subsystem will be the quantitative mode, amplitude and phase data which can be processed by a typical conventional processor to control the test article actuators to perform a closed-loop demonstration.

Figure 42 shows two proposed controllers for the pancake truss. The top portion shows a conventional processor which will control 12 structural modes using 20 sensor signals and 8 actuators. A typical conventional processor would be able to accommodate the 1250 floating point operations per sample (flops) with a rate of 200 samples per second. With assumed housekeeping requirements included, a conversion factor of 1.6 is used to determine a total requirement of 400,000 flops.

The bottom portion of the figure shows the preferred testbed with an integrated optical processor. Here the computational burden is shared by the conventional and optical processor resulting in faster throughput and the potential for control of many more structural modes. The optical processor would identify the modes while the conventional processor might contain the control algorithm and/or actuator commands. The proposed modal processor is derived from optical processing concepts which are currently described in the literature and in laboratory evaluation.

8.3.4 MILESTONE PLAN

A three year program to demonstrate the optical processing for modal sensing and identification is proposed. In the fourth year, a closed-loop control demonstration would be performed.

The major milestones are shown in Figure 43. The first year would be for the design, fabrication and testing of an optical associative memory using a

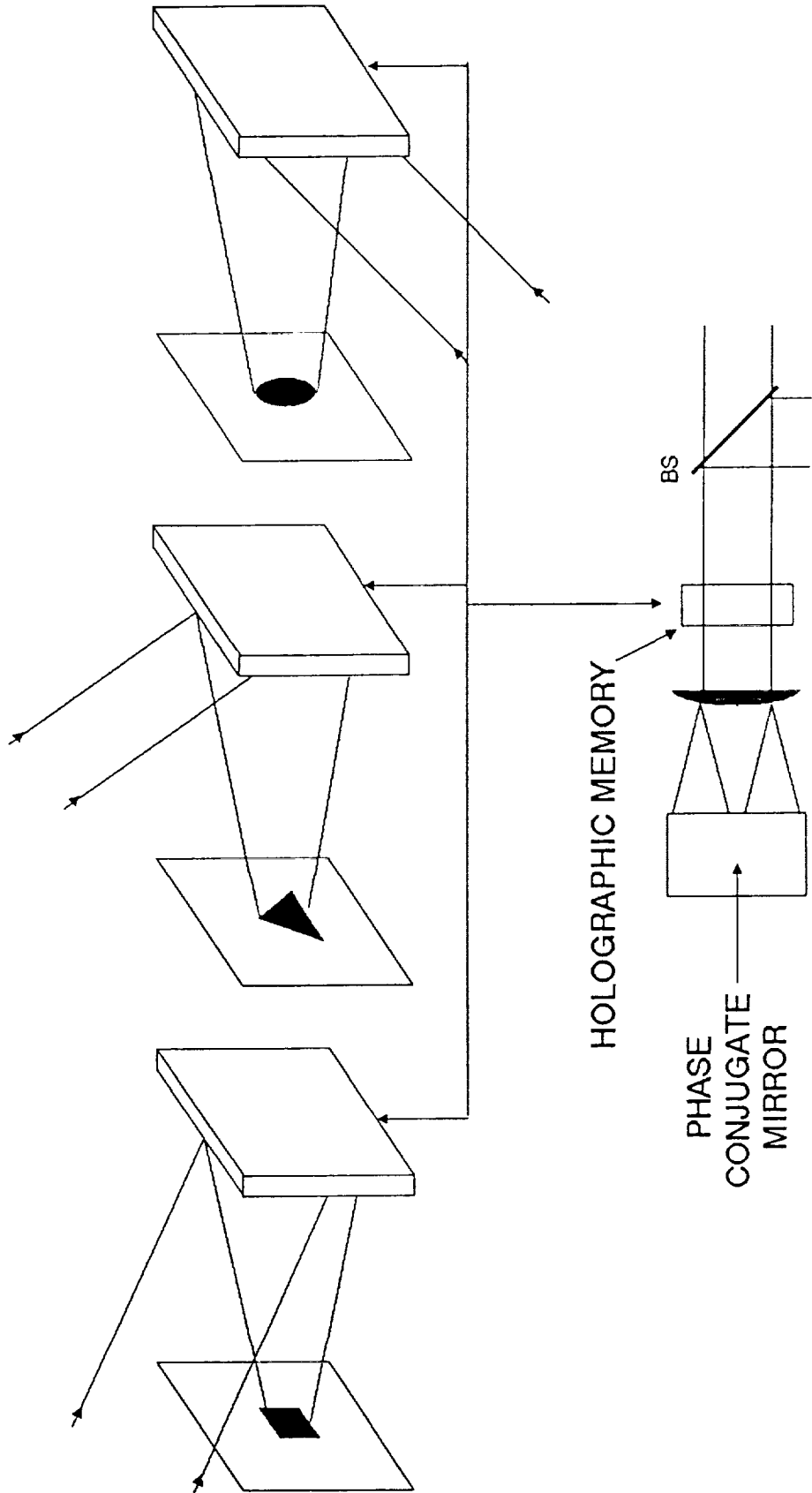
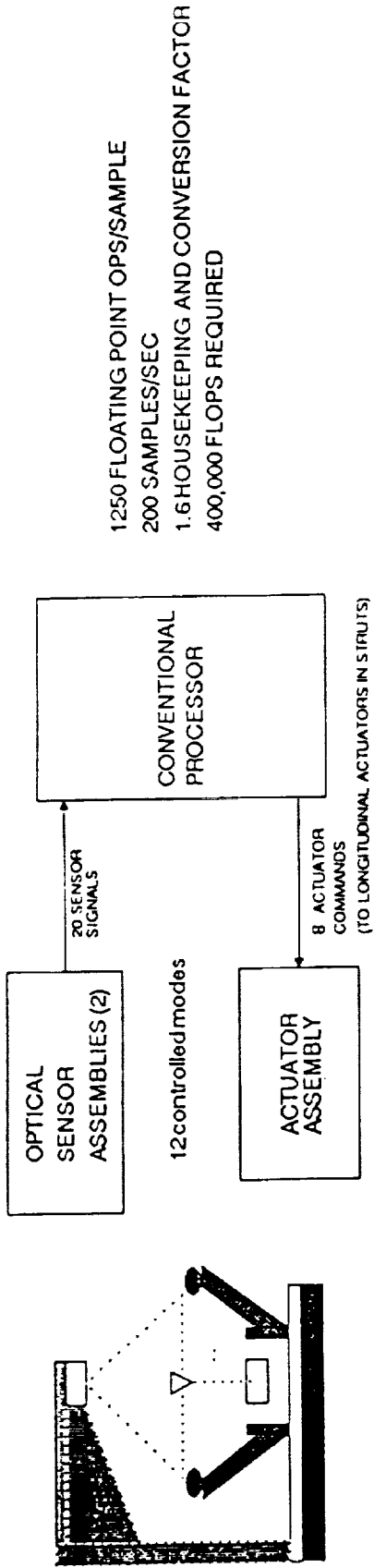


Figure 41. DETAIL OF OPTICAL ASSOCIATIVE MEMORY

WITH CONVENTIONAL CONTROLLER



WITH OPTICAL PROCESSOR INTEGRATED

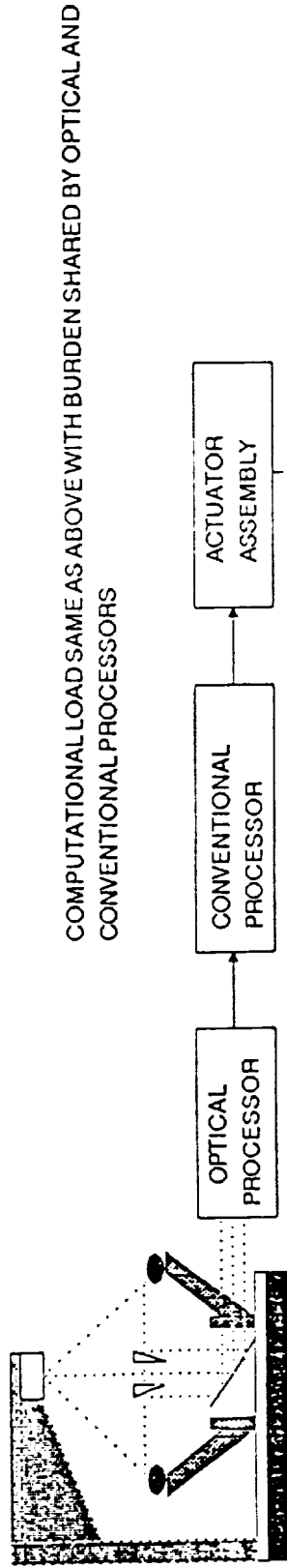


Figure 42. CONTROLLERS FOR PANCAKE TRUSS

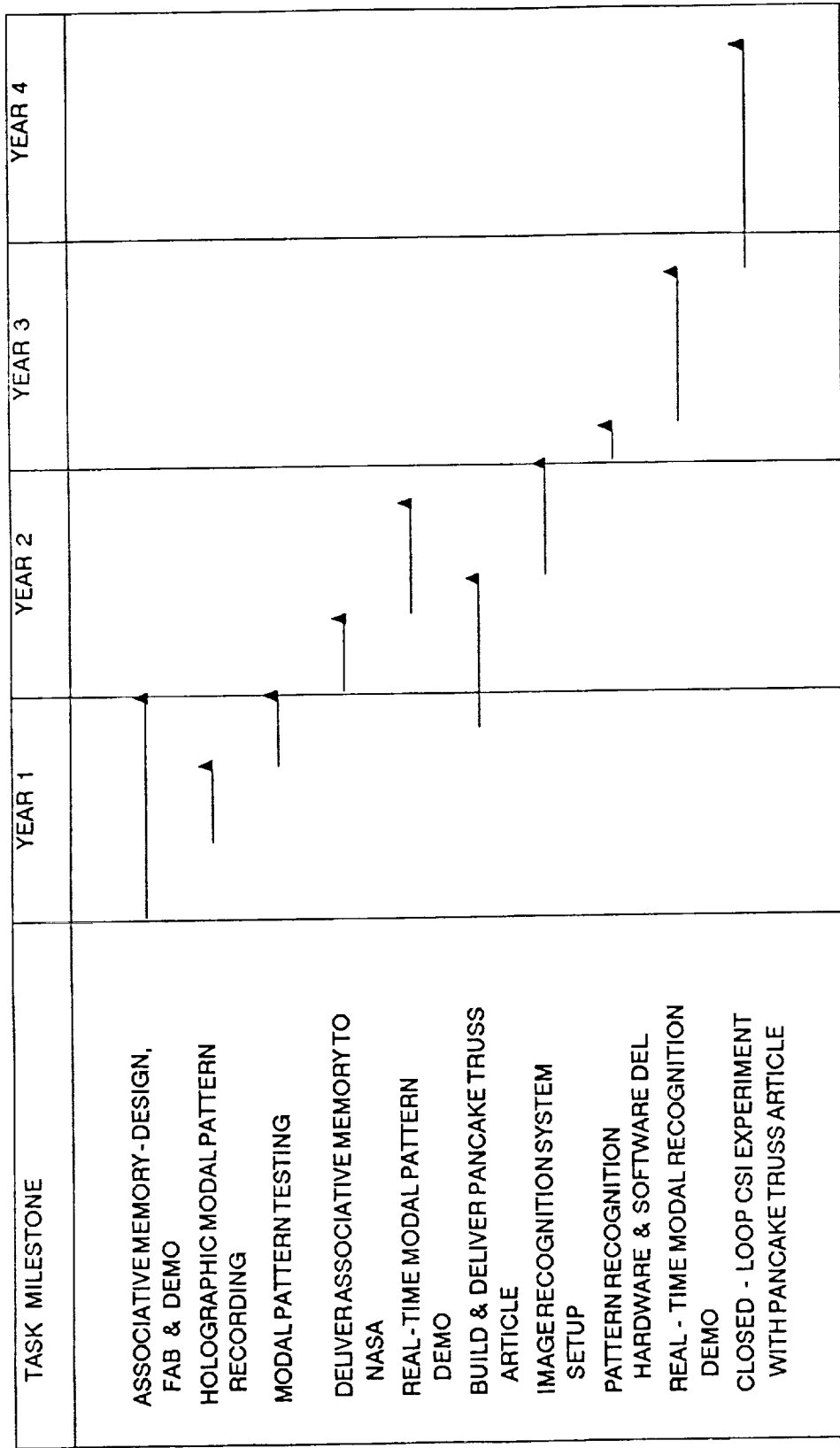


Figure 43. MILESTONE PLAN

readily available photo-refractive material such as BaTiO₃ or barium strontium niobate (BSN). Initially, a series of simple geometric shapes would be stored in a holographic memory using a commercial holographic camera system like the Newport Corporation's HC-1000 model. The camera would then be moved to NASA Langley where it would be used to record examples of modal difference patterns from the NASA optical pattern memory apparatus. We recommend initially using a simple vibrating plate driven by an electromagnetic transducer at several of its lowest frequency modes as the structural test article. Bandwidth of the photo-refractive crystals is not a serious issue if time averaged modal patterns are recorded for this demonstration. These example modal holograms would then be tested in the associative memory subsystem at Cambridge. We would record each mode at several amplitudes to test the memory "amplitude" recall function.

During the first year the pancake truss structure would also be designed and fabricated.

In the second year, the associative memory would be delivered to NASA Langley's optics lab and integrated with the optical modal pattern memory. A real-time demonstration of simple modal identification would be performed at NASA. Again, the vibrating plate test article would be used. The image recognition system would be set up using as much off-the-shelf hardware and software, such as a PC-based image processing system would offer. The pancake truss system would be completed and transferred to NASA.

In the third year, modal pattern recognition experiments would be performed using the pancake truss structure as a test article. The holograms would be formed by omnidirectional reflection of the laser illuminator from the four reference "doorknob" reflectors at the corners of the test article. (Retro-reflectors could not be used in this case.) Software and hardware for modal recognition would be completed and delivered to NASA for real-time mode identification.

If these critical demonstration milestones are achieved by the end of the third year, a closed-loop actuator experiment would be designed and implemented in the fourth year.

This demonstration plan represents a challenging schedule of unique milestones which advance the state of the art of optical processing for structural control. A large amount of interaction with NASA will be necessary for this effort to be successful. This will take full advantage of the facilities, knowledge and experience in optical devices and control structure interaction at both NASA Langley and Photon Research.

9.0 REFERENCES

1. Robert Strunce, et. al., An Investigation of Enabling Technologies for Large Precision Space Systems. Volume III: Survey of Enabling Technologies, The Charles Stark Draper Laboratory, CSDL-R-1499, November 1981. This report is written under contract number F30602-81-C-0180, also known as AFRPI-TR-82-074-VOL-3.
2. Richard Bryant, "Nonlinear Optical Materials: A Technology in Search of Applications," Laser Focus World, October 1989.
3. N. B. Aldridge, "Optical Image Processing in GaAs and BSO," SPIE, vol. 812, 1987.
4. Amnon Yariv and Pochi Yeh, Optical Waves in Crystals, New York: John Wiley & Sons, 1983, vol. 1, p. 589.
5. R. A. Hann and P. Bloor, "Organic Material for Non-Linear Optics," Royal Society of Chemistry, Publication No. 69, 1989.
6. R. Weiss, "At RADC Hanscom, A Two-Pronged Opto Program," Lasers & Optronics, May 1989.
7. E. Labuda, "Photonic Processing Sees the Light of Data," Electronic Engineering Times, Jan 29, 1990.
8. A. Bindra, "Future Seen in Optical Processor," Electronic Engineering Times, Jan 15, 1990.
9. J. A. Neff, R. A. Athole, S. H. Lee, "2-Dimensional Spatial Light Modulators: A Tutorial," Procedures of the IEEE, vol. 78, No. 5, May 1990.
10. "Magneto-Optics Spatial Light Modulator Technology: Sight-MOD," Microwave & RF, vol.13, (1974).
11. D. Armitage, J. I. Thackara, and W. D. Eades, "Gallium Arsenide Photoaddressed Liquid-Crystal Spatial Light Modulator," SPIE, vol. 936, (1988).
12. M. K. Giles. J. Z. Smith, and J. M. Florence " Fourier Plane Modeling of the TI Deformable Mirror Device," SPIE, vol. 936, (1988).
13. A. Bindra, N. Mokhoff, "AT&T Calls on Photonics," Electronic Engineering Times, December 25, 1989.
14. P. S. Guilfoyle and F. F. Zeise, "General Purpose Reconfigurable Programmable Optical Digital Computer", Procedures of the 4th International Supercomputer Conference, ICS 89, p. 8, 1989.
15. Peter S. Guilfoyle and Jackson W. Wiley, "Combinatorial Logic Based Digital Optical Computing Architectures," Applied Optics, 1988, 27, No. 9:13.
16. M. A. Habli, M. A. G. Abushagur, and H. J. Caulfield, "Solving System of Linear Equations Using the Bimodal Optical Computer (Experimental Results)," SPIE Advances in Optical Information Processing III, 1988, 936:6.
17. Caroline J. Perlee and David P. Casasent, "Optical Matrix - Vector Processing for Computational Fluid Dynamics," SPIE Advances in Optical

Information Processing III, 1988, 936:14.

18. M. A. G. Abushagur, H. J. Caulfield, "Hybrid Optoelectronic Nonlinear Algebra Processor," SPIE, vol. 936 (1988).
19. D. Casasent, J. Jackson, "Optical Linear Algebra Processor: Laboratory System Performance for Optical Control Applications," SPIE, vol. 639 (1986).
20. Igor Aleksander, Natural Computing Architectures, Cambridge, MA, The M.I.T. Press, 1989.
21. R. K. Kostuk, J. W. Goopman, L. Hesselink, "Design Considerations for Holographic Optical Interconnects," Applied Optics, 26, 1987.
22. VanderLugt, "Interferometric Spectrum Analyzer," Applied Optics, vol. 20, no. 16, 1981, pp. 2770-2779.
23. J.W. Goodman, Introduction to Fourier Optics, McGraw-Hill, NY (1968).
24. R. Lontz, "Optical Processing Panel Report," ET Technology Assessment Report, October 1989.
25. J. L. Horner and J. R. Leger, "Pattern Recognition with Binary Phase-Only Filters," Applied Optics, 24, 1985, 609.
26. P. Psaltis, E. G. Paek, S. S. Venkatesh, "Optical Image Subtraction with a Binary Spatial Light Modulator," Optical Engineering, 23, 1984, 695.
27. J. L. Horner and P. D. Gianino, "Phase-Only Match-Go Filtering," Applied Optics, 23, 1984, 812.



Report Documentation Page

1. Report No. NASA CR-4399		2. Government Accession No.		3. Recipient's Catalog No.	
4. Title and Subtitle Advanced Optical Sensing and Processing Technologies for the Distributed Control of Large Flexible Spacecraft			5. Report Date October 1991		
			6. Performing Organization Code		
7. Author(s) G. M. Williams and J. C. Fraser			8. Performing Organization Report No.		
			10. Work Unit No. 590-14-11-02		
9. Performing Organization Name and Address McDonnell Douglas Space Systems Company 5301 Bolsa Avenue Huntington Beach, CA 92647-2048			11. Contract or Grant No. NAS1-18763		
			13. Type of Report and Period Covered Contractor Report		
12. Sponsoring Agency Name and Address National Aeronautics and Space Administration Langley Research Center Hampton, VA 23665-5225			14. Sponsoring Agency Code		
			15. Supplementary Notes G. M. Williams and J. C. Fraser: Photon Research Associates, Cambridge, Massachusetts. This report was prepared by Photon Research Associates, Cambridge Research Division, 1033 Massachusetts Avenue, Cambridge, Massachusetts 02138, under subcontract number 89521150H to McDonnell Douglas Space Systems Company. Langley Technical Monitor: Sharon S. Welch Final Report - Task 3		
16. Abstract The objective of this study effort was to examine state-of-the-art optical sensing and processing technology applied to control the motion of flexible spacecraft. Proposed large flexible space systems, such as optical telescopes and antennas, will require control over vast surfaces. Most likely distributed control will be necessary involving many sensors to accurately measure the surface. A similarly large number of actuators must act upon the system. Recent advances in optical technologies may provide very lightweight and rapid sensor and processors. The technical approach used to meet this study goal included reviewing proposed NASA missions to assess system needs and requirements. A candidate mission was chosen as a baseline study spacecraft for comparison of conventional and optical control components. Control system requirements of the baseline system were used for designing both a control system containing current off-the-shelf components and a system utilizing electro-optical devices for sensing and processing. State-of-the-art surveys of conventional sensor, actuator, and processor technologies and advanced optical technologies were performed. A technology development plan is presented that presents a logical, effective way to develop and integrate advancing technologies. The last portion of this study effort was the development of a laboratory demonstration plan.					
17. Key Words (Suggested by Author(s)) Optical processing, Large Spacecraft, control/structures interaction, distributed sensing.			18. Distribution Statement Unclassified - Unlimited Subject Category 35		
19. Security Classif. (of this report) Unclassified		20. Security Classif. (of this page) Unclassified		21. No. of pages 132	22. Price A07

